Figure 23.1
Standard color look-up tables for orientation imaging.
Left: c-axis orientation image (COI) made with color look-up table (CLUT) shown on right;
right from top to bottom: stereographic projection and 180 · 180 matrix of CLUT; c-axis pole figure with contours at 0.5 uniform density; orientations and directions as in Figure 22.6.
(a) Simple azimuth and inclination coding;
(b) color coding with CIP-Standard CLUT;
(c) color coding with CIP-Spectrum CLUT.
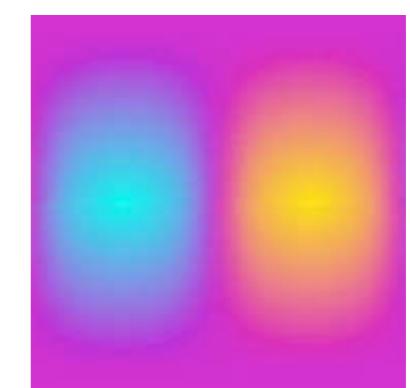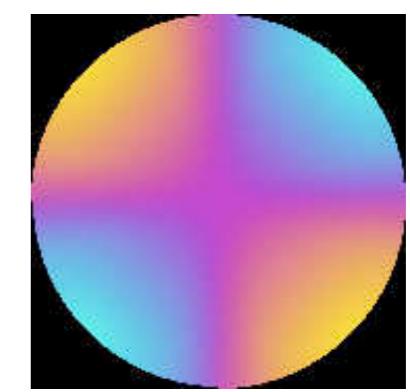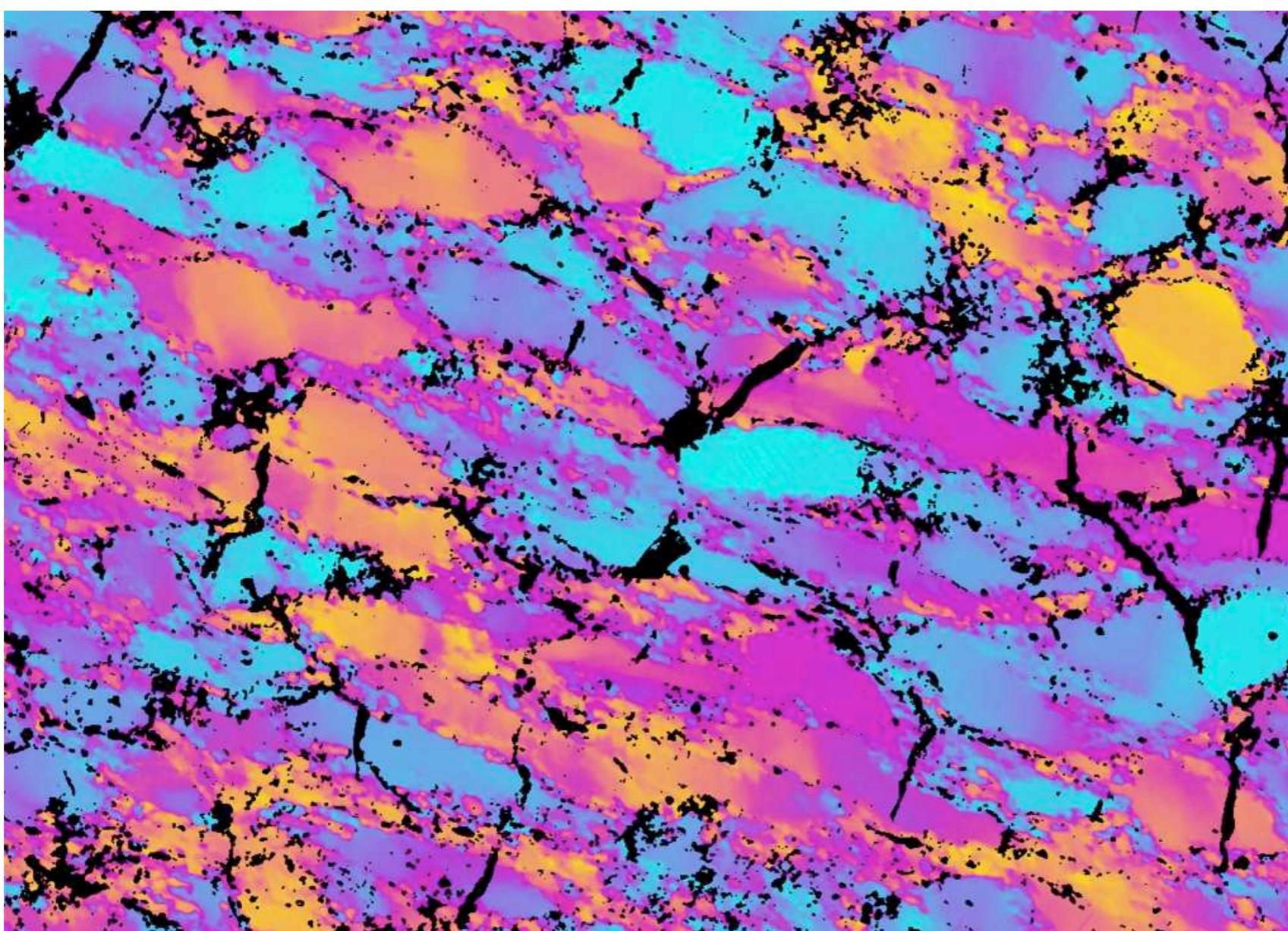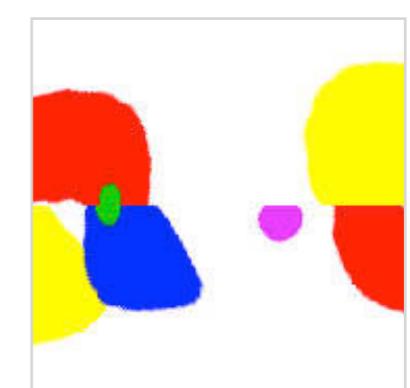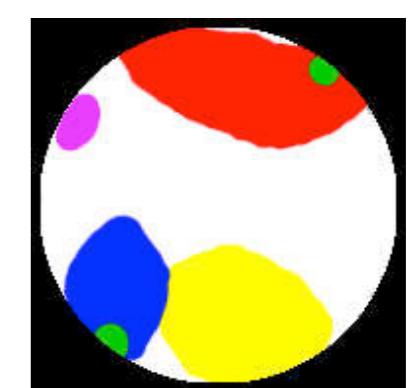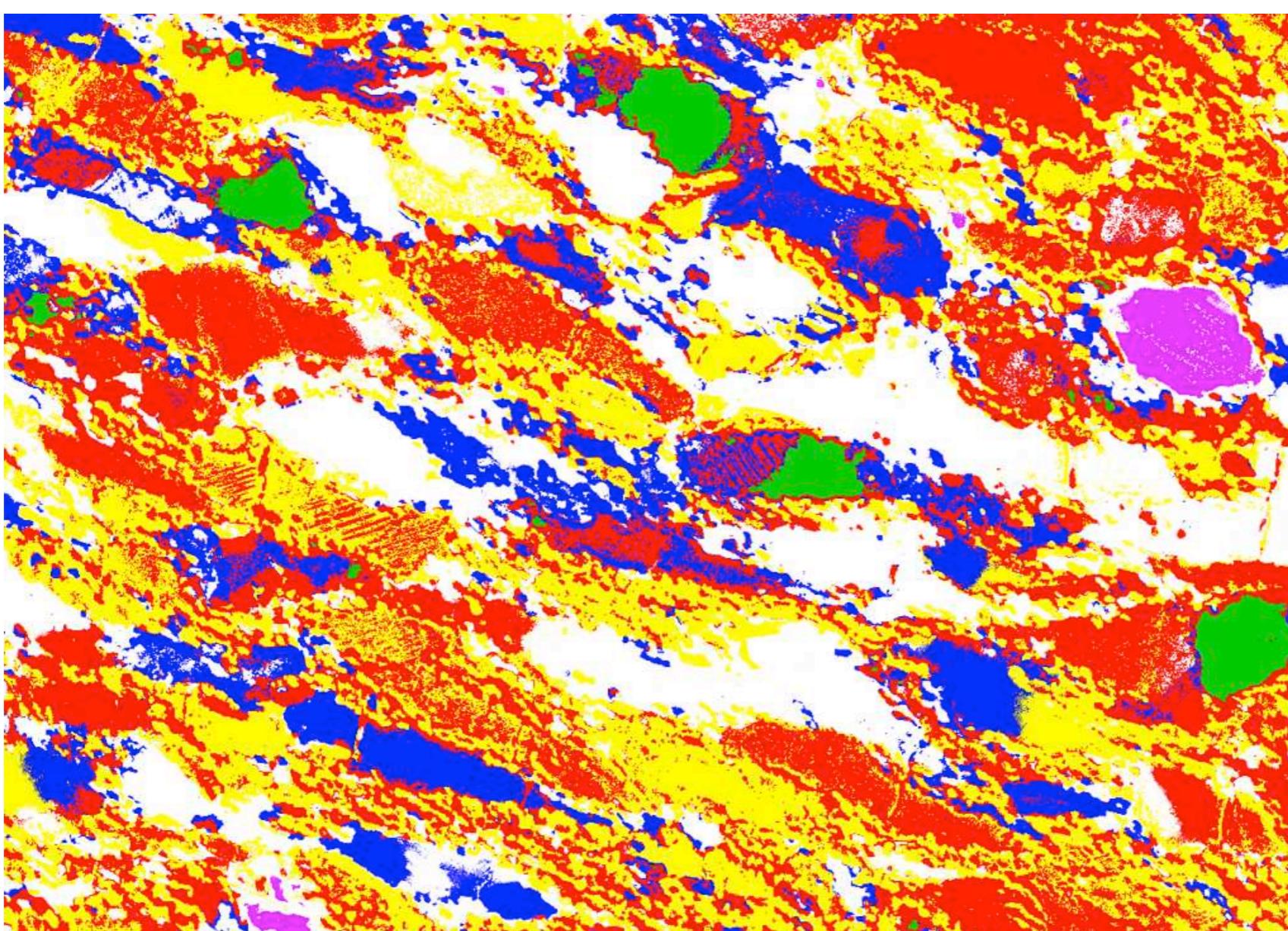
Figure 23.2
Special color look-up tables for orientation imaging.
Compare to Figure 23.1.
(a) Positive CLUT: conoscopic image used to re-create view of section under cross polarization with wave plate inserted;
(b) Problem adapted CLUT: created by coloring regions in the pole figure highlighting different maxima with different colors;
in both cases, (a) and (b), the square CLUT is derived from the stereographic form by inverting the Schmidt projection.

a

Euler angles (ψ_1, ϕ, ψ_2)

b
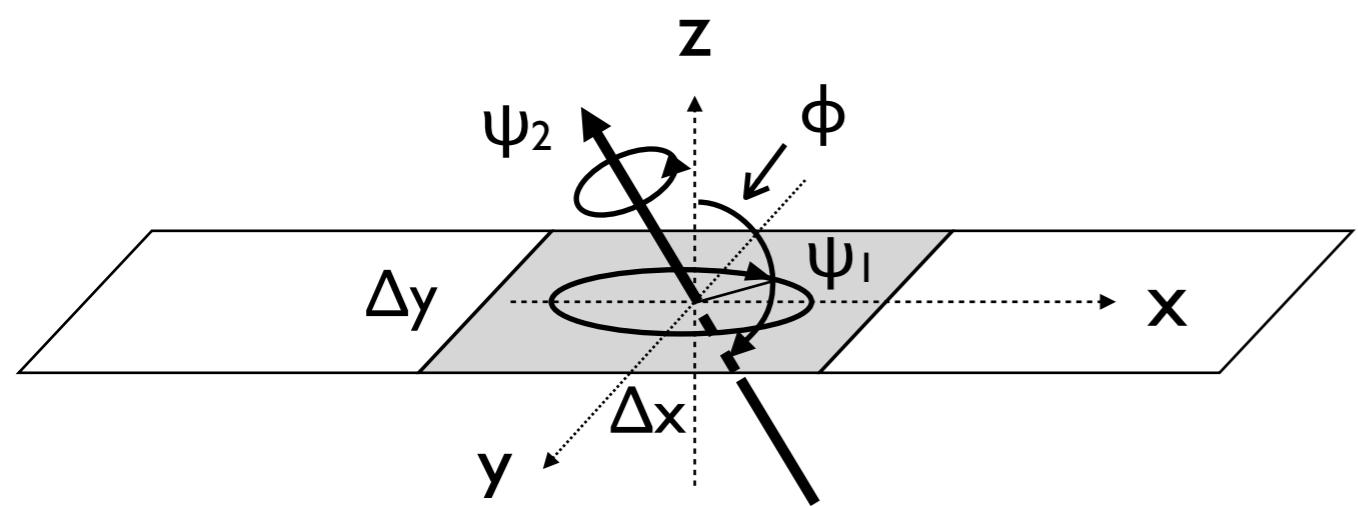
orientation (φ, θ) of c-axis
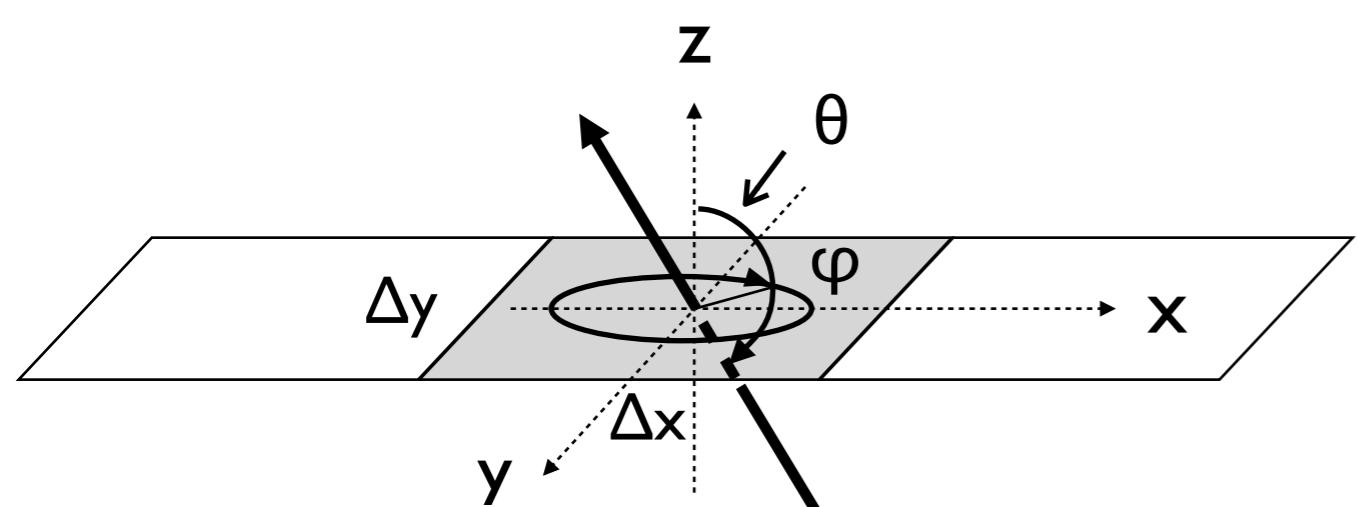
Figure 23.3
Orientation imaging.
(a) EBSD: full crystallographic orientation defined by 3 Euler angles (ψ_1, ϕ, ψ_2) at every pixel in X-Y image plane;
(b) CIP: c-axis orientation defined by azimuth and inclination (φ, θ), at every pixel in X-Y image plane.
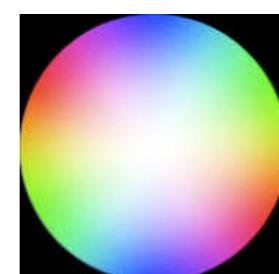
Figure 23.4

CIP orientation imaging of quartz mylonite.

(a) Images of azimuth (AZI) and inclination (INC) with histograms of φ and θ;

(b) c-axis orientation images (COI) with color look-up tables (CLUT); frame indicates area that has been analyzed with EBSD for comparison (see Figure 23.5, 23.6 and 23.7).
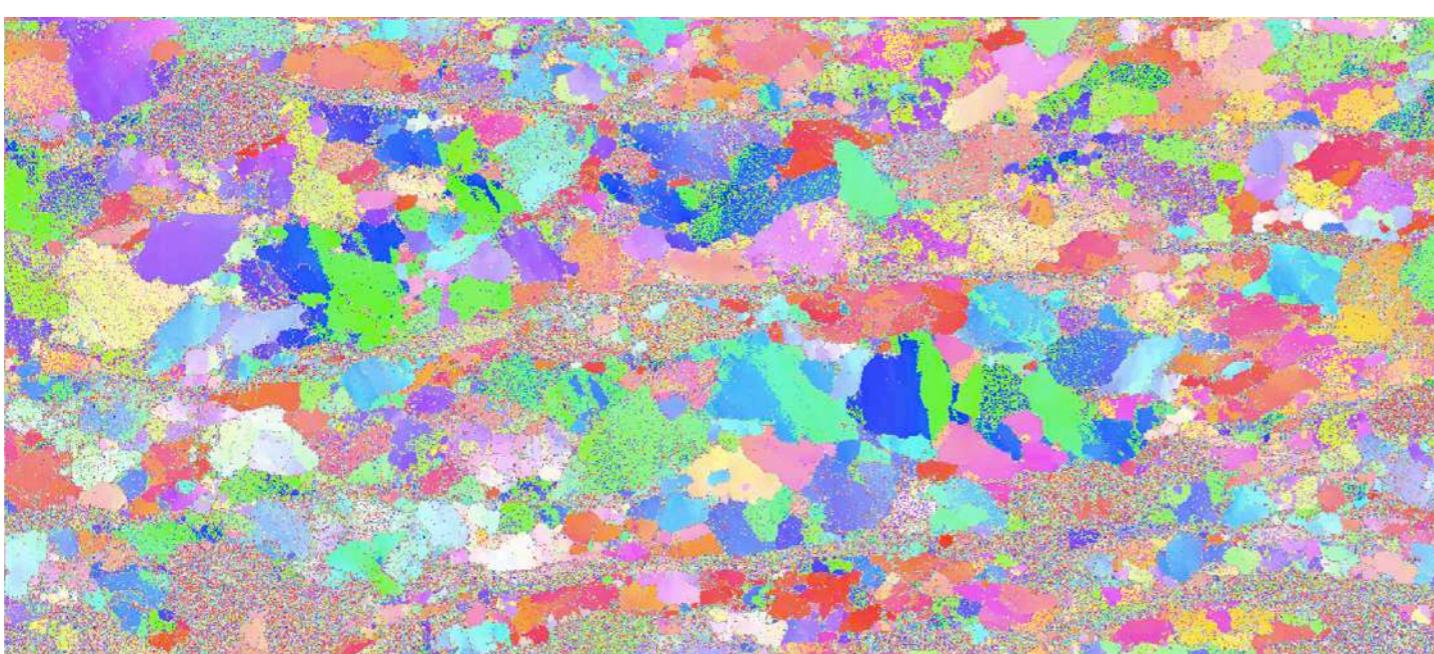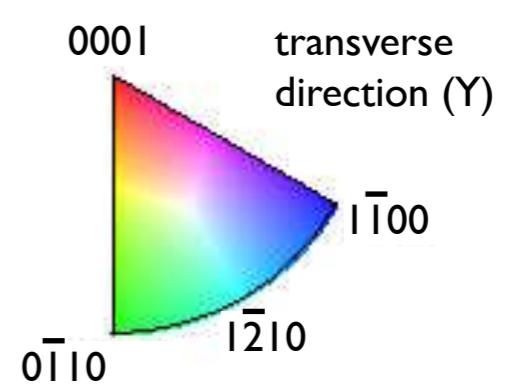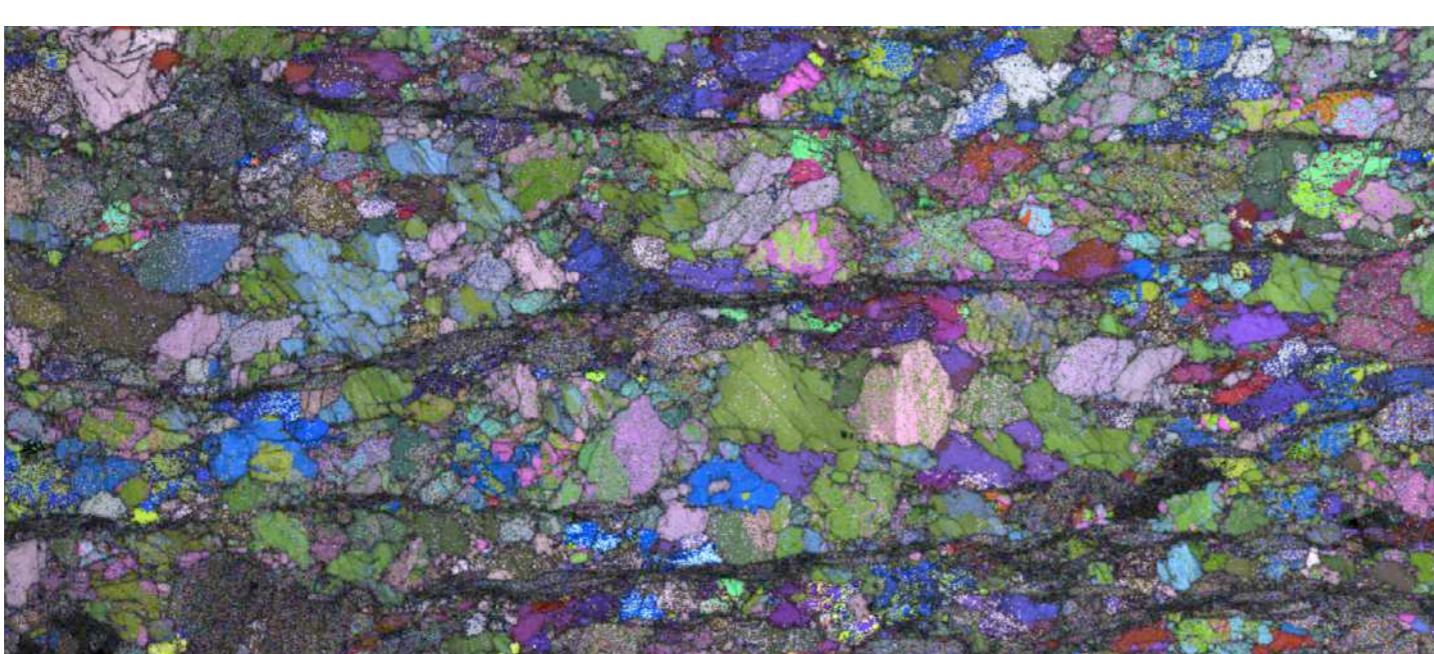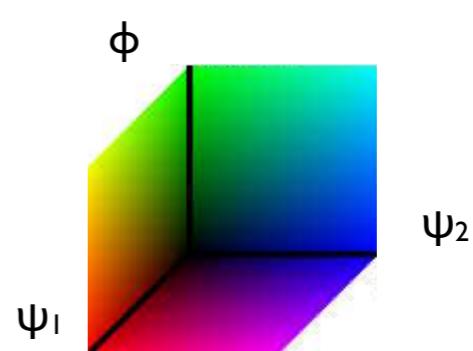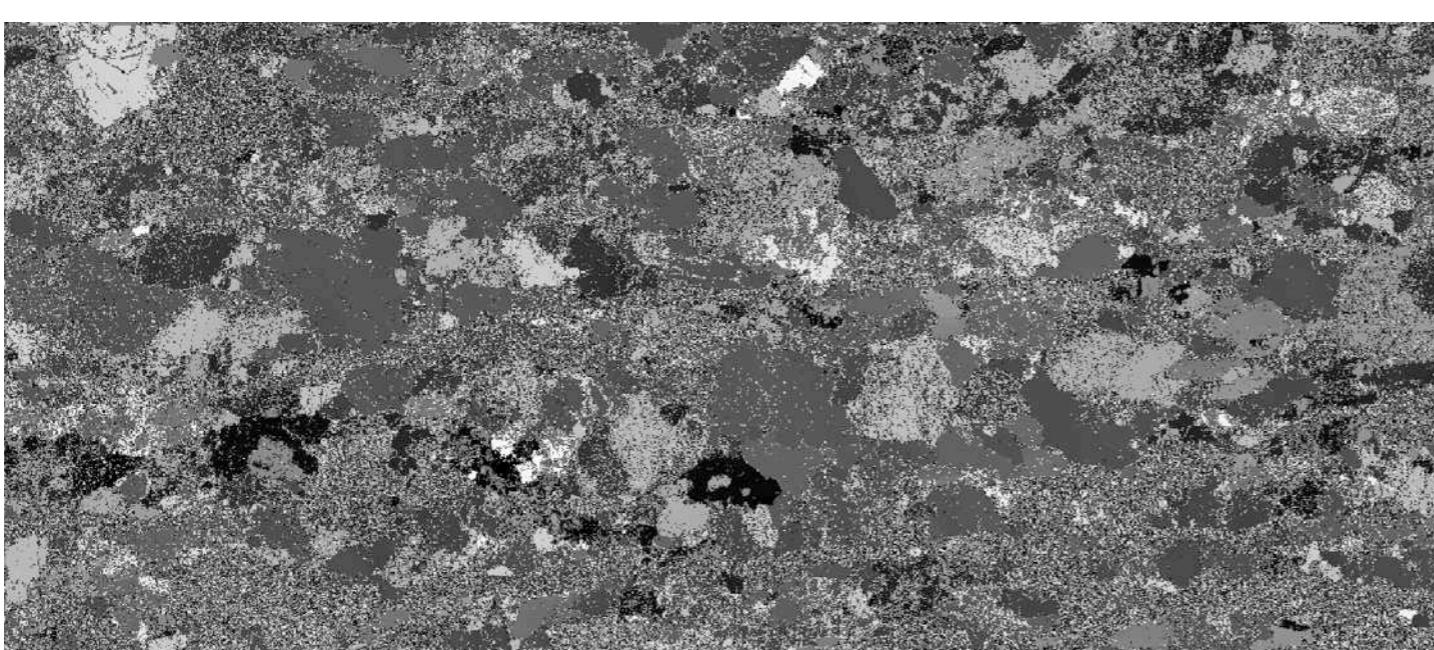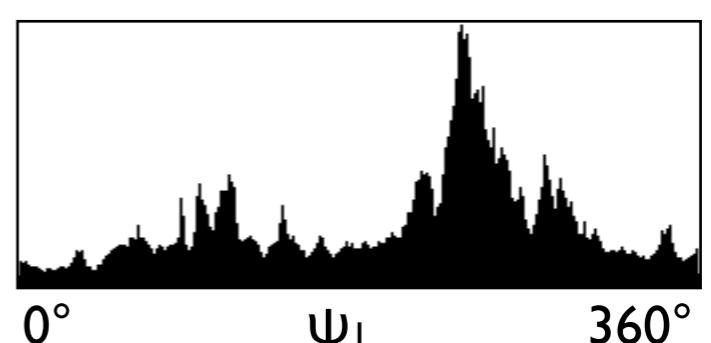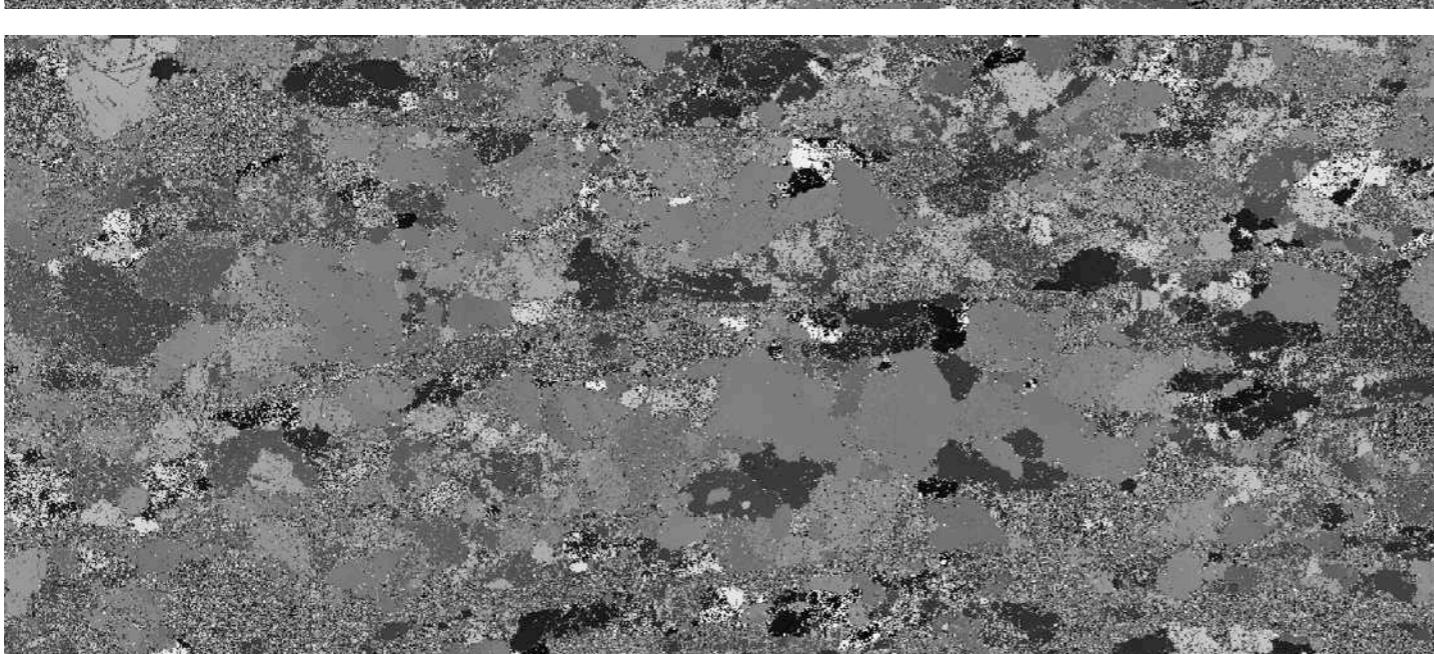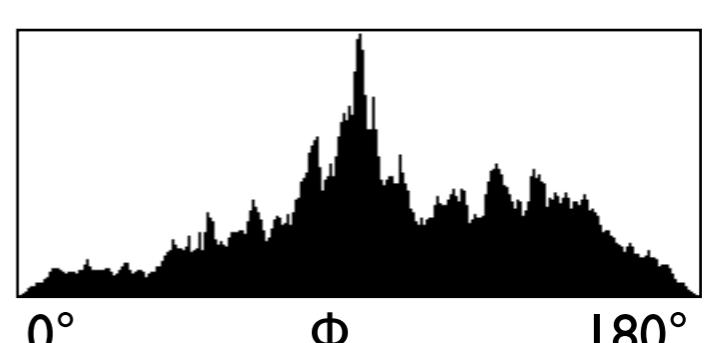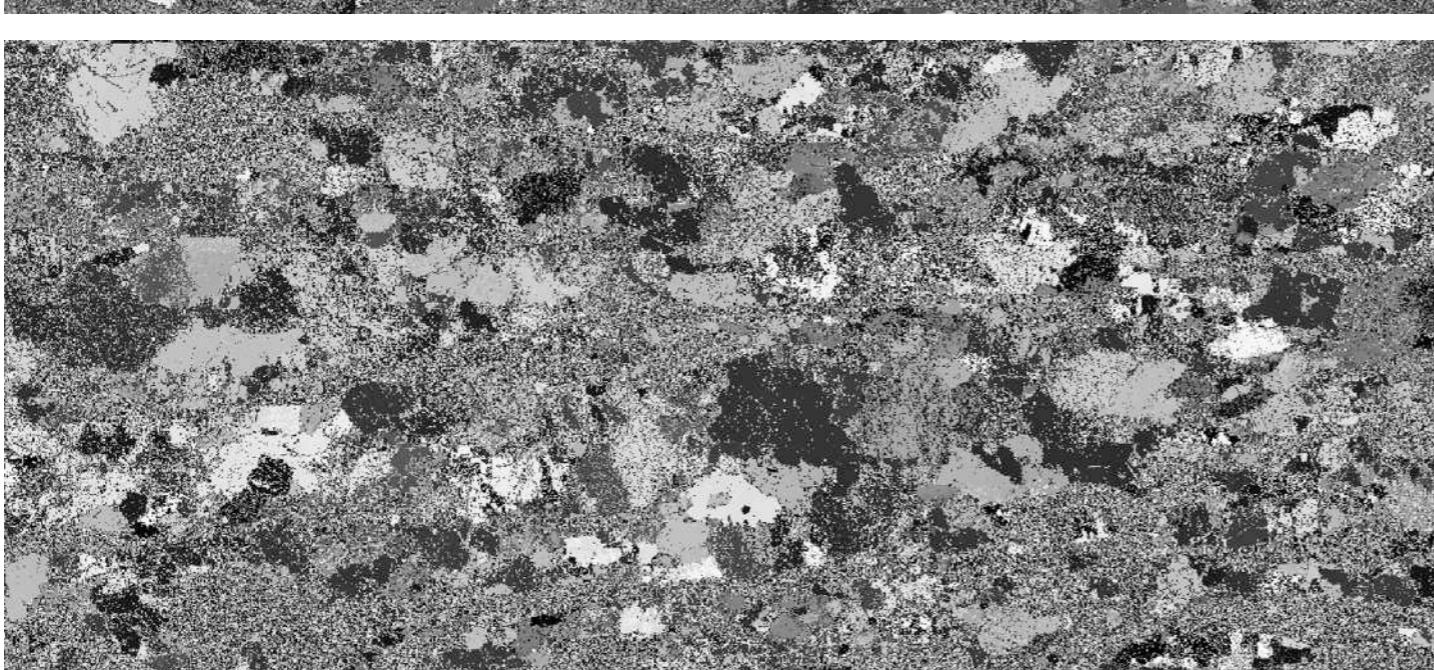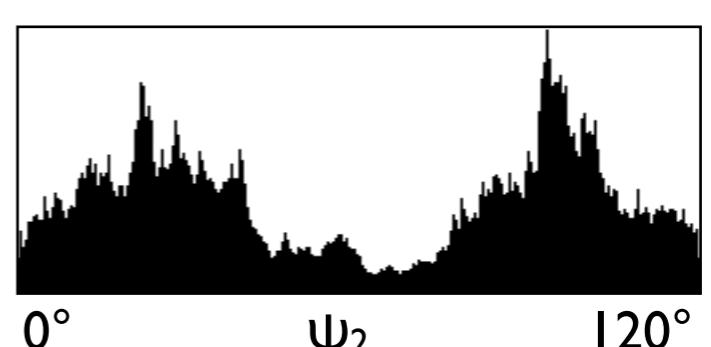
Figure 23.5

EBSD orientation imaging of quartz mylonite.

(a) Orientation image using Inverse Pole Figure (IPF) coloring shown on right; inverse pole figure for the transverse direction (image normal) shown on right;

(b) Euler image with R = ψ_1, G = ϕ, B = ψ_2;

(c) images of RGB color channels of (b) with histograms of ψ_1, ϕ, and ψ_2 on right.
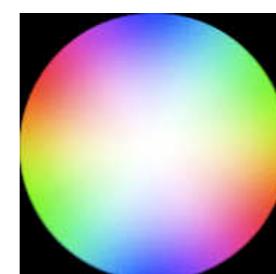
Figure 23.6
CIP coloring of EBSD orientation image.
(a) Images of azimuth (AZI) and inclination (INC) calculated from Euler angles (Figure 23.5.c) using Lazy EBSD macro with histogram shown on right; Al = Aluminium element map, acquired with SEM, used to create mask for (b);
(b) c-axis orientation images (COI) derived from AZI and INC (a) with color look-up tables (CLUT) shown on right.
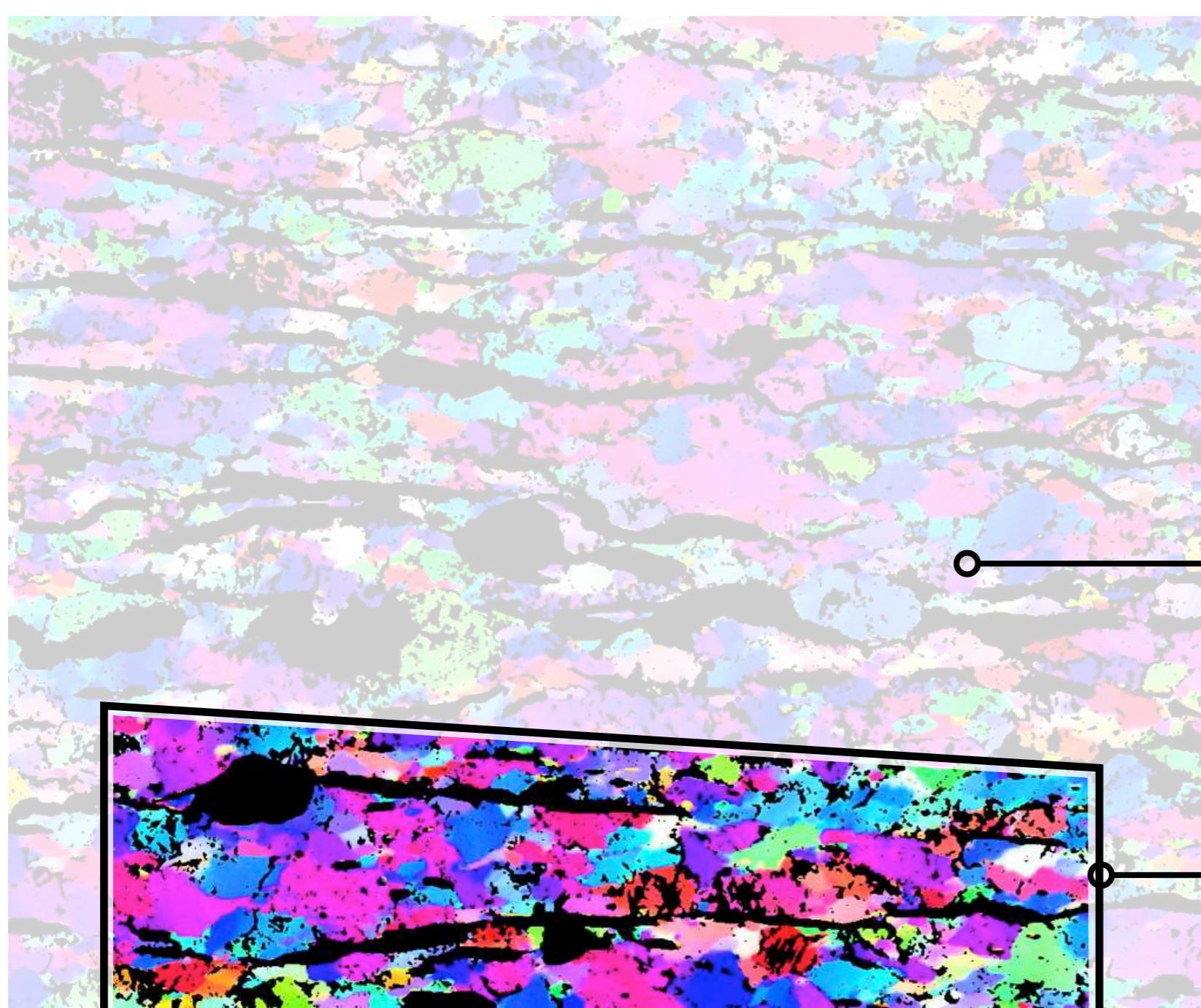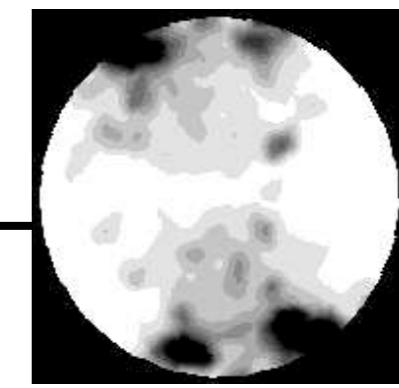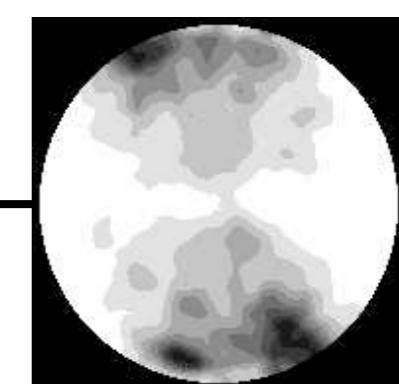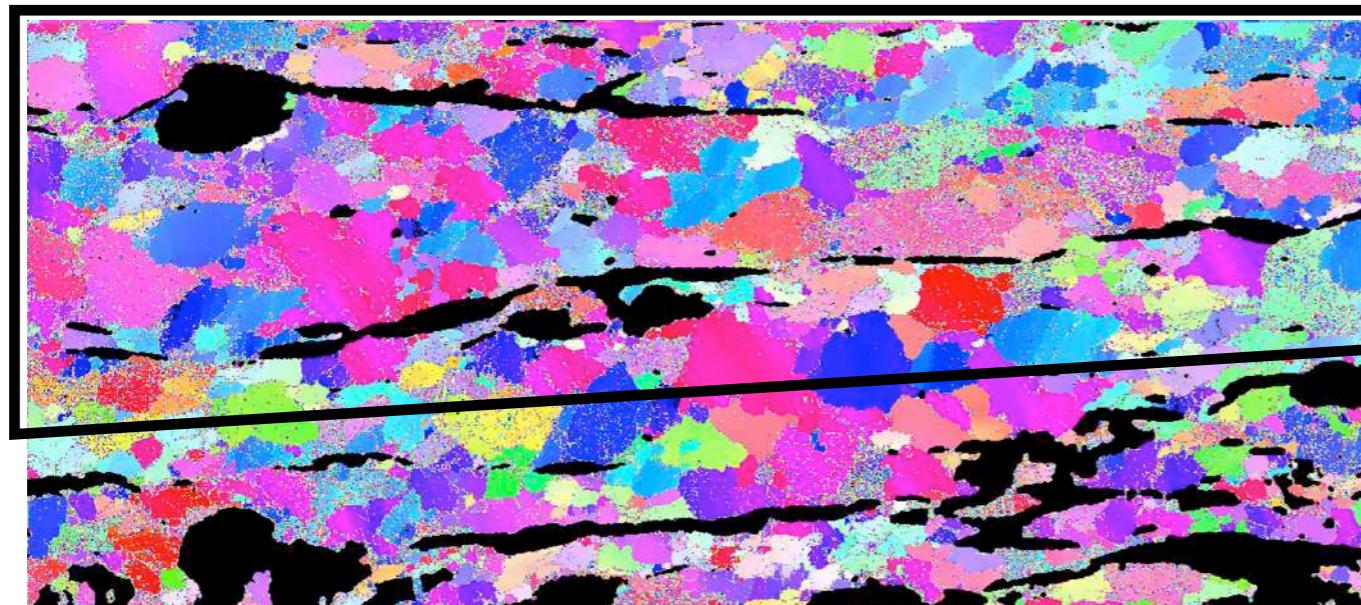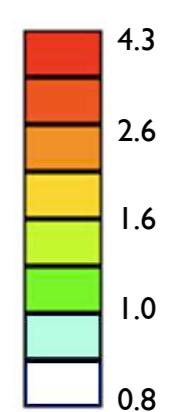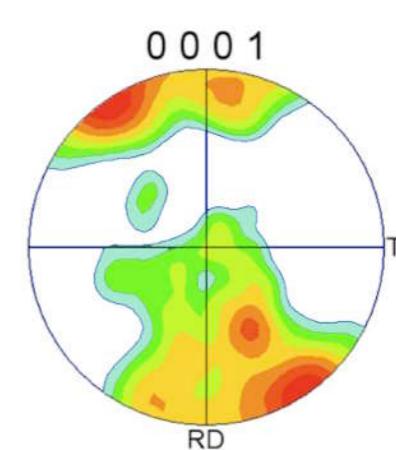
Figure 23.7
Comparison of CIP and EBSD.
(a) CIP-derived c-axis orientation image (COI) with color look-up table (CLUT) and pole figures on right: (bulk) applies to total area, (detail) to area of overlap with EBSD-derived COI;
(b) EBSD-derived COI with EBSD pole figure on right (0001 = c-axis pole figure);
area of overlap is outlined in both COIs.
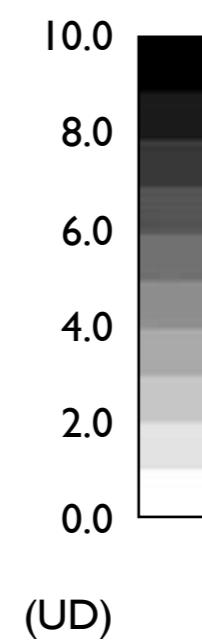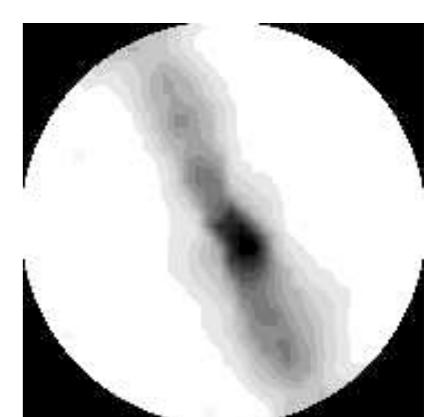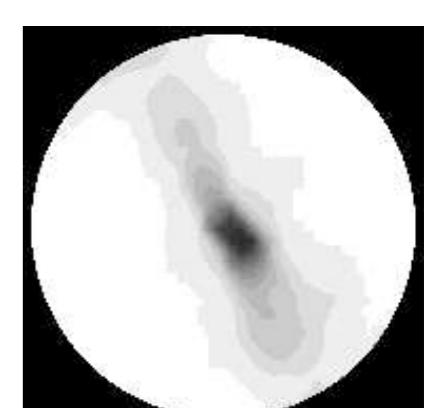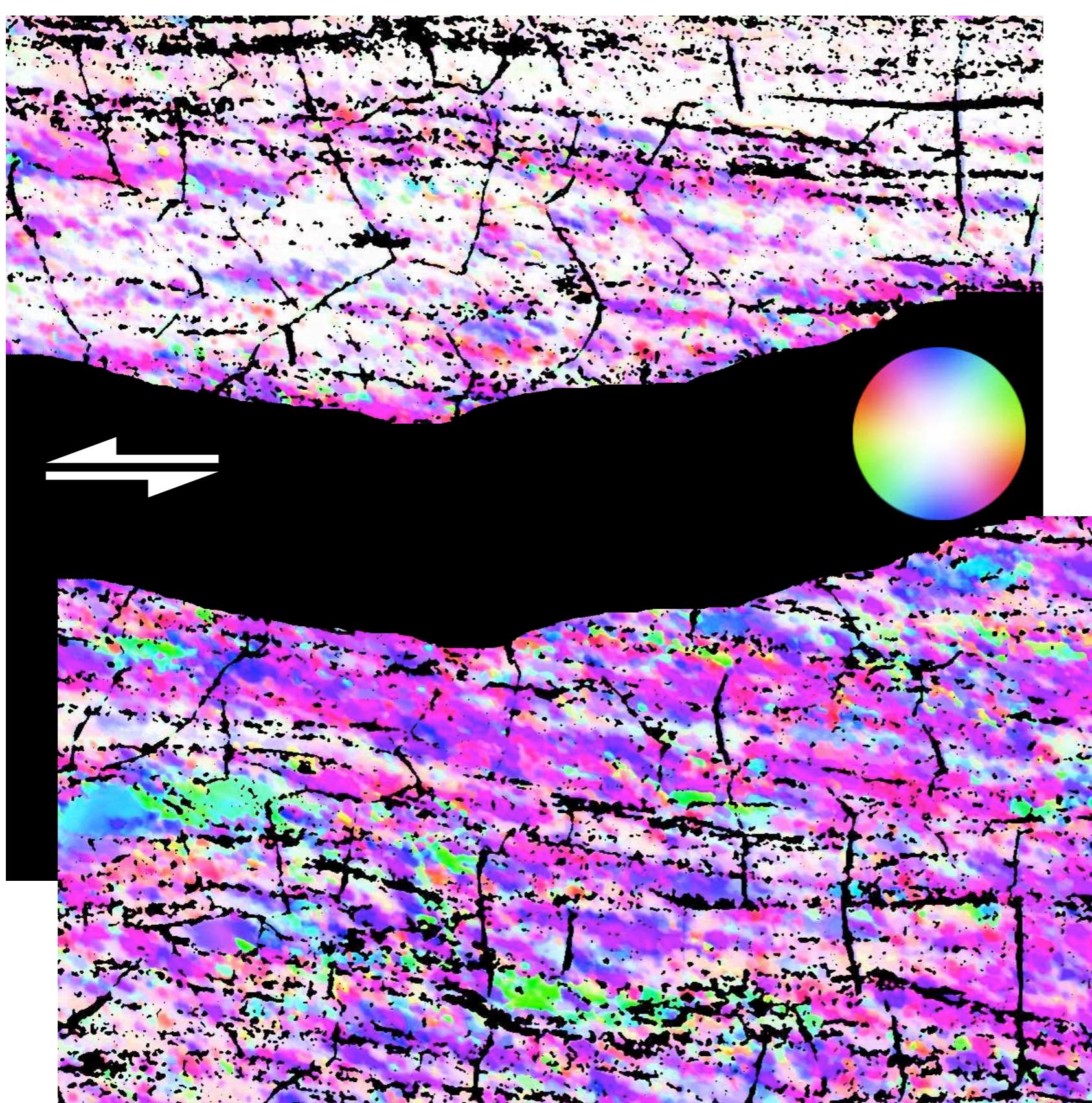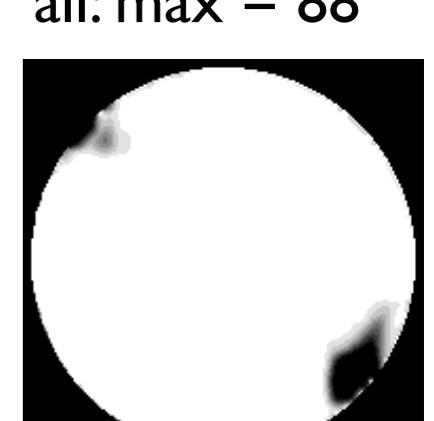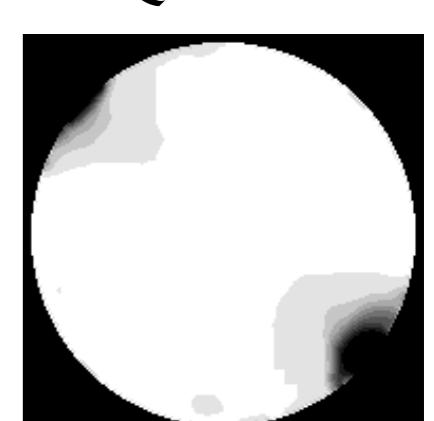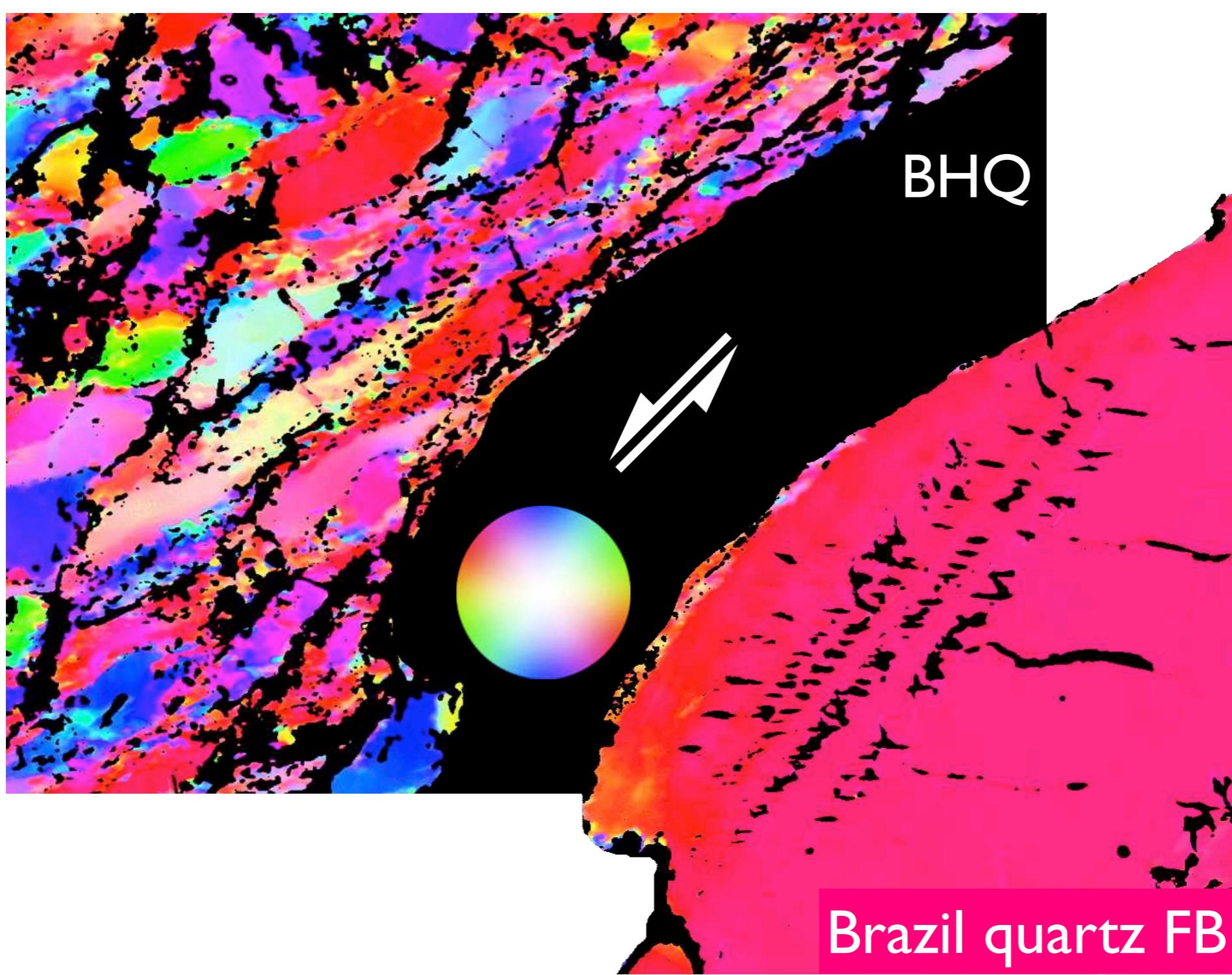
Figure 23.8
Masking for area of interest.
(a) c-axis orientation image (COI) of experimentally sheared quartzite (experimental samples by Jan Tullis) with strain gradient from top to bottom: two complementary masks are used to evaluate top and bottom part separately; on the right: pole figures of the top part (Y_{max}), the bottom part (rhomb) and the entire sample (girdle);
(b) COI of experimentally sheared quartzite (BHQ) and of forcing block (FB) shown separately at right; below: pole figures of BHQ, of entire image and of (FB); contours are 1 - 10 times uniform, pole figure maxima are indicated; shear sense is indicated in (a) and (b).
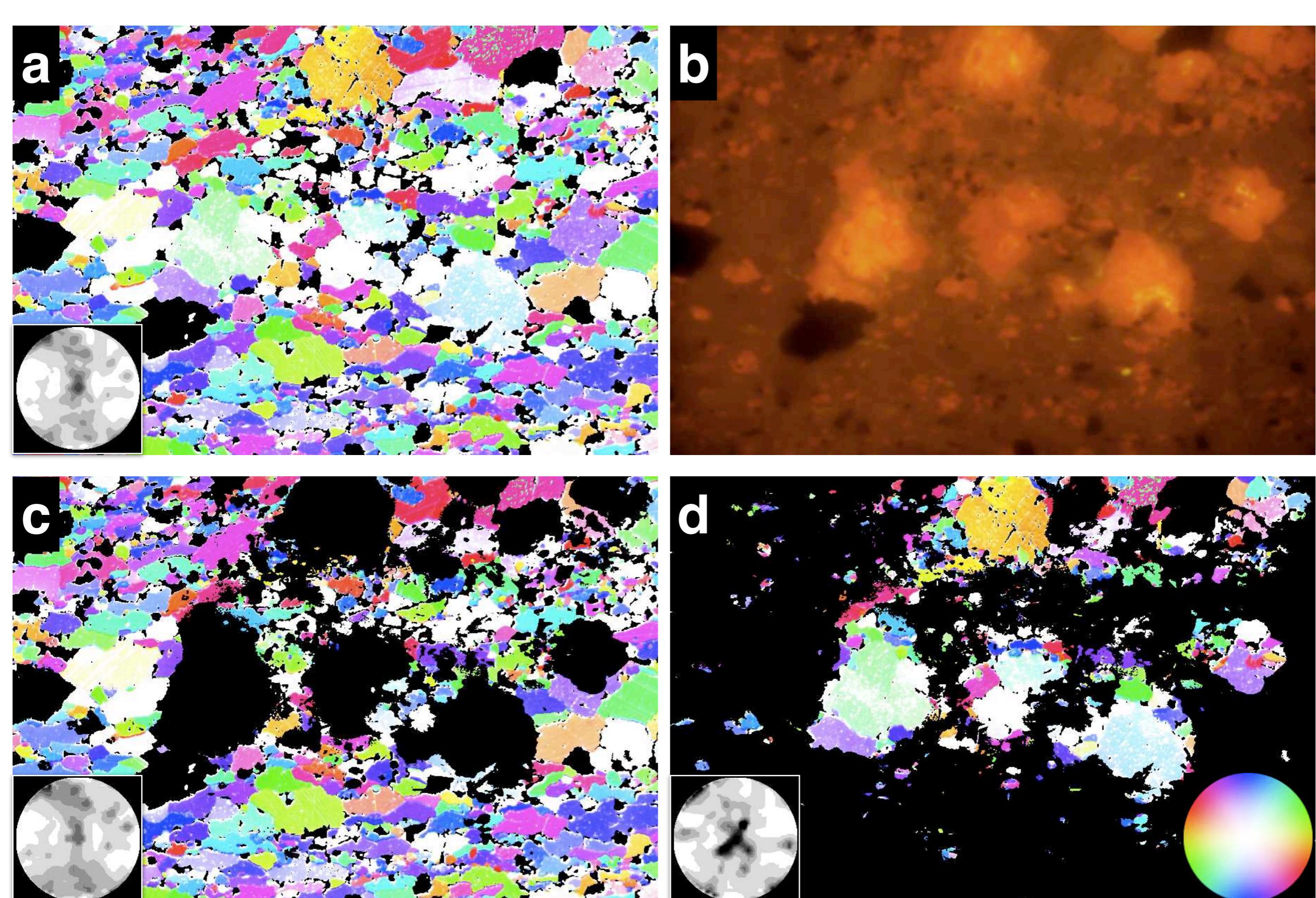
Figure 23.9
Masking for different mineral phases.
Calcite-dolomite marble (sample courtesy Nils Oesterling):
(a) c-axis orientation image (COI) and pole figure of entire sample;
(b) cathodo-luminescence (CL) image, showing dolomite in bright orange;
(c) COI and pole figure of calcite; black = dolomite mask;
(d) COI and pole figure of dolomite; black = calcite mask.

a

orientation (φ, θ) of c-axis

b
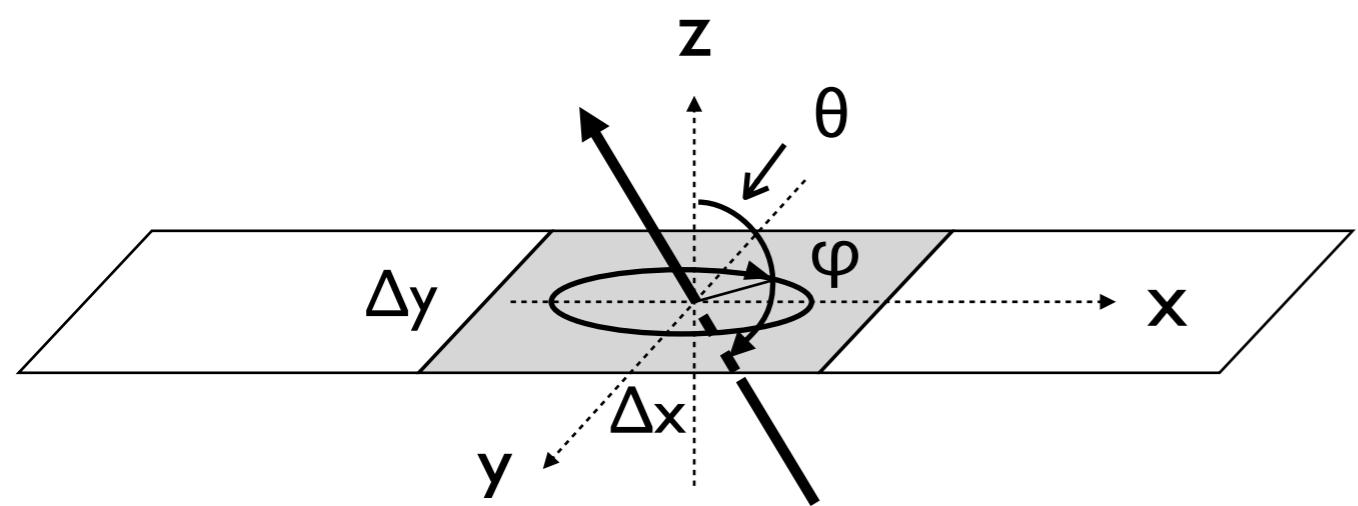
misorientation (β) of c-axis
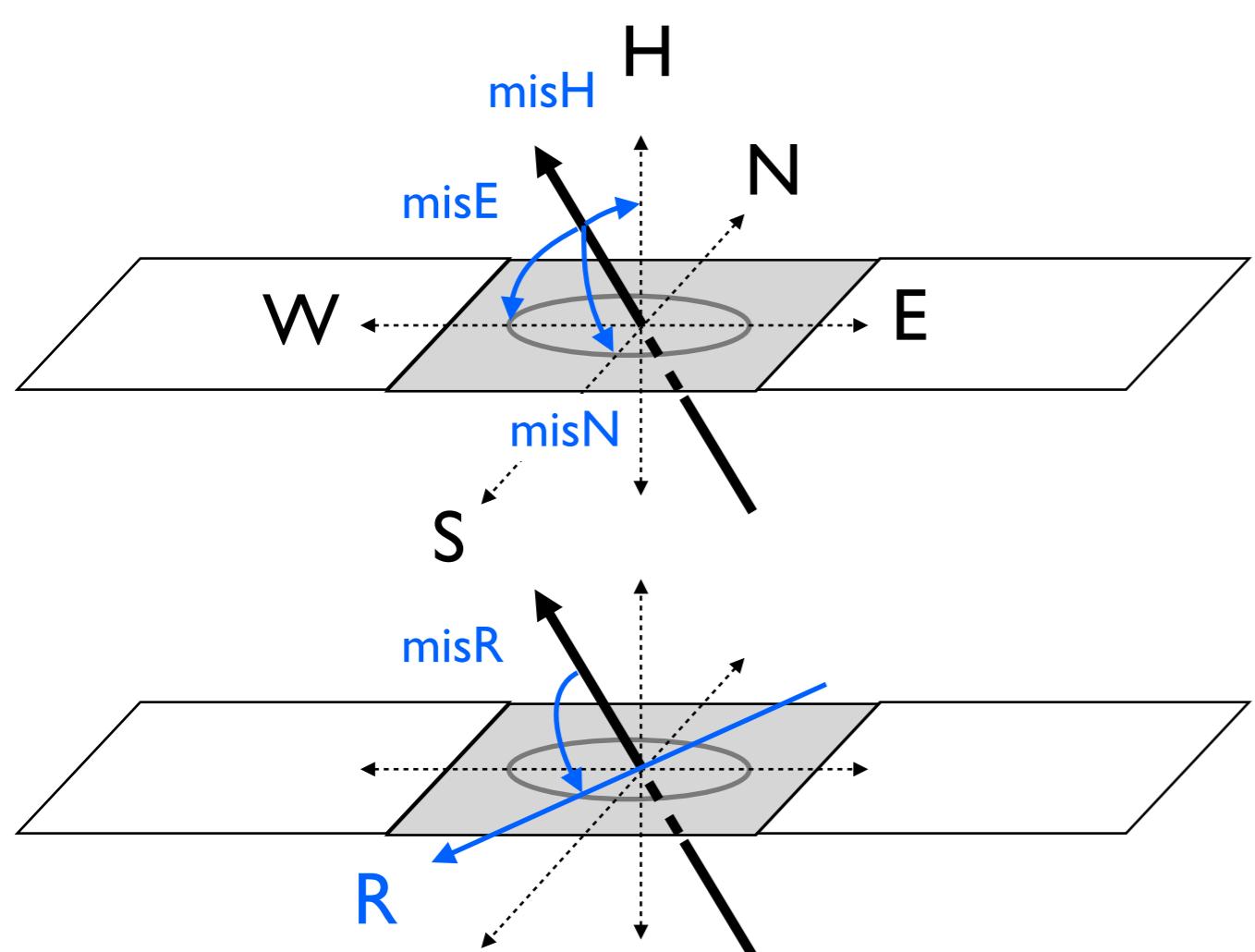
Figure 23.10
Misorientation imaging.
Schematic representation of orientations and misorientations:
(a) orientation image: c-axis orientation is given by azimuth and inclination (φ, θ), at every pixel of the x-y image plane;
(b) misorientation image: misorientation (β) of c-axis with respect to principal directions (misE, misN, misH) or selected reference direction (misR).
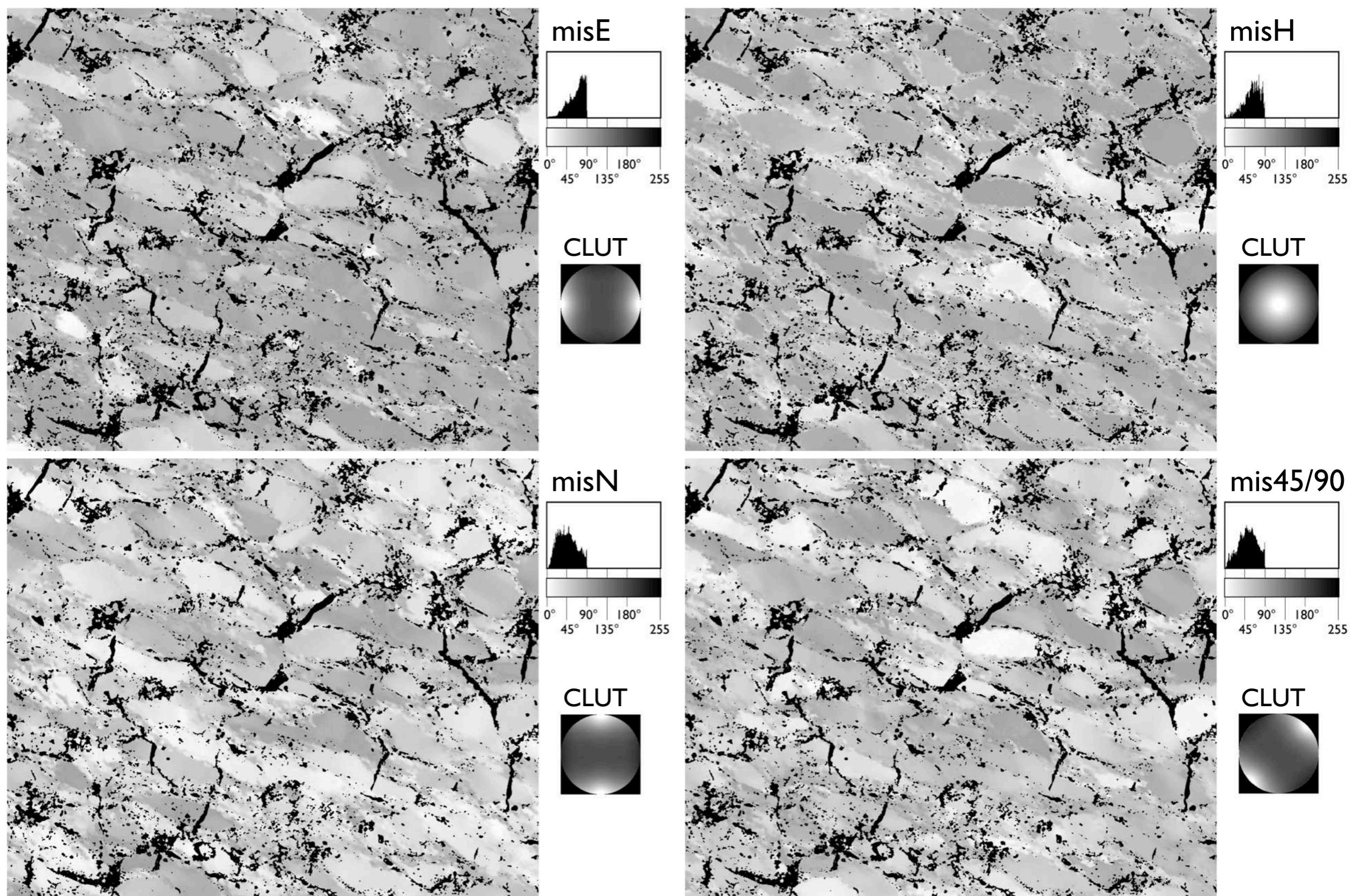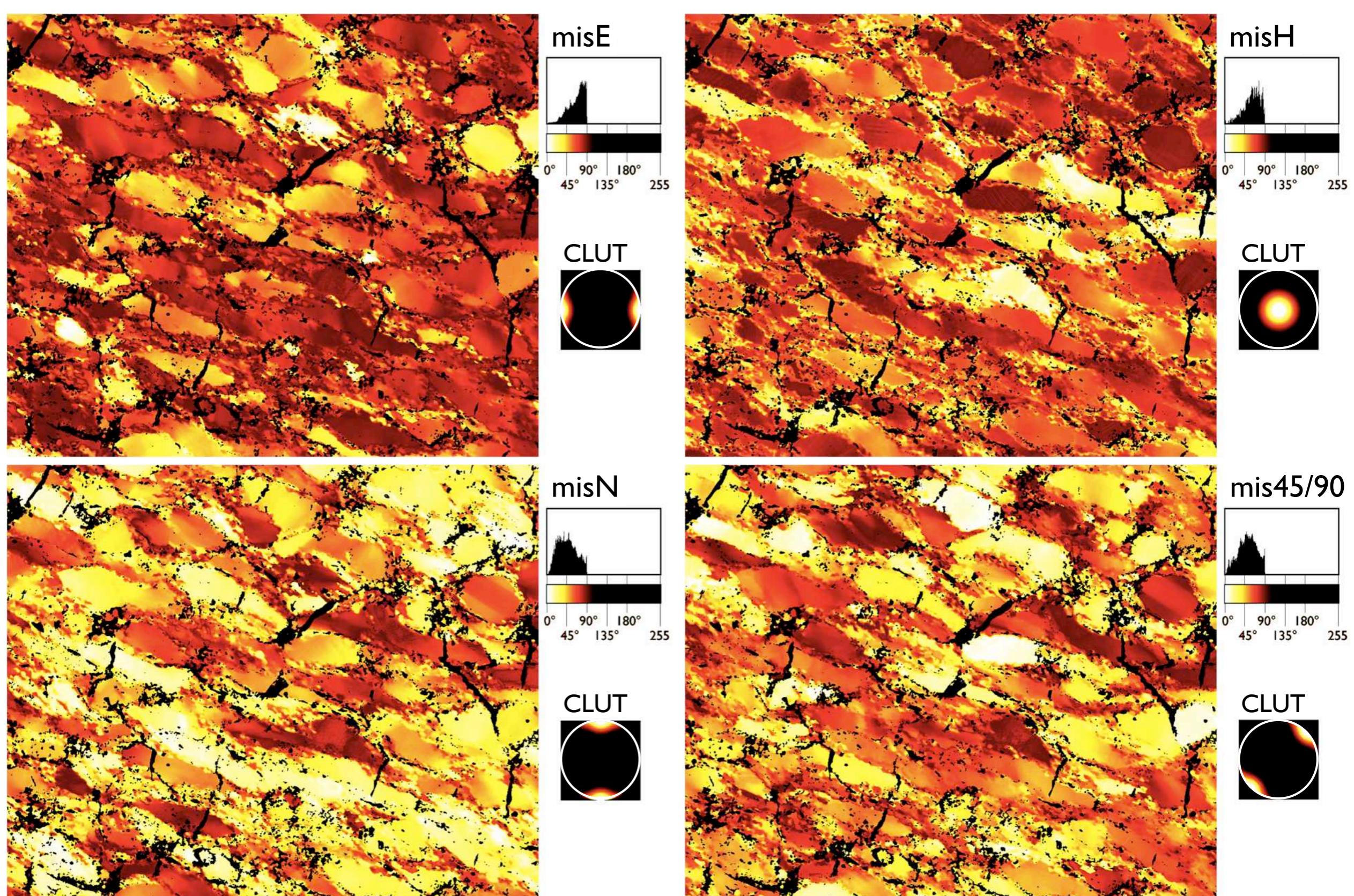
Figure 23.11

Principal misorientation images.

Misorientation images (MOI) with histogram and color look-up table (CLUT).

(a) MOI of misE, misN, misH and mis45/90 as grayscale;

(b) same as (a) with 'Fire -1' (Image SXM look-up table), contrast enhanced to 0° - 90° range;

misE = East (positive x), azimuth = 90°, inclination = 90°;

misN = North (positive y), azimuth = 0°, inclination = 90°;

misH = Heaven (Up, positive z), inclination = 0°;

mis45/90 = Northeast, azimuth = 45°, inclination = 90°.
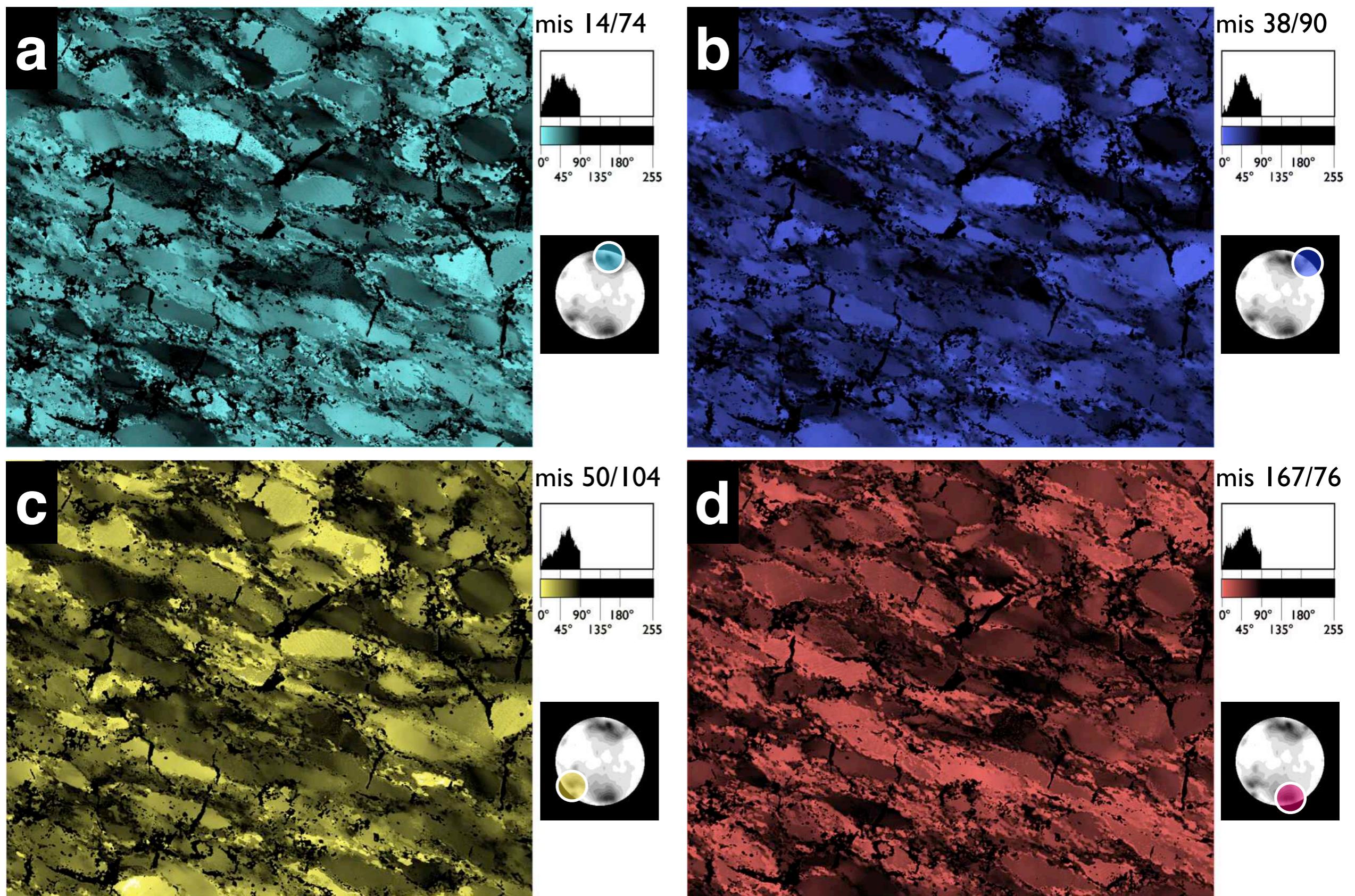
Figure 23.12
Misorientation images of pole figure maxima.
Color-coded misorientation images are shown with histograms:
(a) reference direction = azimuth = 14°, inclination = 74°;
(b) reference direction = azimuth = 38°, inclination = 90°;
(c) reference direction = azimuth = 50°, inclination = 104°;
(d) reference direction = azimuth = 167°, inclination = 76°.
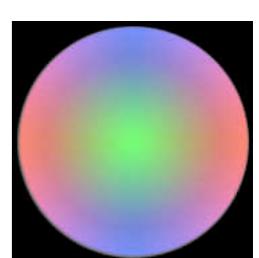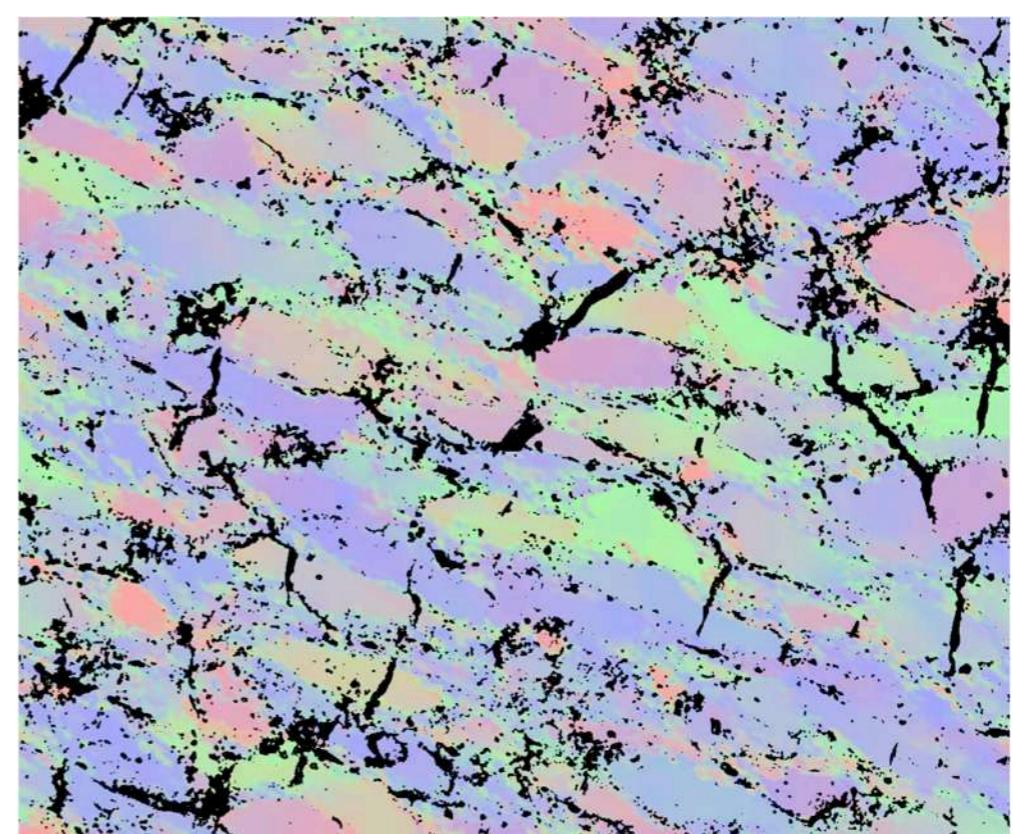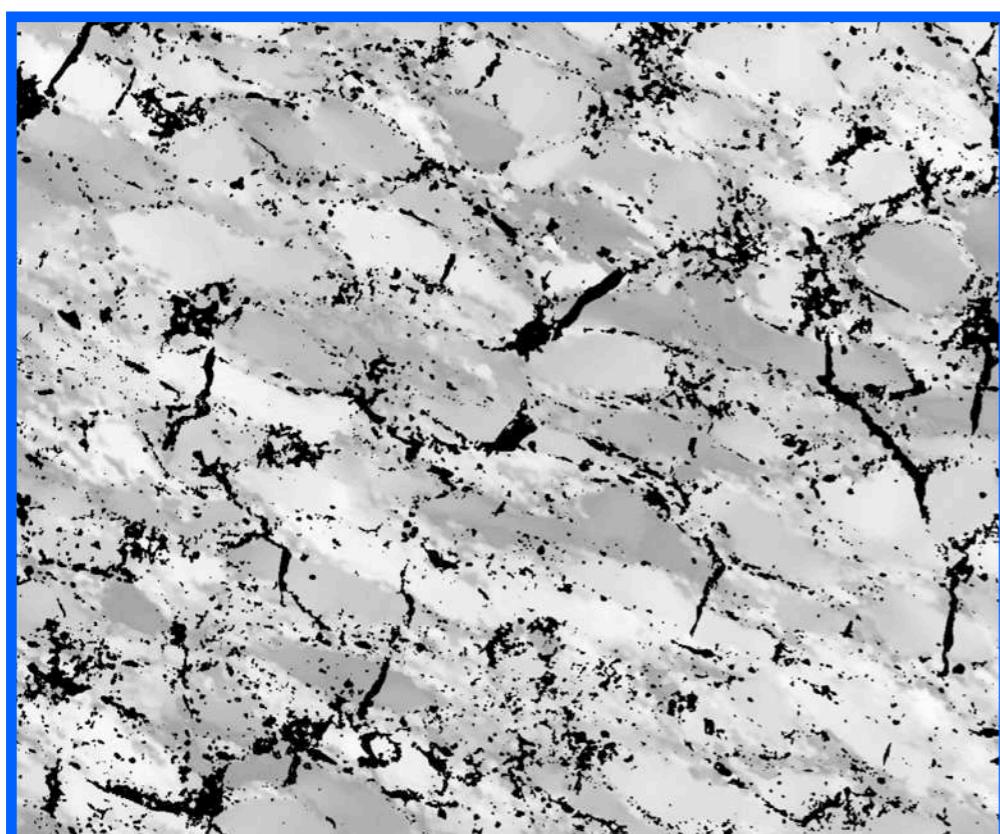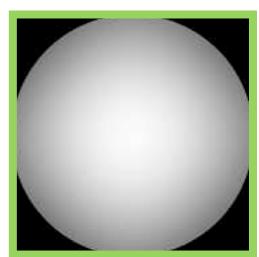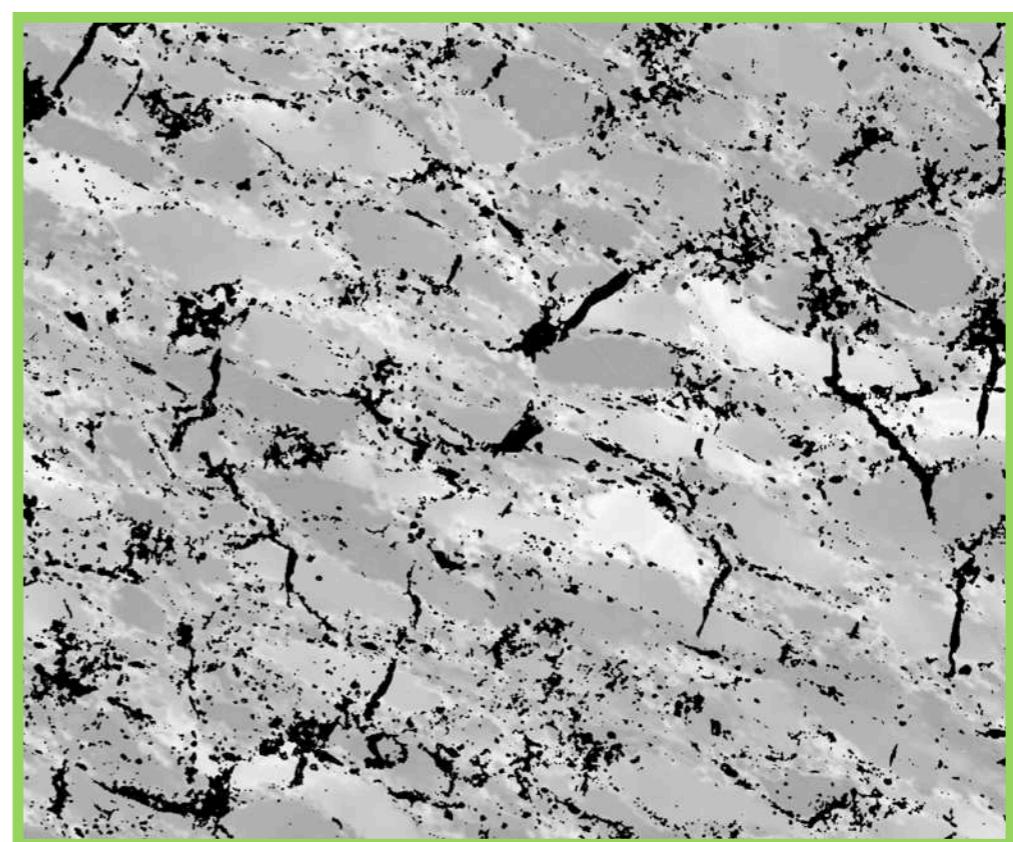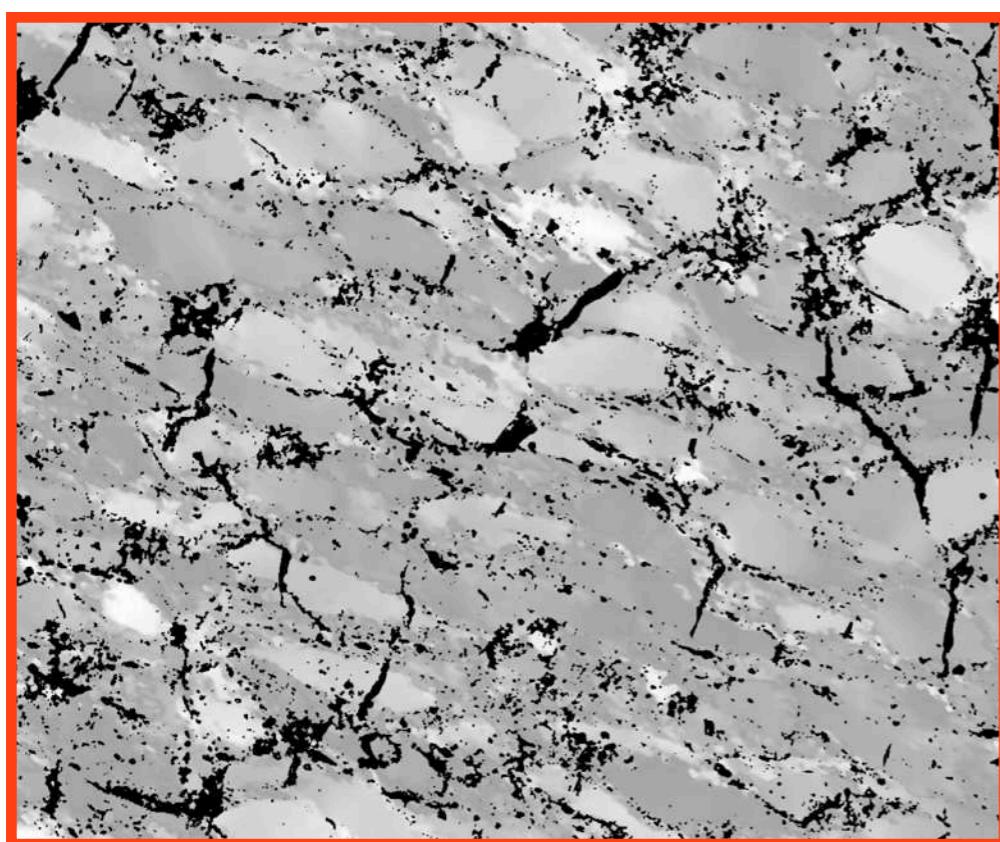
Figure 23.13

Orientation image from principal misorientation images.

The c-axis orientation image (COI) is generated by copying 3 principal misorientation images (MOI) into color channels of RGB image:

Red = misE; Green = misH; Blue = misN.

Note pale colors of COI (lower right): due to small range of misorientations, only 90 (of 256) gray values are used.
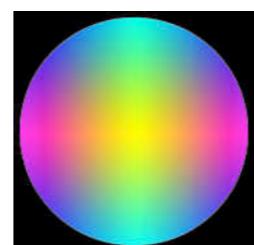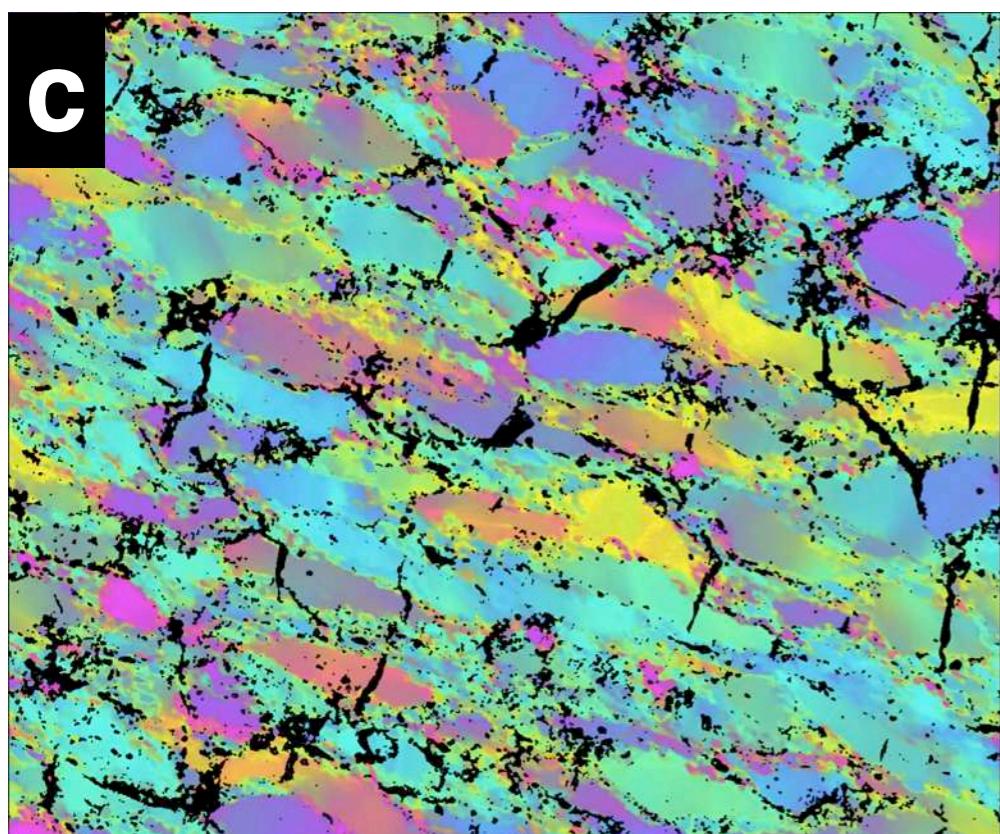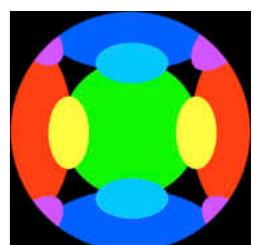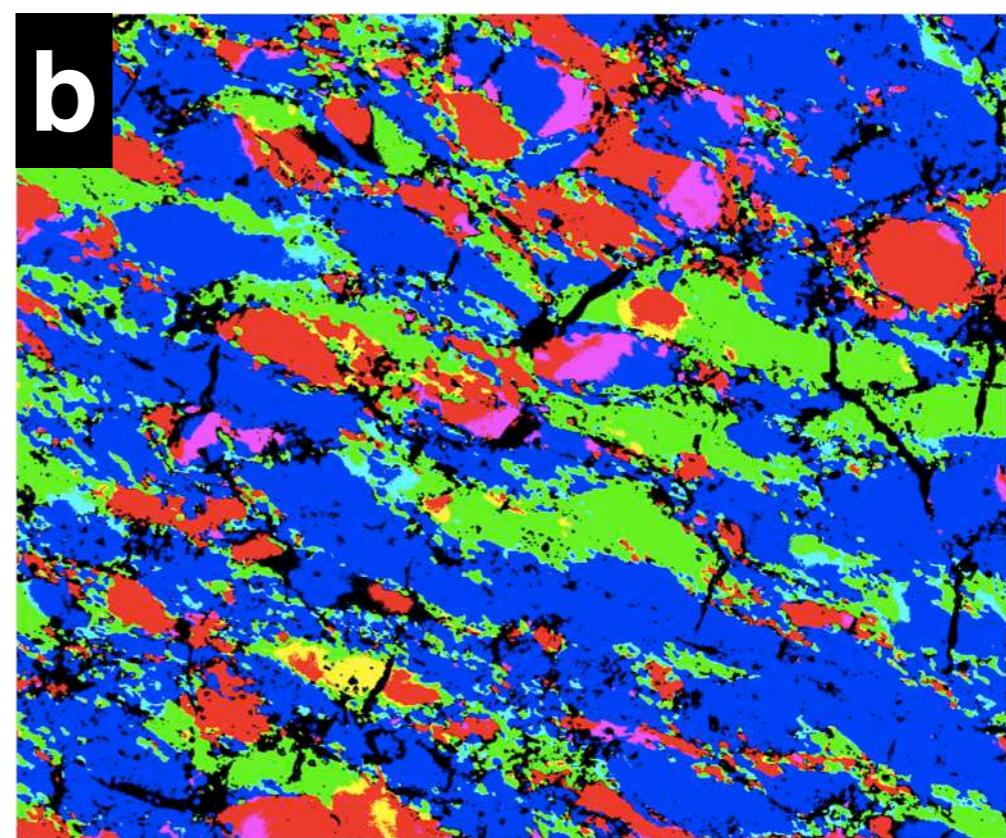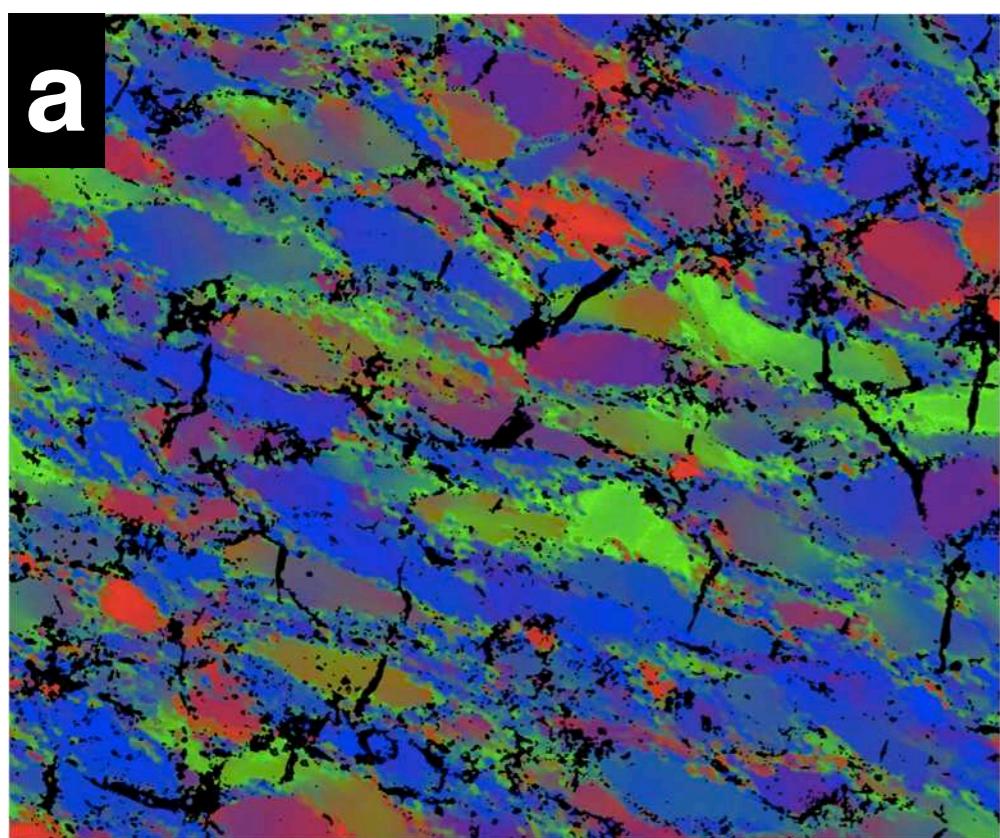
Figure 23.14

Orientation image from enhanced misorientation images.

Same COI as Figure 23.13:

(a) using 'Enhance Contrast' command in Process menu;

(b) using thresholding of each color channel at gray value corresponding to a misorientation of 60°;

(c) channels re-arranged: Red = misN; Green = misE; Blue = misH, and inverted.
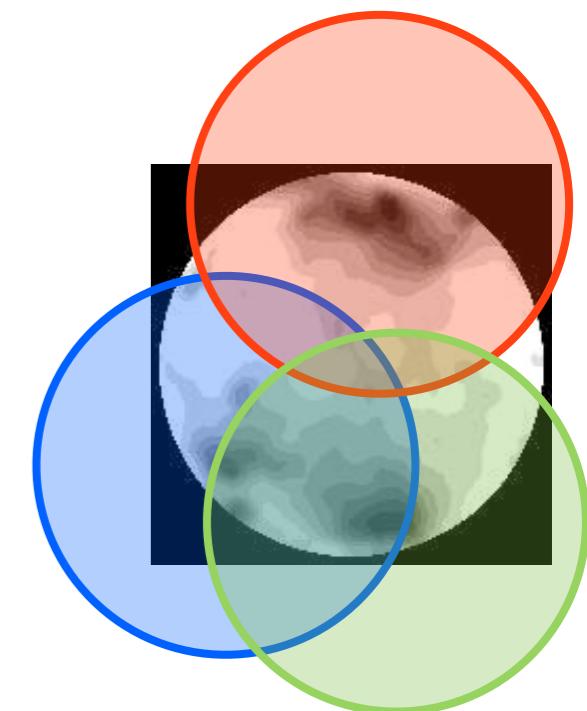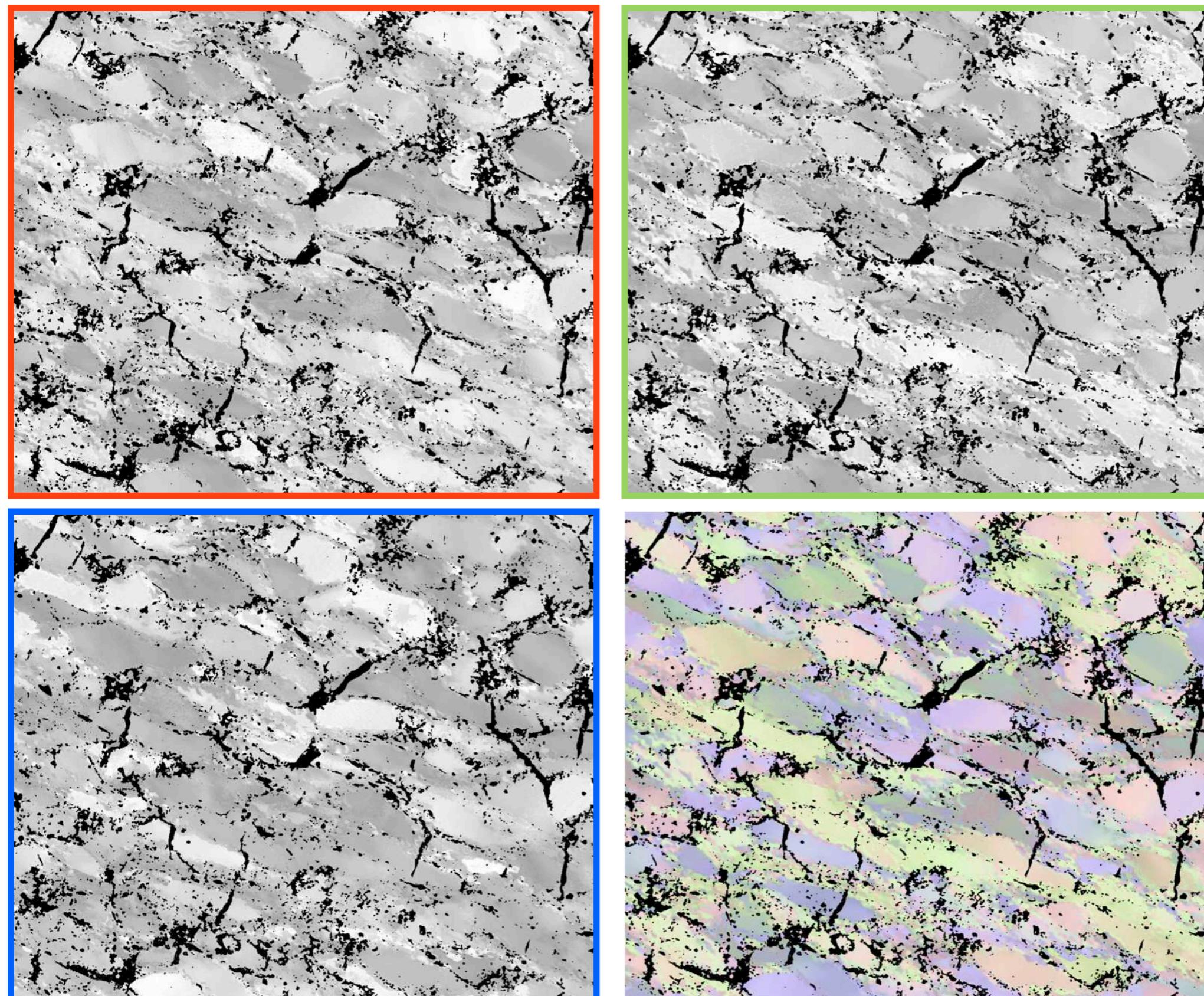
Figure 23.15

Orientation image from selected orientations.

The c-axis orientation image (COI) is generated by copying 3 misorientation images (MOIs) into color channels of RGB image; the reference directions correspond to the first three maxima of the pole figure:

Red = 14°/74°; Green = 167°/76°; Blue = 50°/104°; cones of 90° misorientation are indicated schematically on pole figure.

Note pale colors of COI (lower right): due to small range of misorientation, only 90 (of 256) gray values are used.
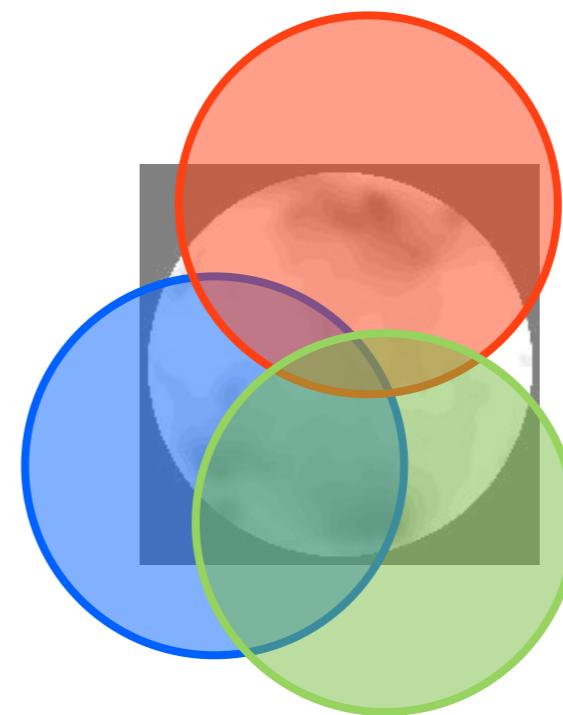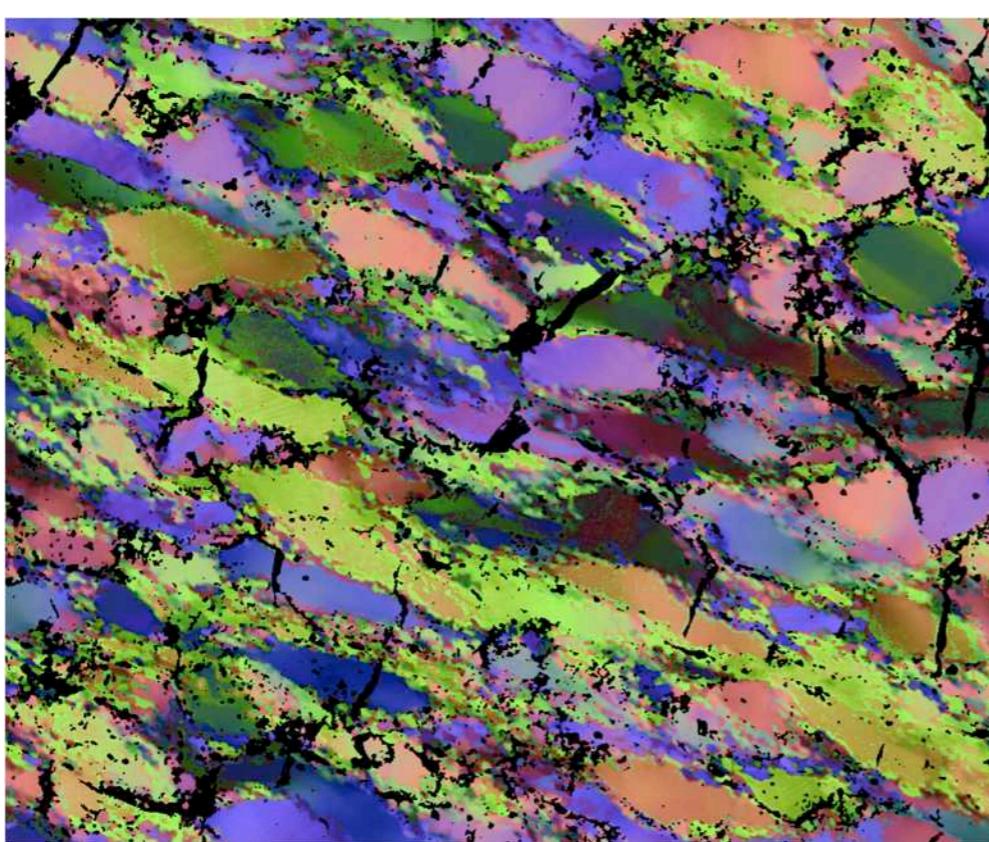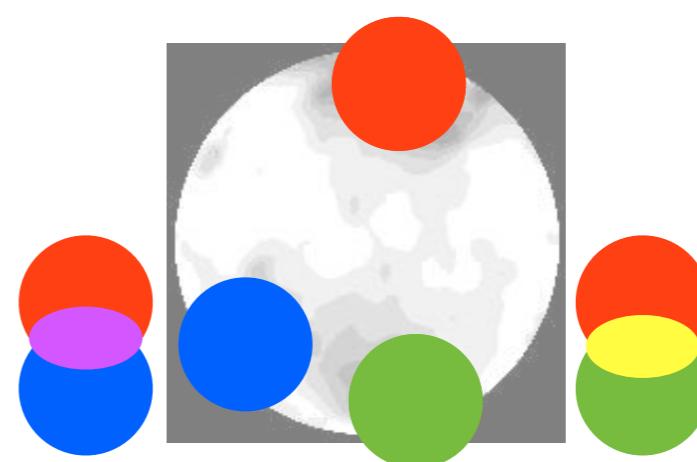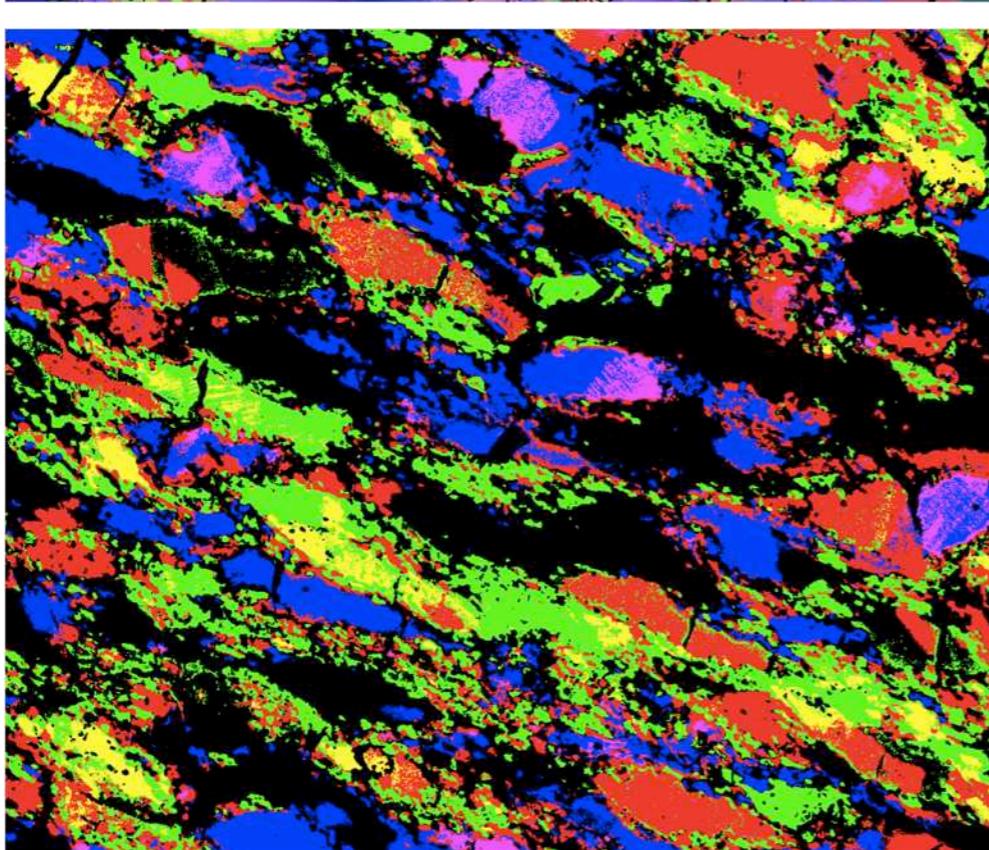
Figure 23.16
Orientation image from enhanced selected orientations.
Same COI as Figure 22.15:
(a) using 'Enhance Contrast' command in Process menu;
(b) thresholding each color channel at gray value corresponding to a misorientation of 30°; misorientation coloring indicated schematically on pole figures on right.
Note that steep axes (low inclinations) appear black because all 3 maxima are near periphery.
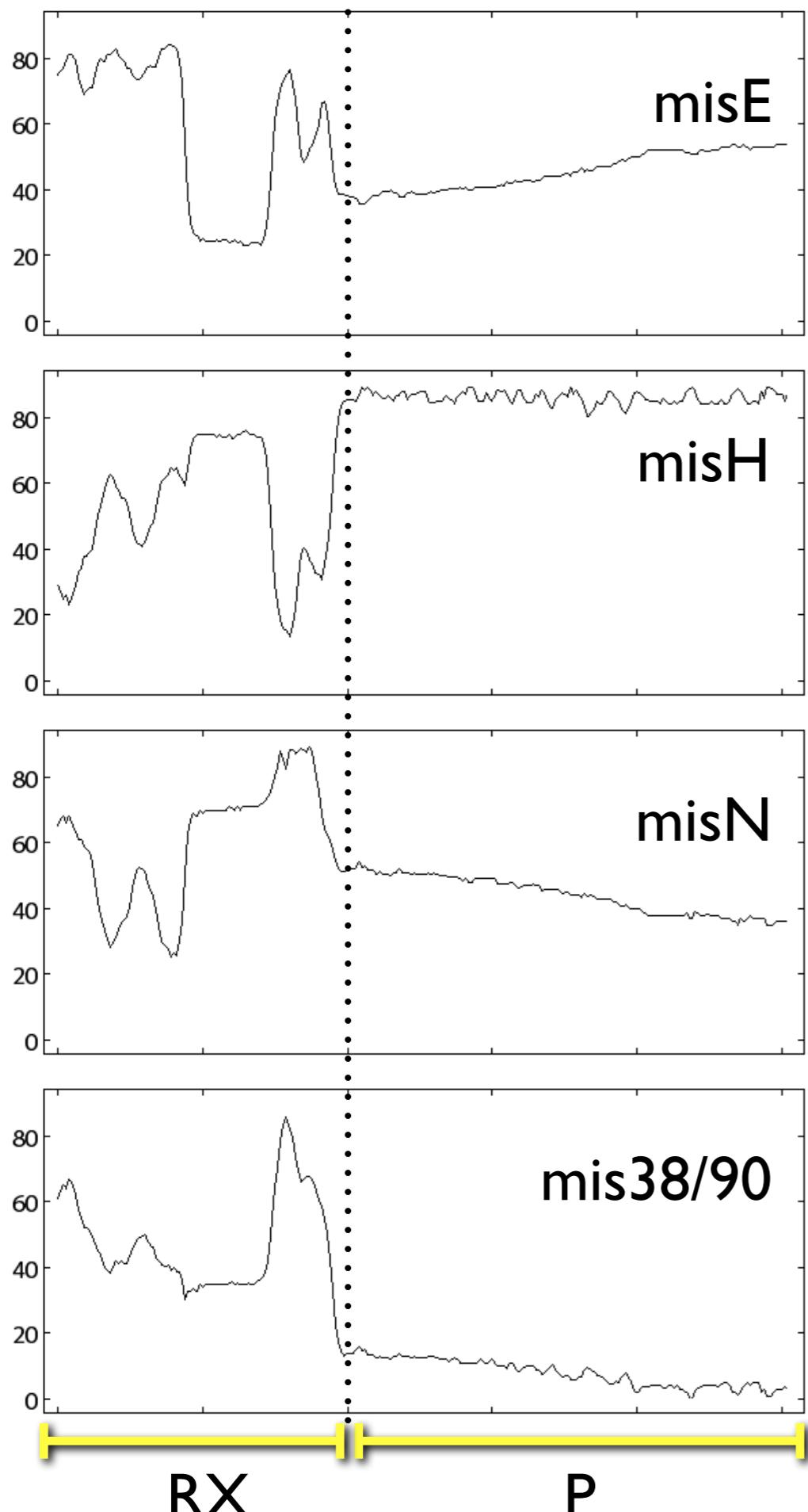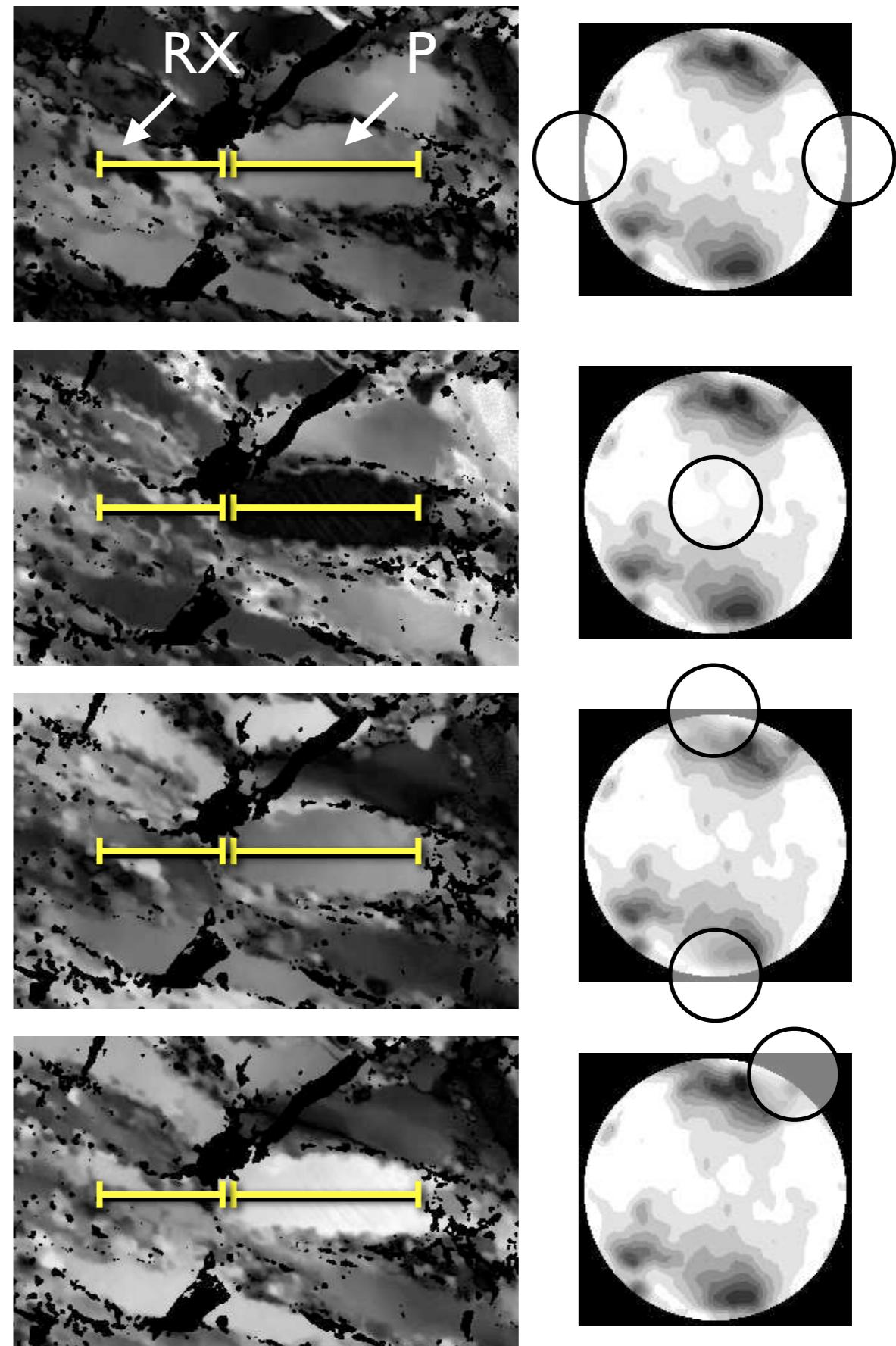
Figure 23.17
Misorientation profiles.
(a) Profiles on misorientation images (MOI) across recrystallized grains (RX) and porphyroclast (P);
(b) contrast-enhanced MOI; traces indicated; reference directions indicated on pole figure on right; misorientations are: with respect to East (misE), Heaven (misH), North (misN) and with respect to (38° / 90°) = c-axis orientation of porphyroclast.
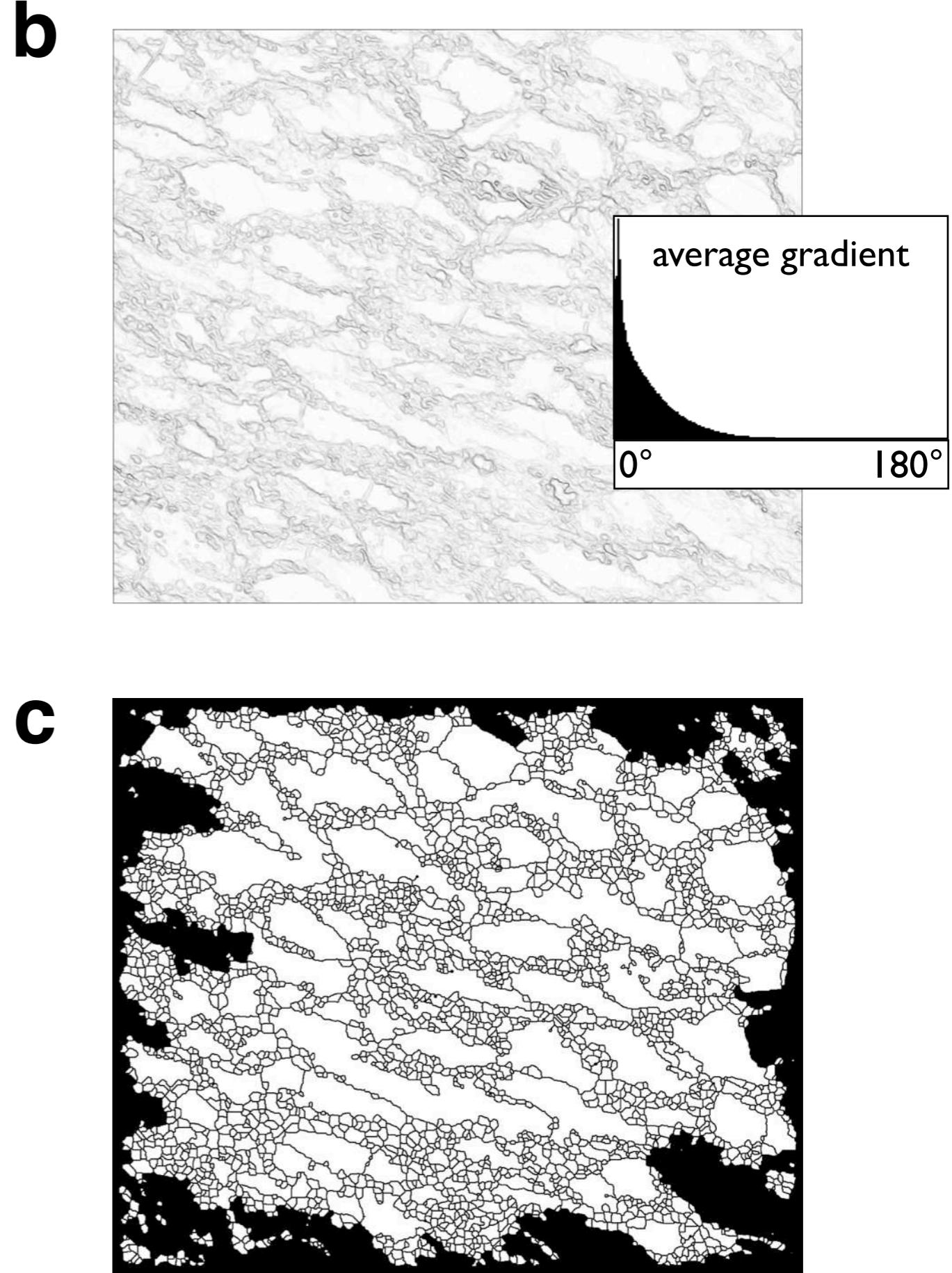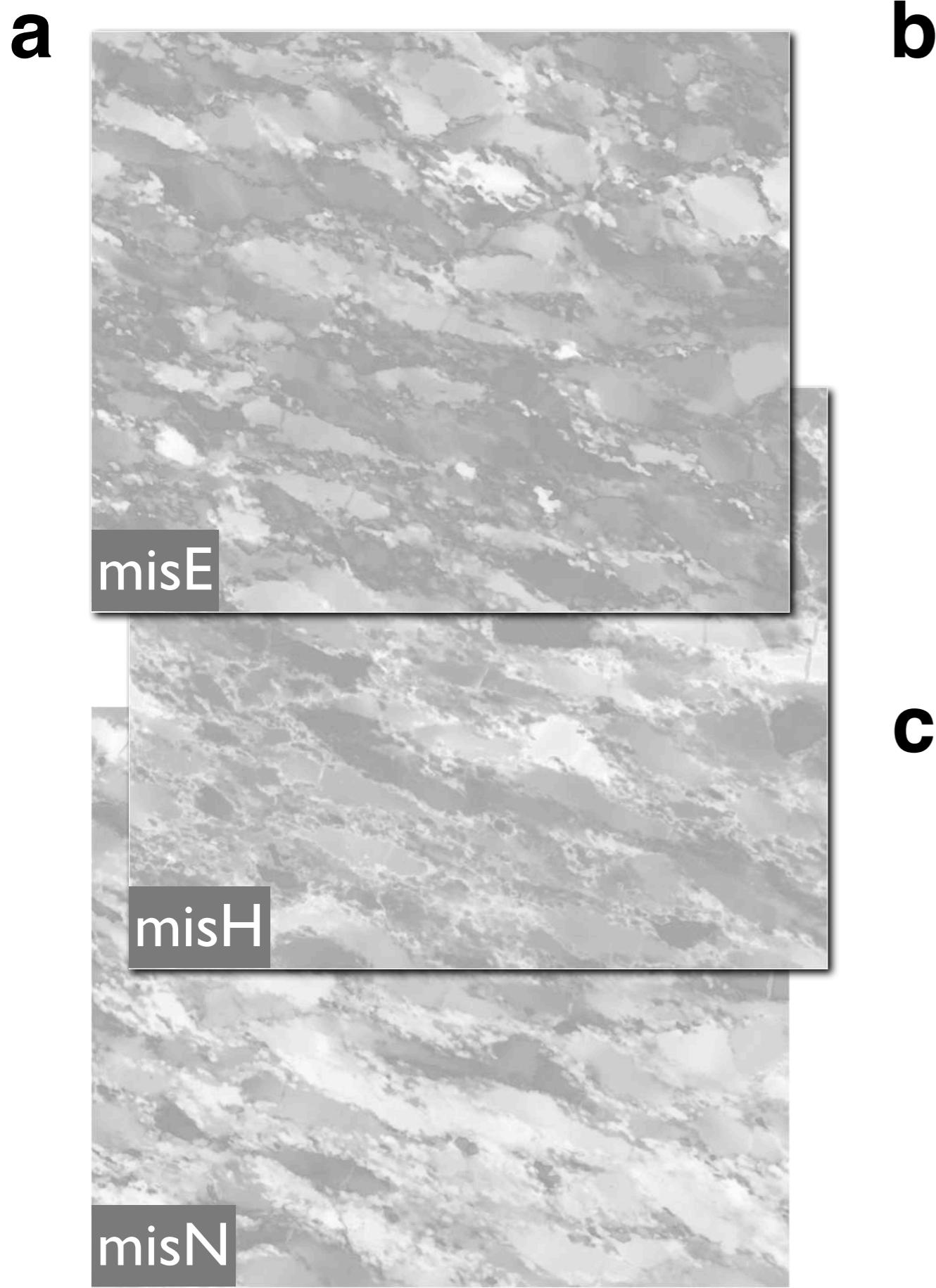
Figure 23.18

Grain boundaries from misorientation images.

(a) Stack of principal misorientation images (MOIs): misE (with respect to to East); misH (with respect to to Heaven); misN (with respect to to North);

(b) edge detection using Lazy grain boundaries macro (Figure 7.19 ff, after Heilbronner 2000); grey values in histogram represent the sums of three misorientation gradients;

(c) grain boundary map.
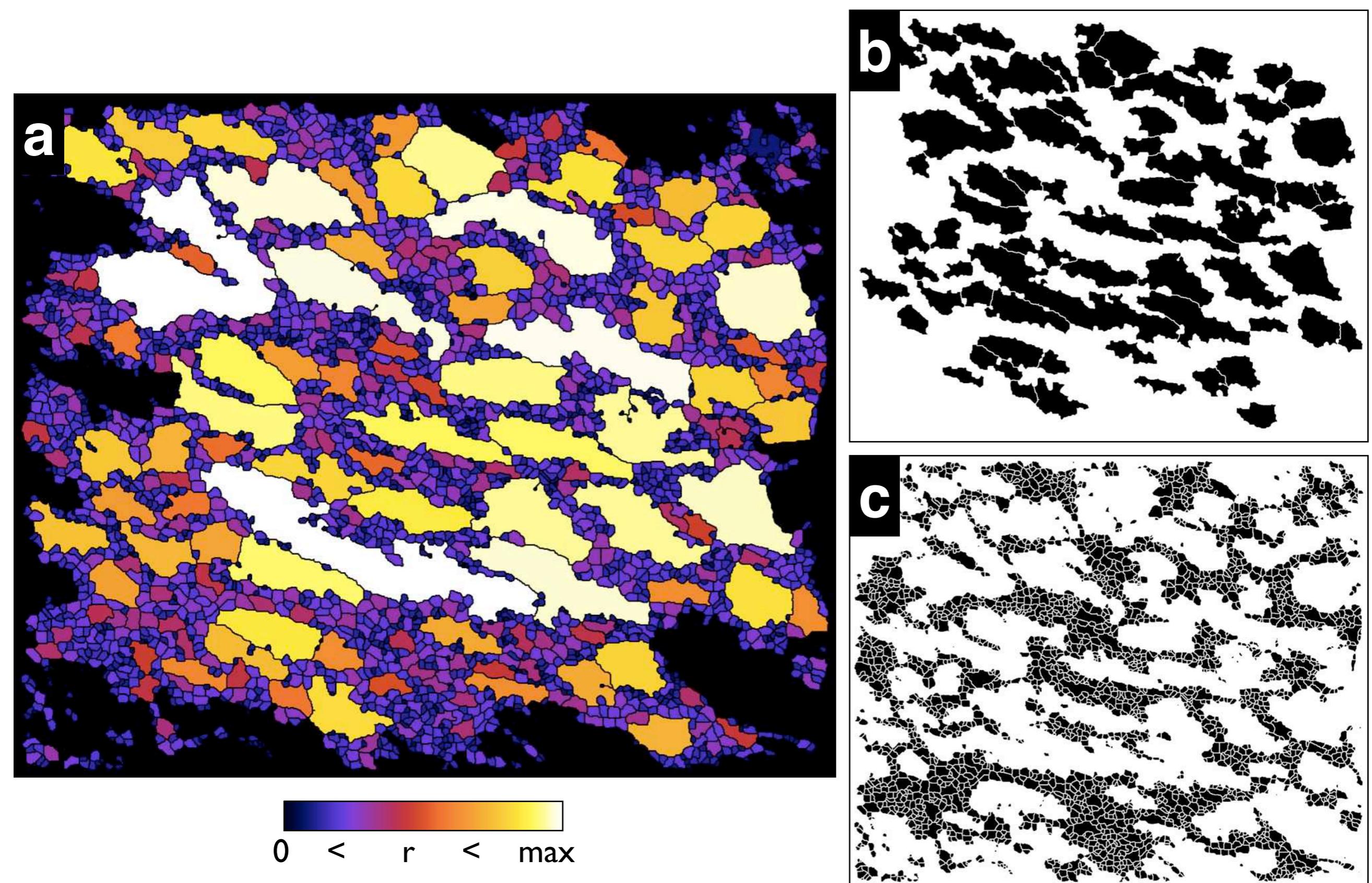
Figure 23.19
Grain size maps for masking.
(a) Grain size map of same sample as Figure 23.18, with 'Fire-2' look-up table;
(b) same as (a) thresholded for grains with radius > 30 pixel;
(c) same as (a) thresholded for grains with radius < 30 pixel.
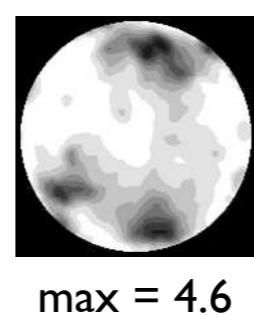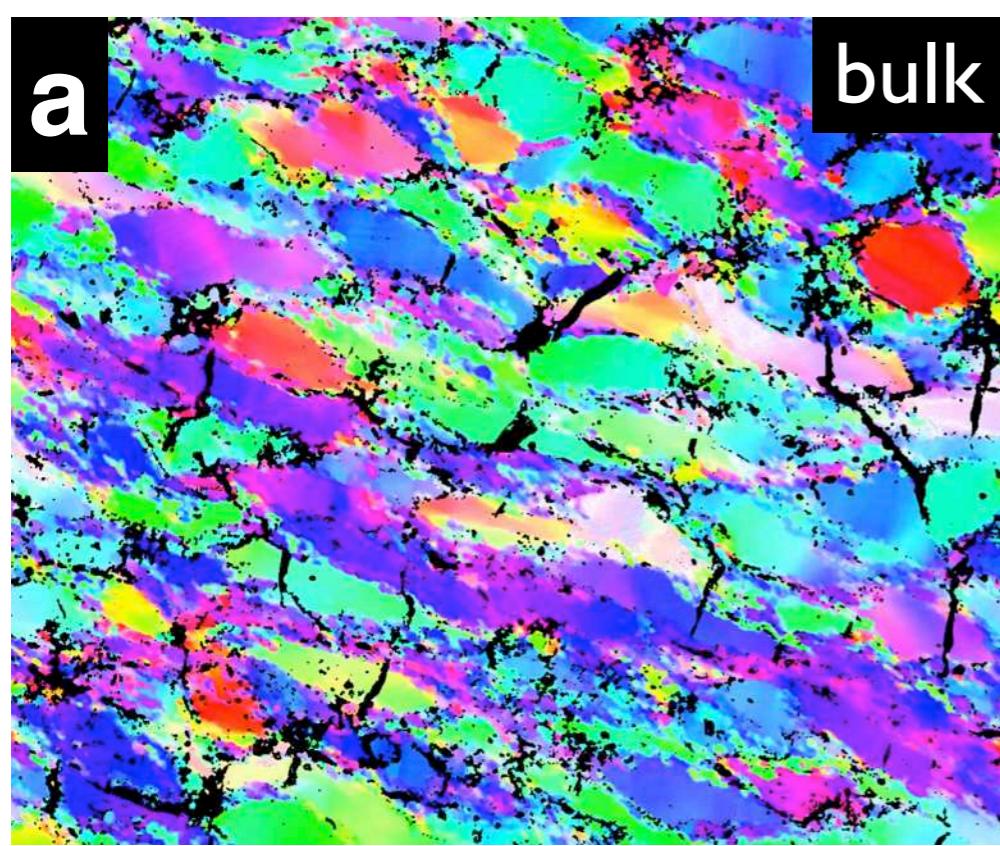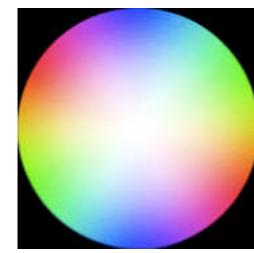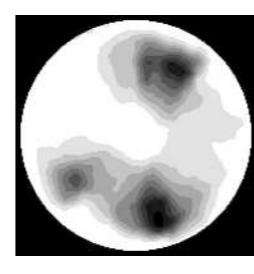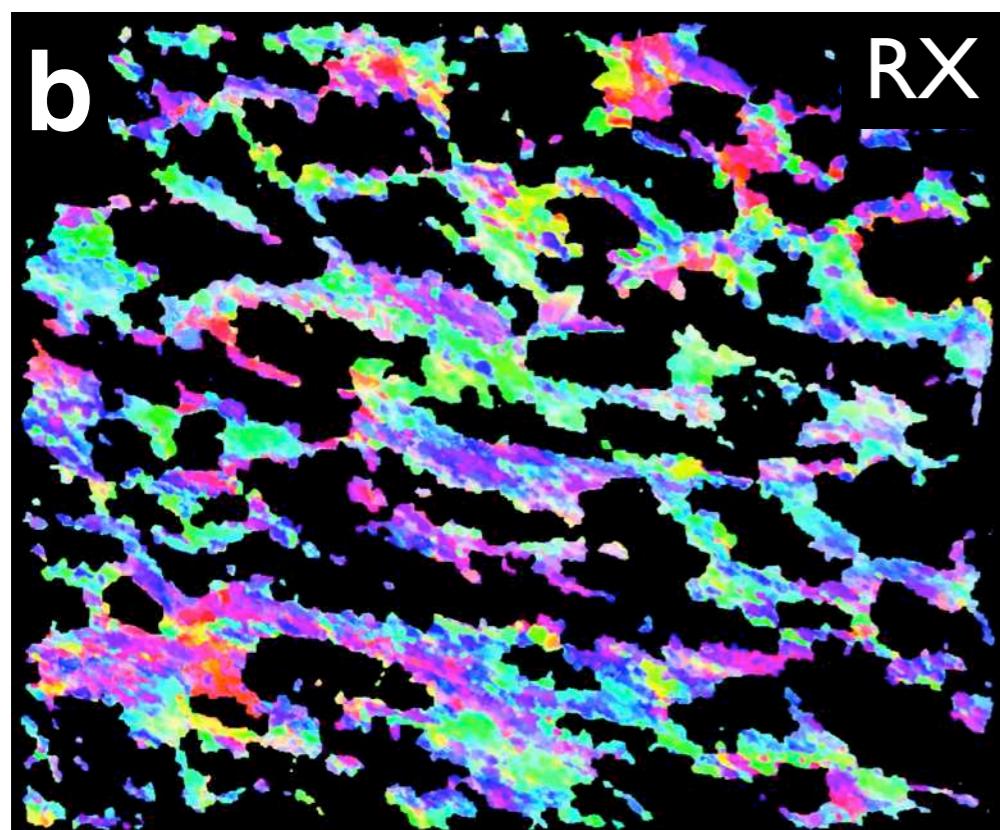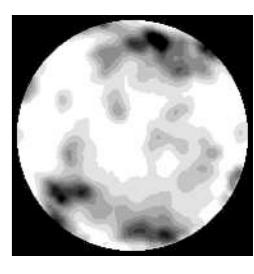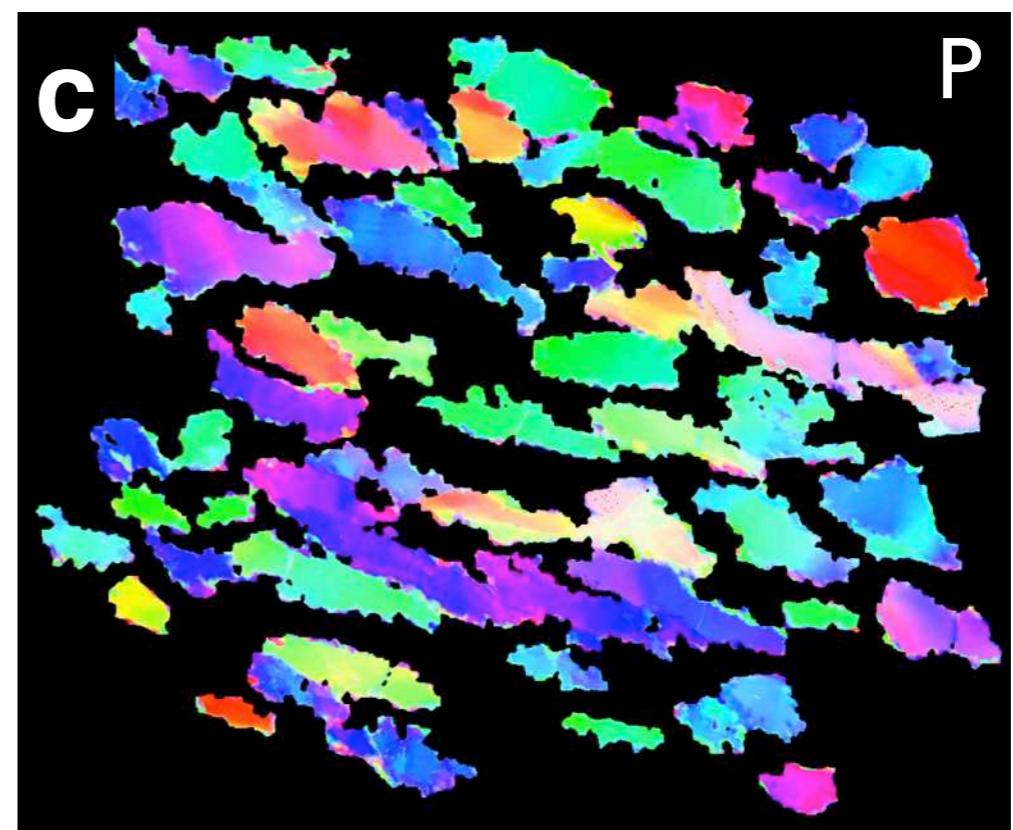
Figure 23.20
Masking for grain size.
Sample of dynamically recrystallized quartzite:
(a) c-axis orientation image (COI) of entire sample
(b) COI of recrystallized grains (RX); black = masked porphyroclasts;
(c) COI of remaining porphyroclasts (P); black = masked recrystallized grains;
corresponding pole figures indicated at lower left: contours at 0.5 increments from 0.5 - 5.0 times uniform density, measured maxima are indicated; Spectrum-CLUT color coding applies to all.
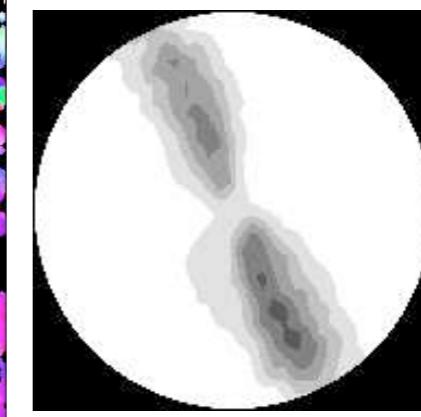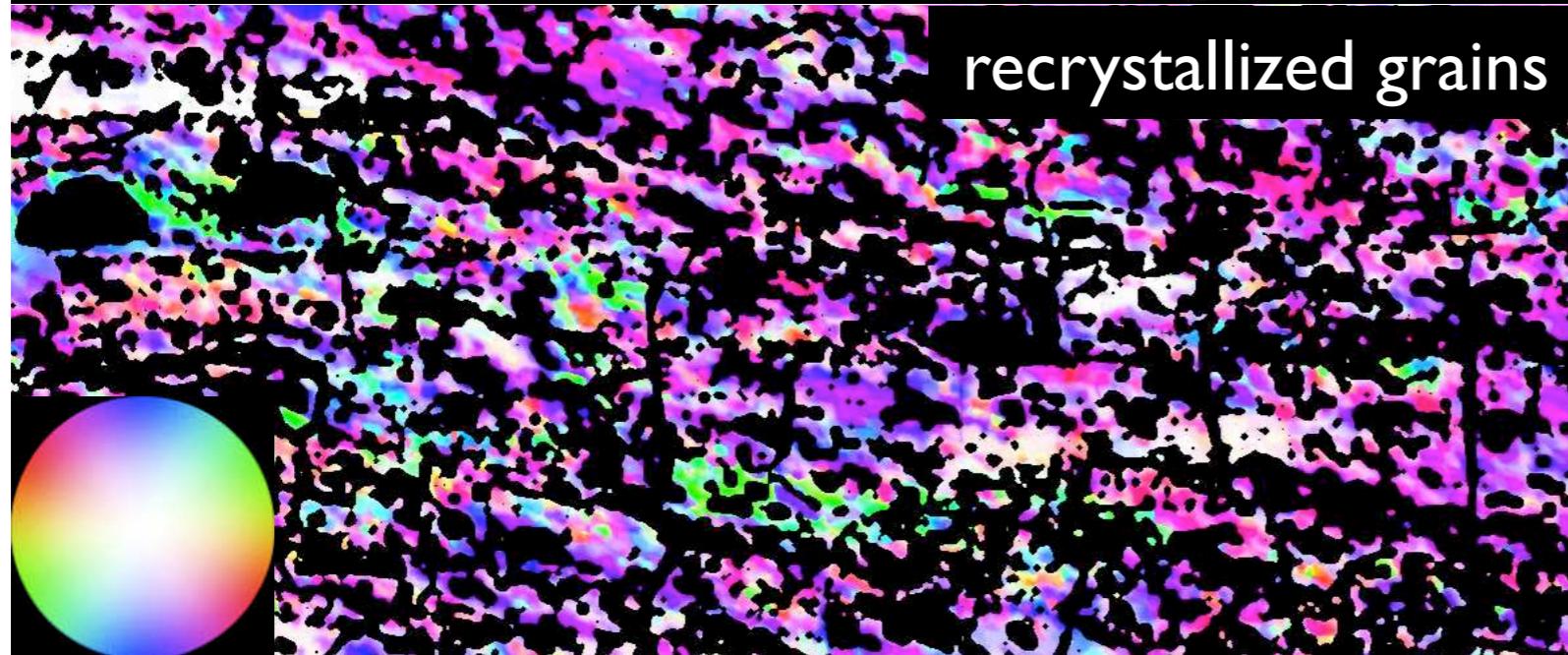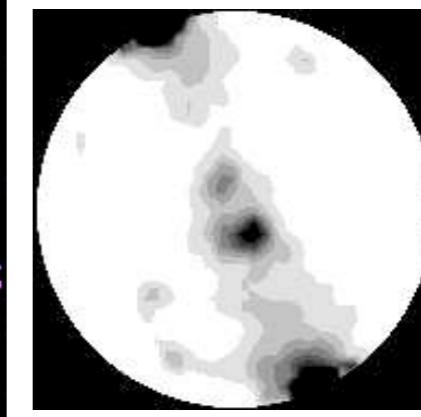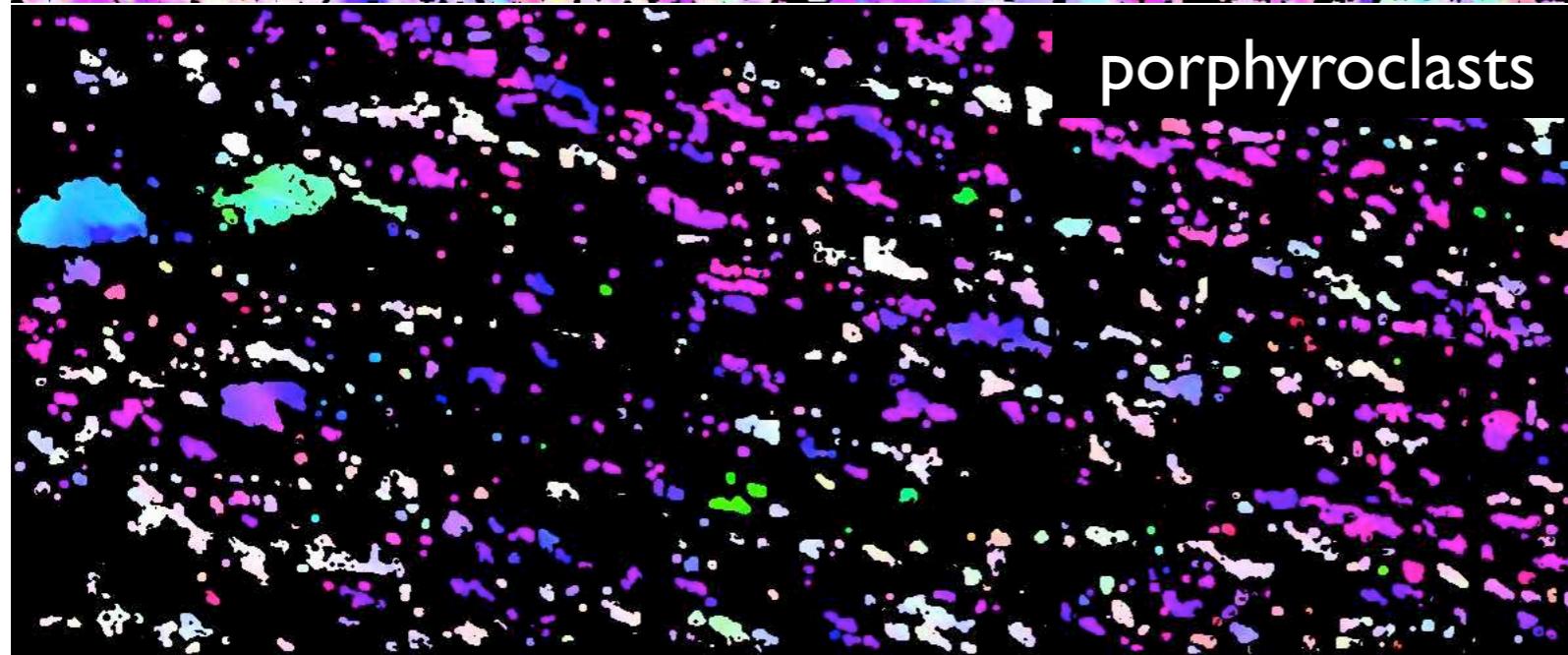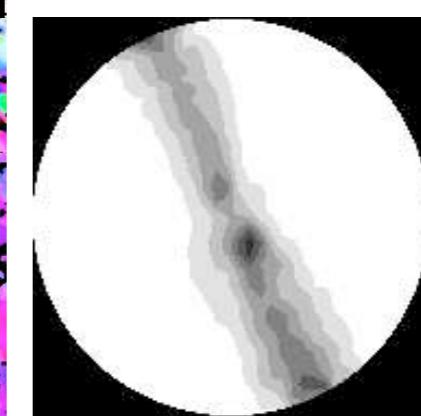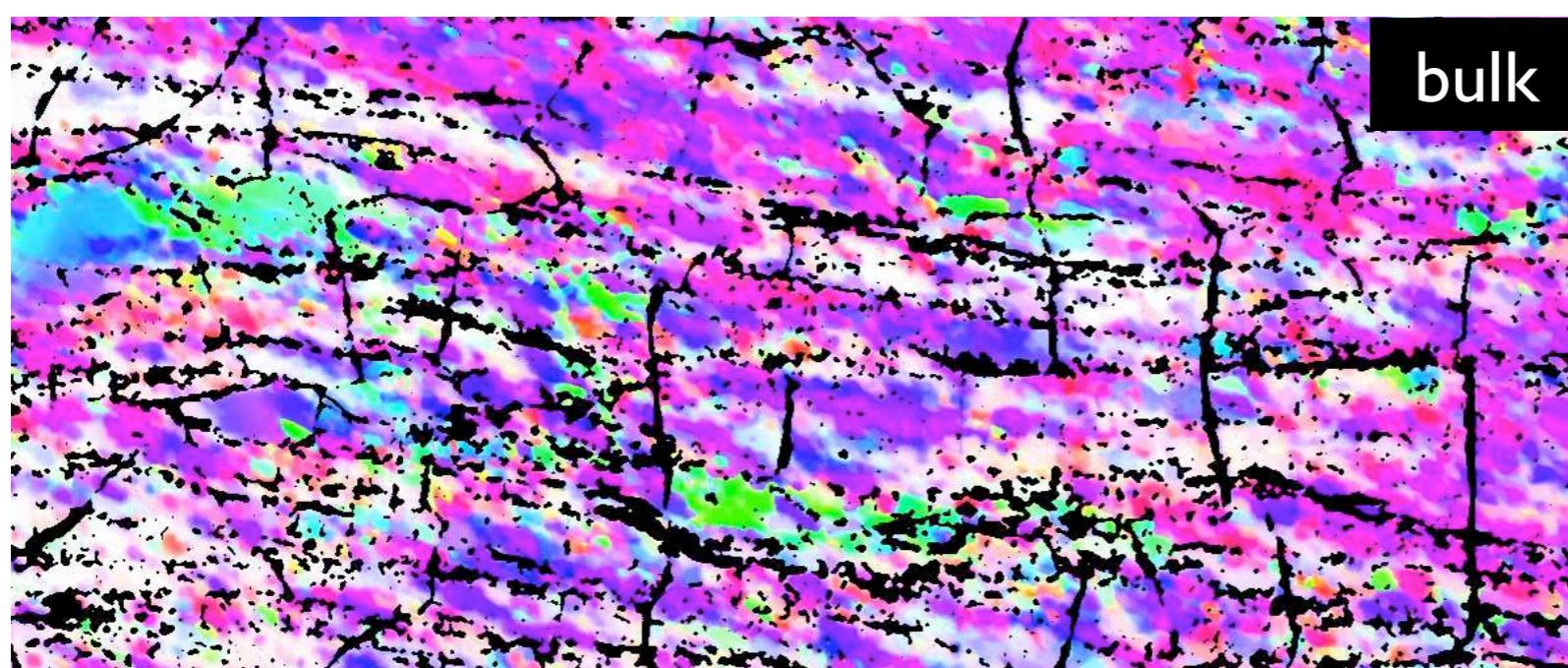
Figure 23.21
Using grain boundary density for masking.
Sample of highly deformed quartzite.
(a) Unmasked c-axis orientation image (COI) (bulk);
(b) COI of areas with low grain boundary density ≈ porphyroclasts (P); black = mask of high grain boundary density;
(c) COI of areas with high boundary density ≈ recrystallized grains (RX); black = mask of low grain boundary density;
corresponding pole figures shown on right with contours from 1.0 - 8.0 times uniform density (UD) at 1.0 x UD
increments; Spectrum-CLUT color coding applies to all.
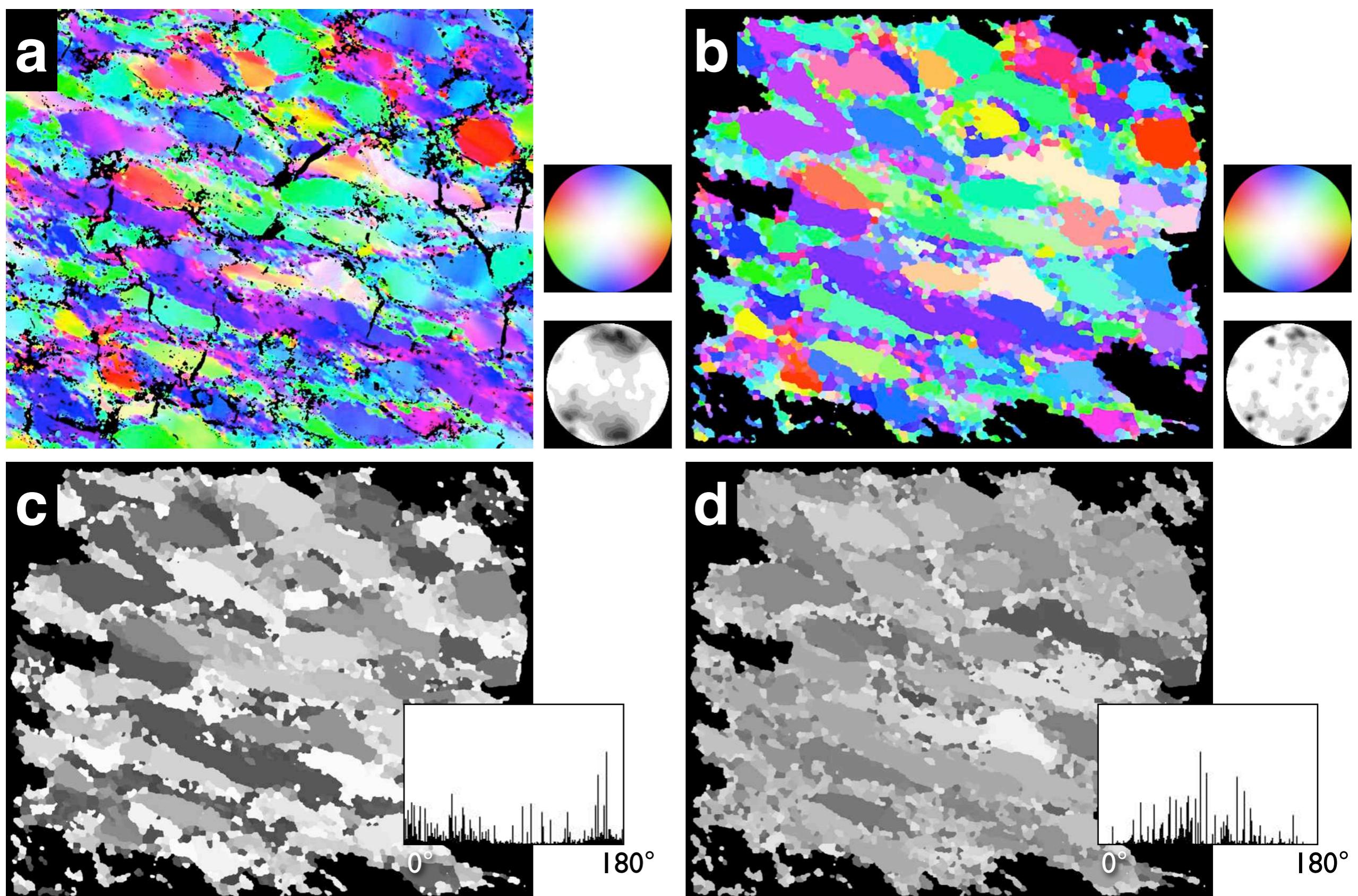
Figure 23.22
Flat grains.
From a stack of azimuth and inclination images and grain map (inverse of grain boundary map), flat grains are derived (Lazy view and handle macro).
(a) Original c-axis orientation image (COI) with pole figure;
(b) flattened COI with pole figure;
(c) flat azimuth image with histogram;
(d) flat inclination image with histogram.
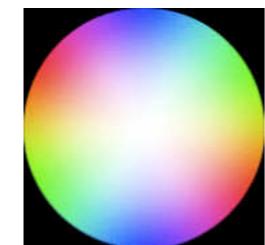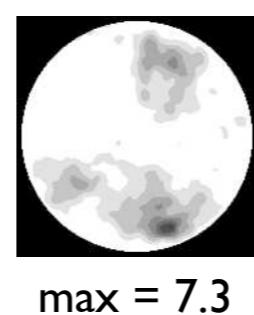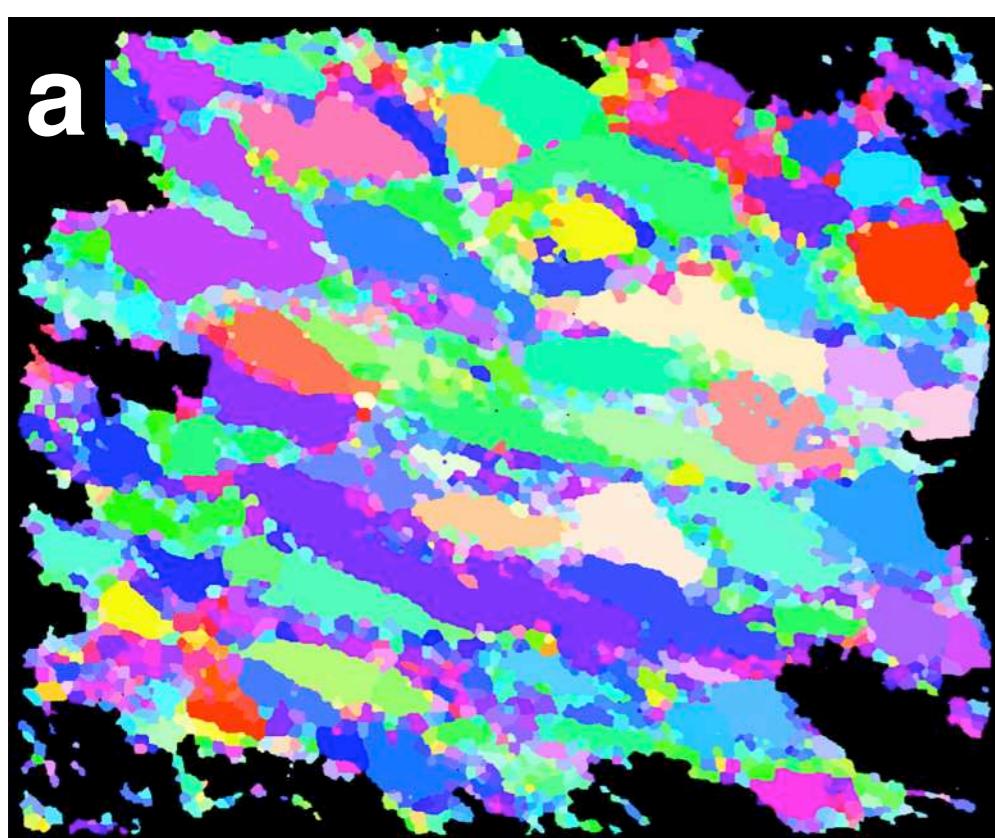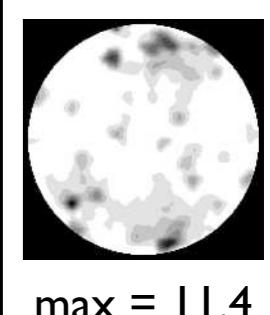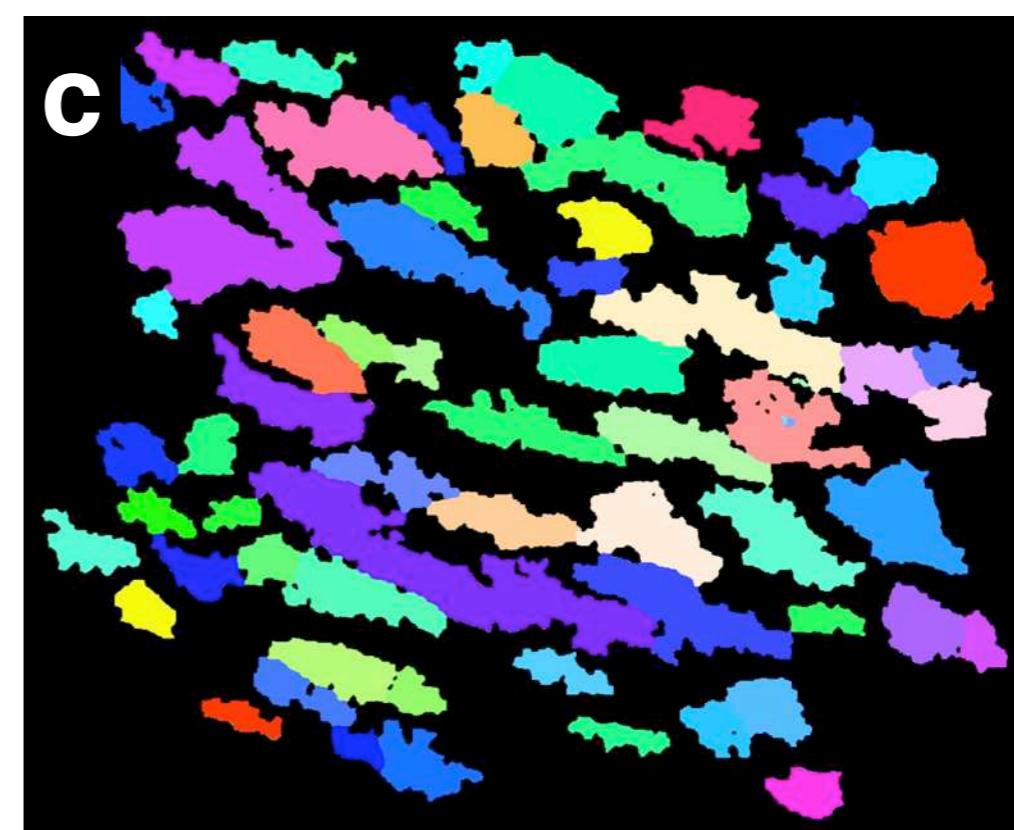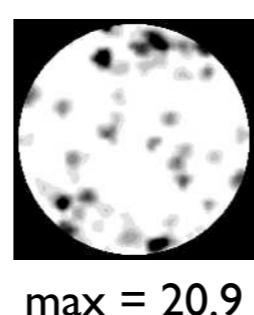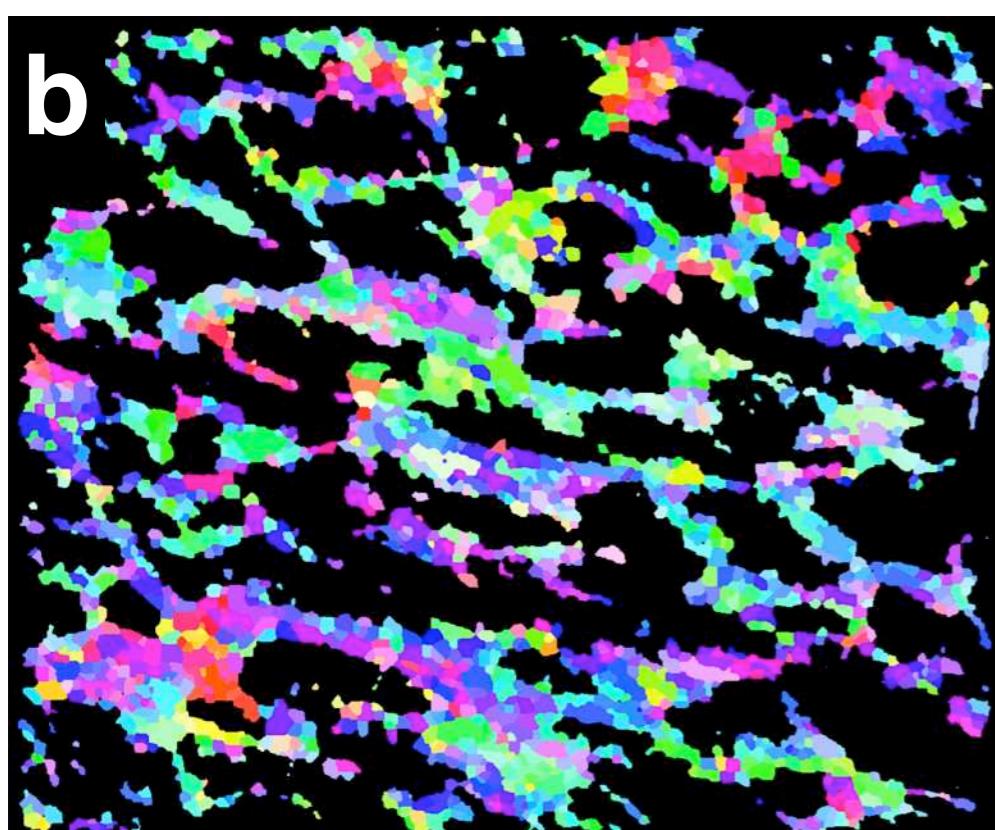
Figure 23.23
Masking flat grains for grain size.
Sample of dynamically recrystallized quartzite:
(a) flat c-axis orientation image (COI) of entire sample
(b) flat COI of recrystallized grains (RX); black = masked porphyroclasts;
(c) flat COI of remaining porphyroclasts (P); black = masked recrystallized grains;
corresponding pole figures indicated at lower left: contours at from 1 - 10 times uniform density (UD) at 1 x UD
increments, measured maxima are indicated; Spectrum-CLUT color coding applies to all.

a

circular cones 2α

α = 30°
UD = 11.6%

b

girdles 2α

α = 15°
UD = 29.4%

c
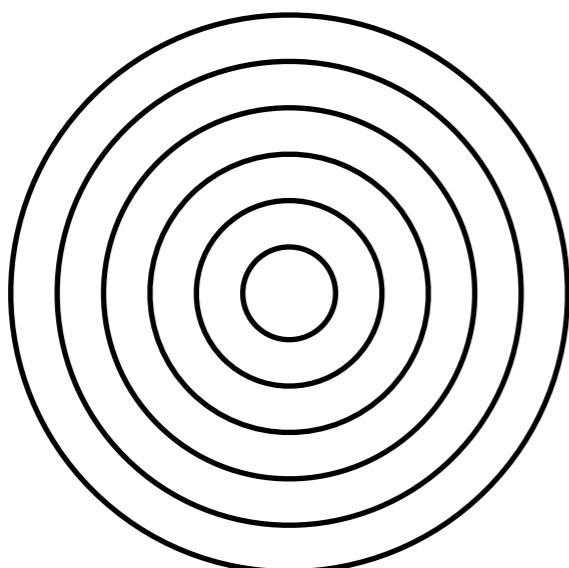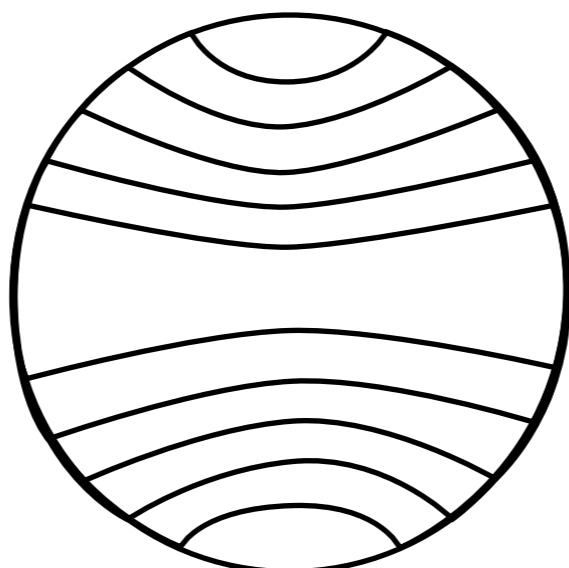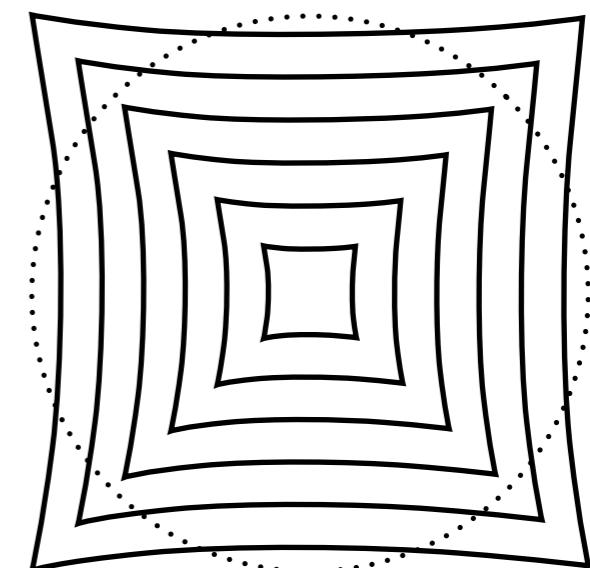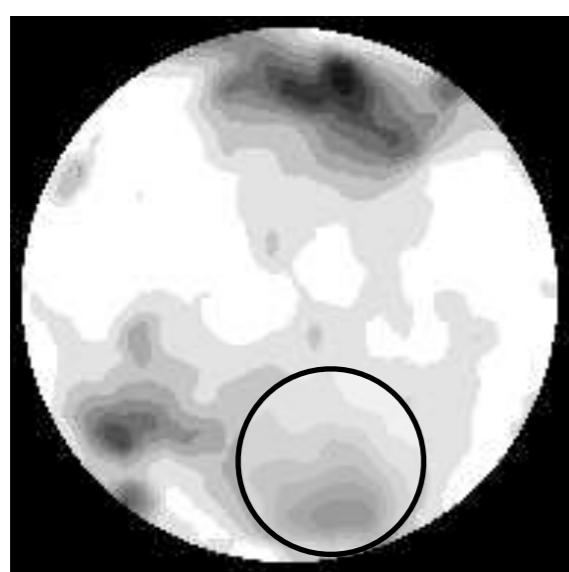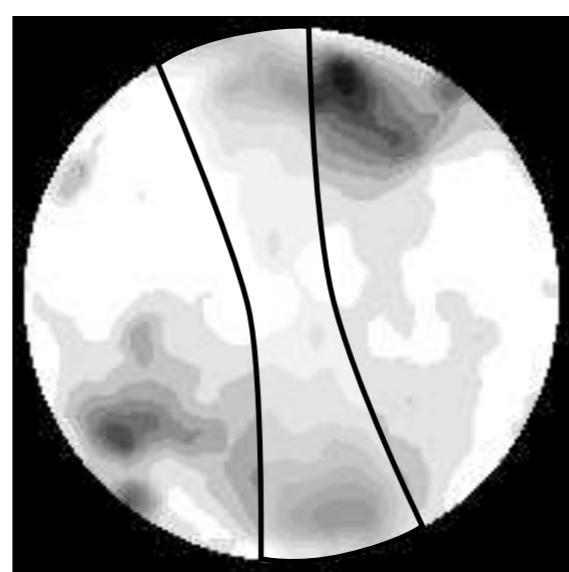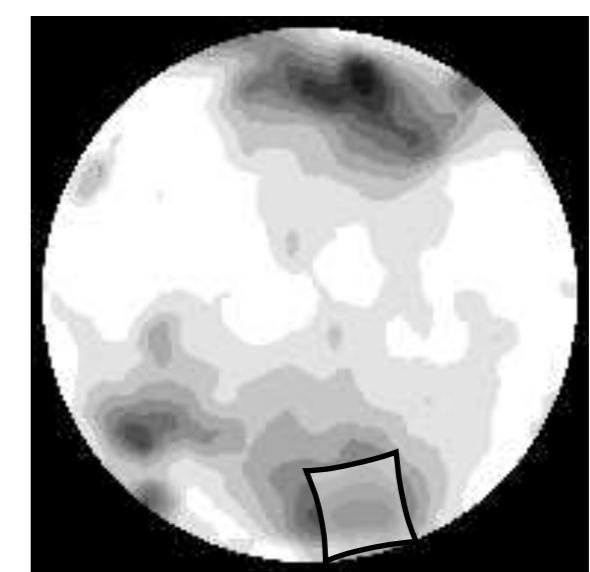
square cones α · α

α = 30°
UD = 4.9%

Figure 23.24
Texture domains.
Schematic representation of 3 types of texture domains:
(a) point maxima: circular cones with opening angle α;
(b) single girdles: 'anti-point-maxima' with half width α;
(c) intersected girdles: square cones of width α.
For each case, an example is shown and the corresponding uniform density, UD, is indicated.

angle α (°)	uniform density of point maximum	width of girdle 2α (°)	uniform density in girdle	width of cone 2α (°)	uniform density in square cone
0	0.00000	0	0.00000	0	0.00000
5	0.00325	10	0.10301	10	0.00572
10	0.01299	20	0.20123	20	0.02236
15	0.02921	30	0.29446	30	0.04908
20	0.05187	40	0.38255	40	0.08501
25	0.08093	50	0.46530	50	0.12925
30	0.11634	60	0.54258	60	0.18086
35	0.15802	70	0.61423	70	0.23887
40	0.20590	80	0.68011	80	0.30227
45	0.25989	90	0.74011	90	0.37005
50	0.31989	100	0.79410	100	0.44117
55	0.38577	110	0.84198	110	0.51454
60	0.45742	120	0.88366	120	0.58911
65	0.53470	130	0.91907	130	0.66377
70	0.61745	140	0.94813	140	0.73743
75	0.70554	150	0.97079	150	0.80899
80	0.79877	160	0.98701	160	0.87734
85	0.89699	170	0.99675	170	0.94138
90	1.00000	180	1.00000	180	1.00000

Table 23.1

Uniform densities in single maxima and girdle distributions.
The angle α denotes half of the opening angle of a single maximum or a girdle, and half of the width of a square cone.
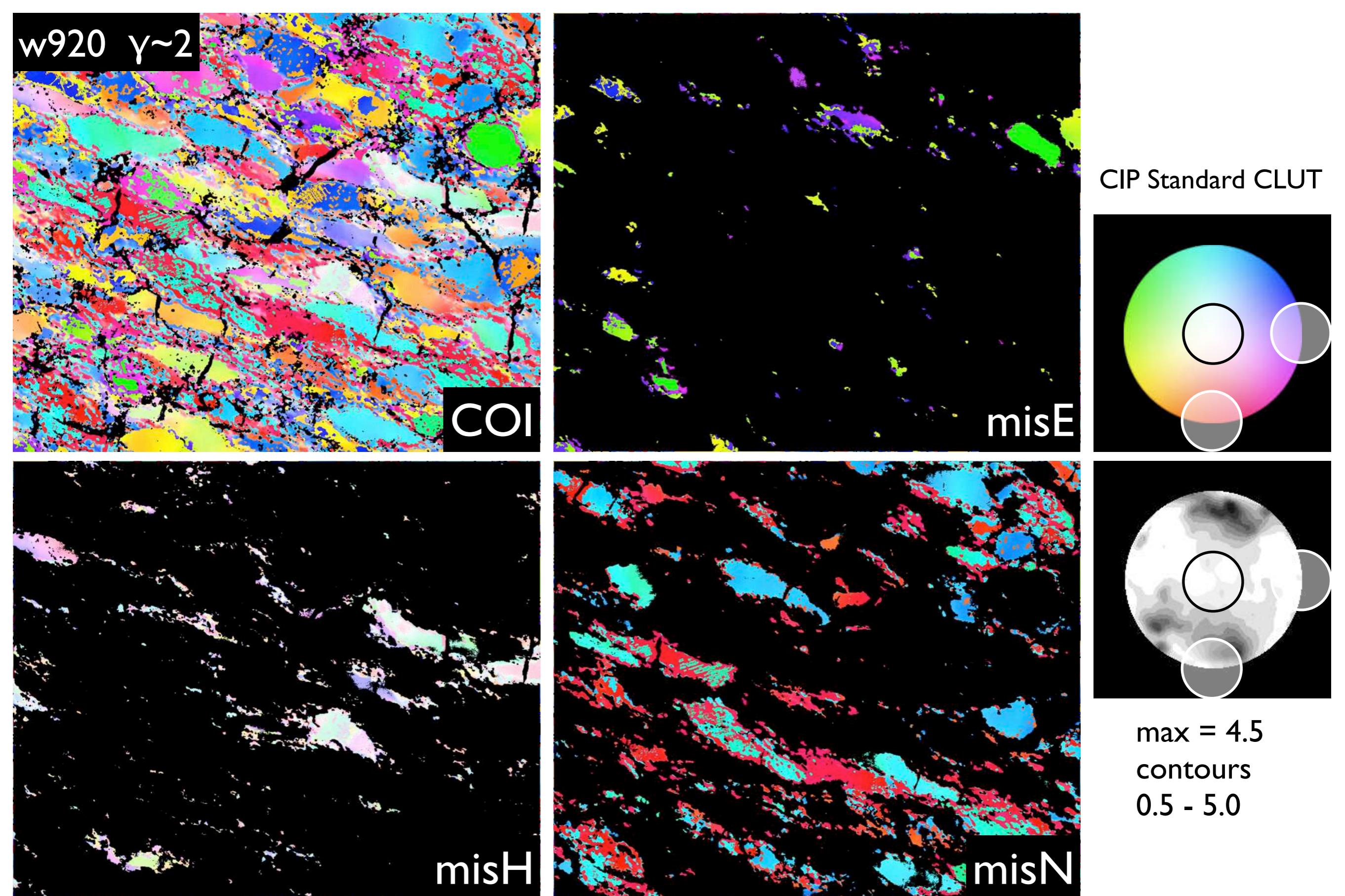
Figure 23.25
Orientation tracking I.
Low-strain sample w920: c-axis orientation image (COI) is masked using thresholded misorientation images (misE, misH, misN); threshold level = 30, i.e., cones of 30° opening angle are considered; CLUT and c-axis pole figure with schematic indication of texture domains on the right.
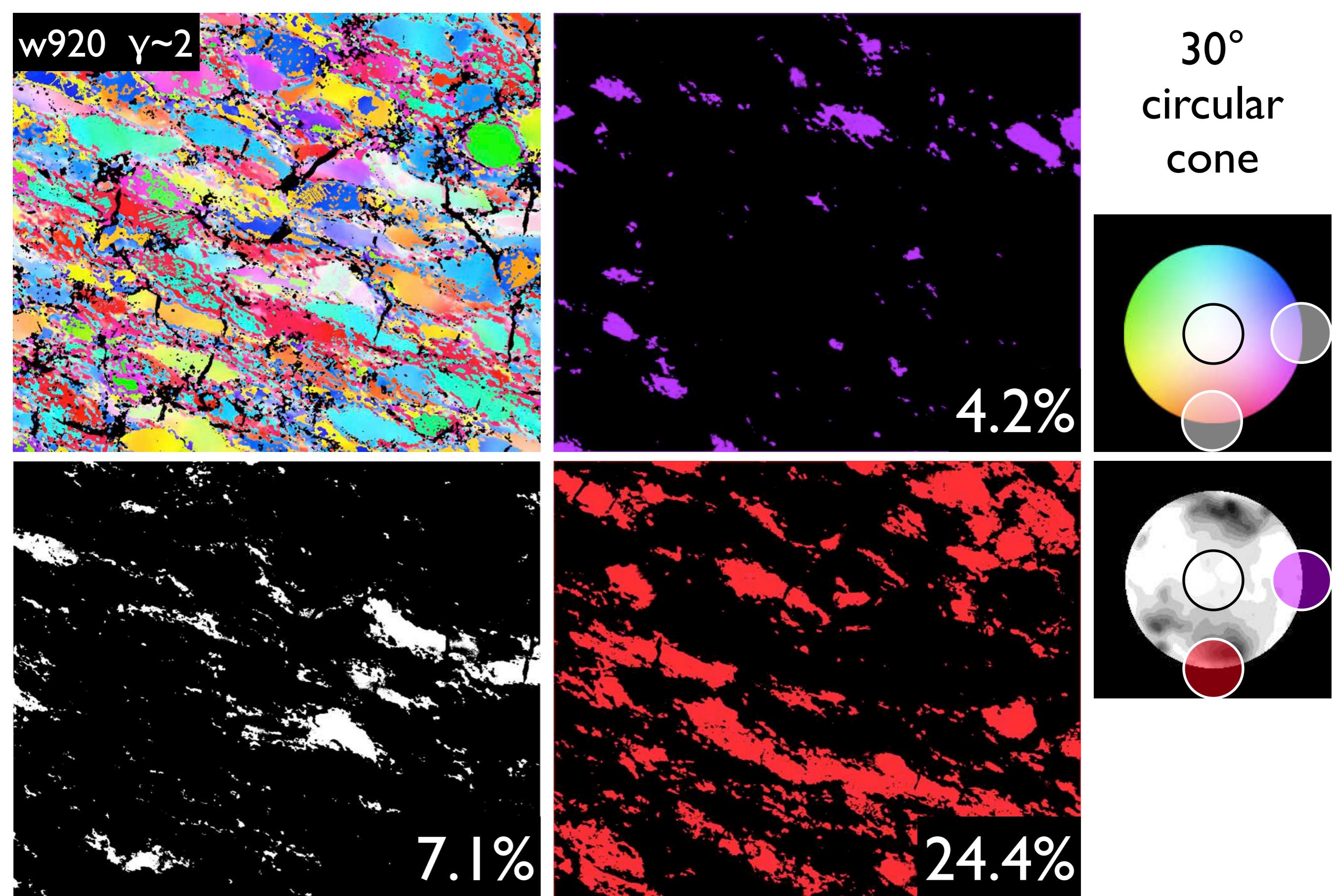
Figure 23.26
Orientation tracking II.
Low-strain sample w920: texture domains are color-coded thresholded misorientation images (misE, misH, misN);
threshold level = 30, i.e., 30° cones are considered; CLUT and c-axis pole figure with schematic indication of texture
domains on the right.
Measured area fraction of each domain is indicated, uniform density (UD) for 30° cone is 11.6%. Enrichment in domains
is: 0.4 x, 0.6 x and 2.1 x.
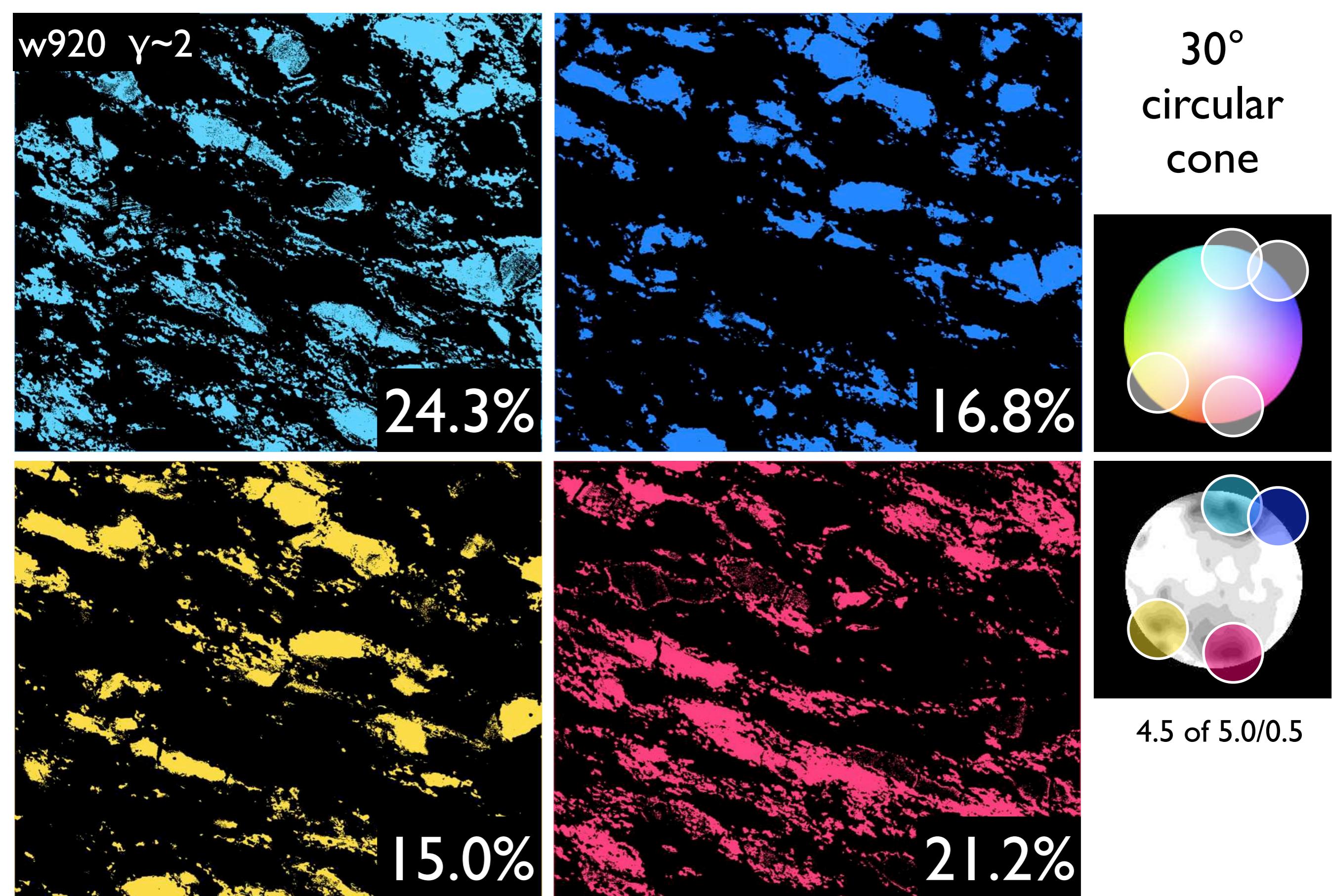
Figure 23.27

Orientation tracking III.

Low-strain sample w920: texture domains are shown as color-coded thresholded misorientation images (with respect to 4 pole figure maxima); threshold level = 30, i.e., 30° cones are considered; CLUT and c-axis pole figure with schematic indication of texture domains on the right.

Measured area fraction of each domain is indicated, uniform density (UD) for 30° cone is 11.6%. Enrichment in domains is: 2.0 x, 1.4 x UD, 1.3 x and 1.8 x.
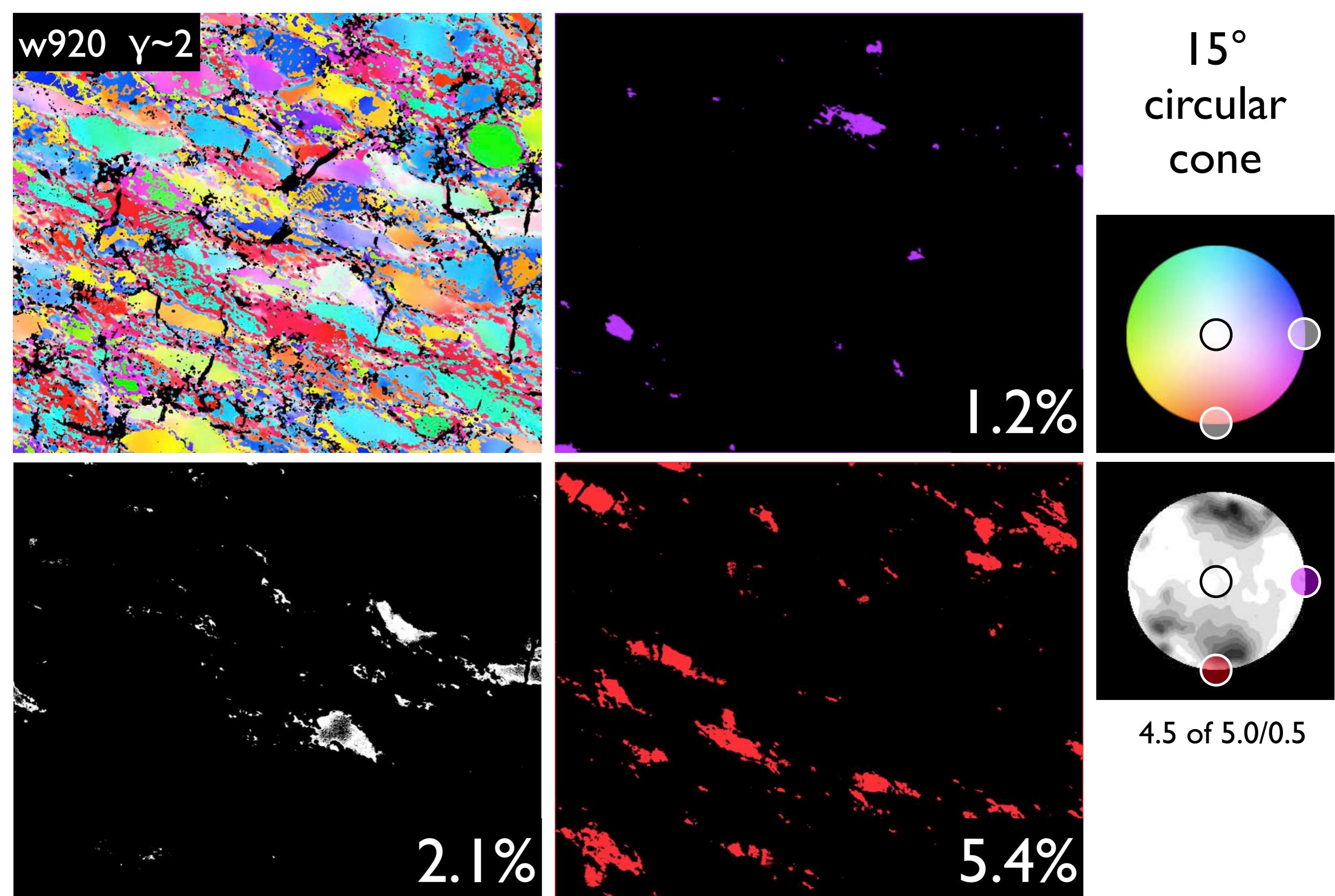
Figure 23.28
Orientation tracking IV.
Low-strain sample w920: texture domains are color-coded thresholded misorientation images (misE, misH, misN); threshold level = 15, i.e., 15° cones are considered; CLUT and c-axis pole figure with schematic indication of texture domains on the right.
Measured area fraction of each domain is indicated, uniform density (UD) for 15° cone is 2.9%. Enrichment in domains is: 0.4 x, 0.7 x and 1.9 x.
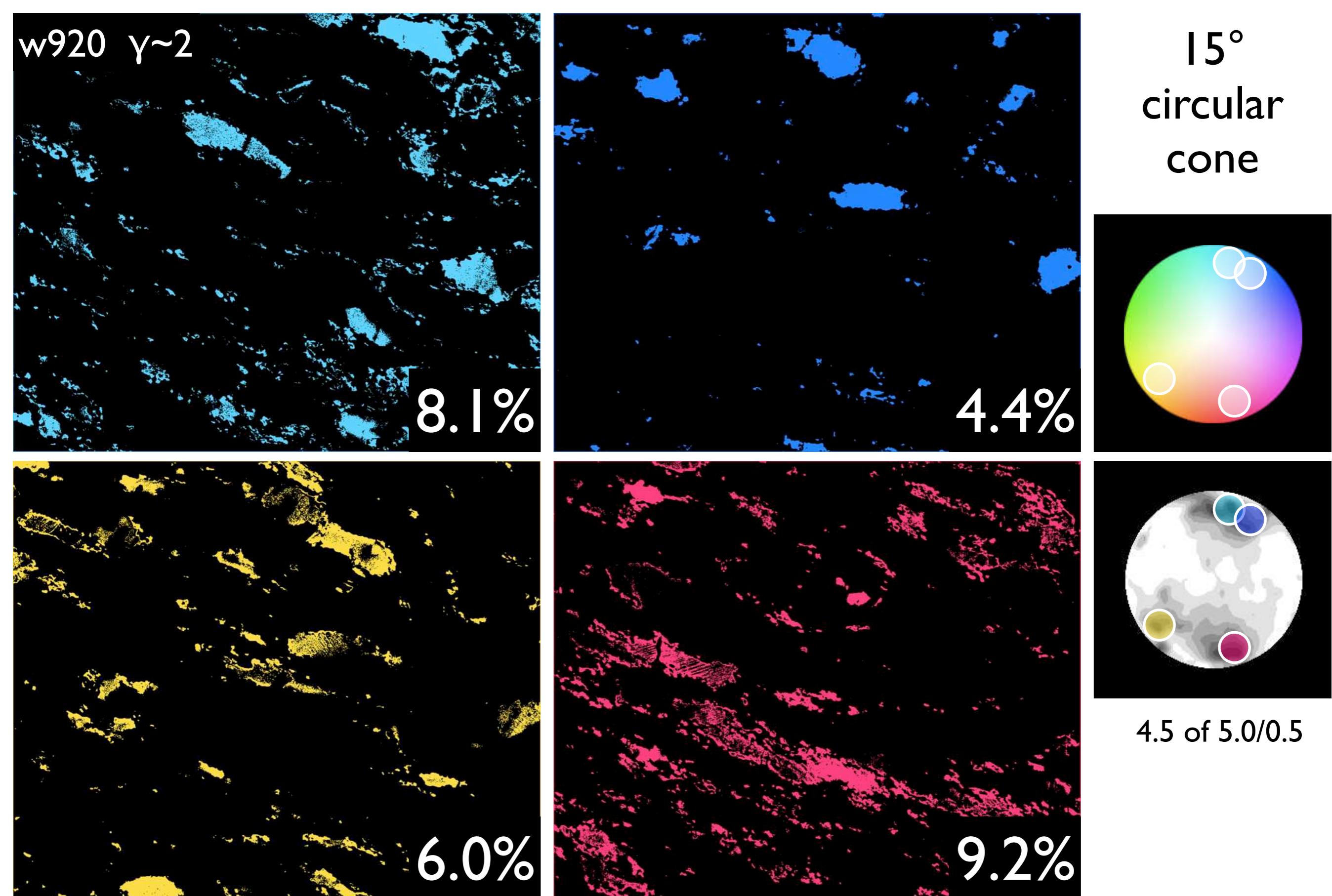
Figure 23.29
Orientation tracking V.
Low-strain sample w920: texture domains are shown as color-coded thresholded misorientation images (with respect to 4 pole figure maxima); threshold level = 15, i.e., 15° cones are considered; CLUT and c-axis pole figure with schematic indication of texture domains on the right.
Measured area fraction of each domain is indicated, uniform density (UD) for 15° cone is 2.9%. Enrichment in domains is: 2.8 x, 1.5 x, 2.1 x and 3.2 x.
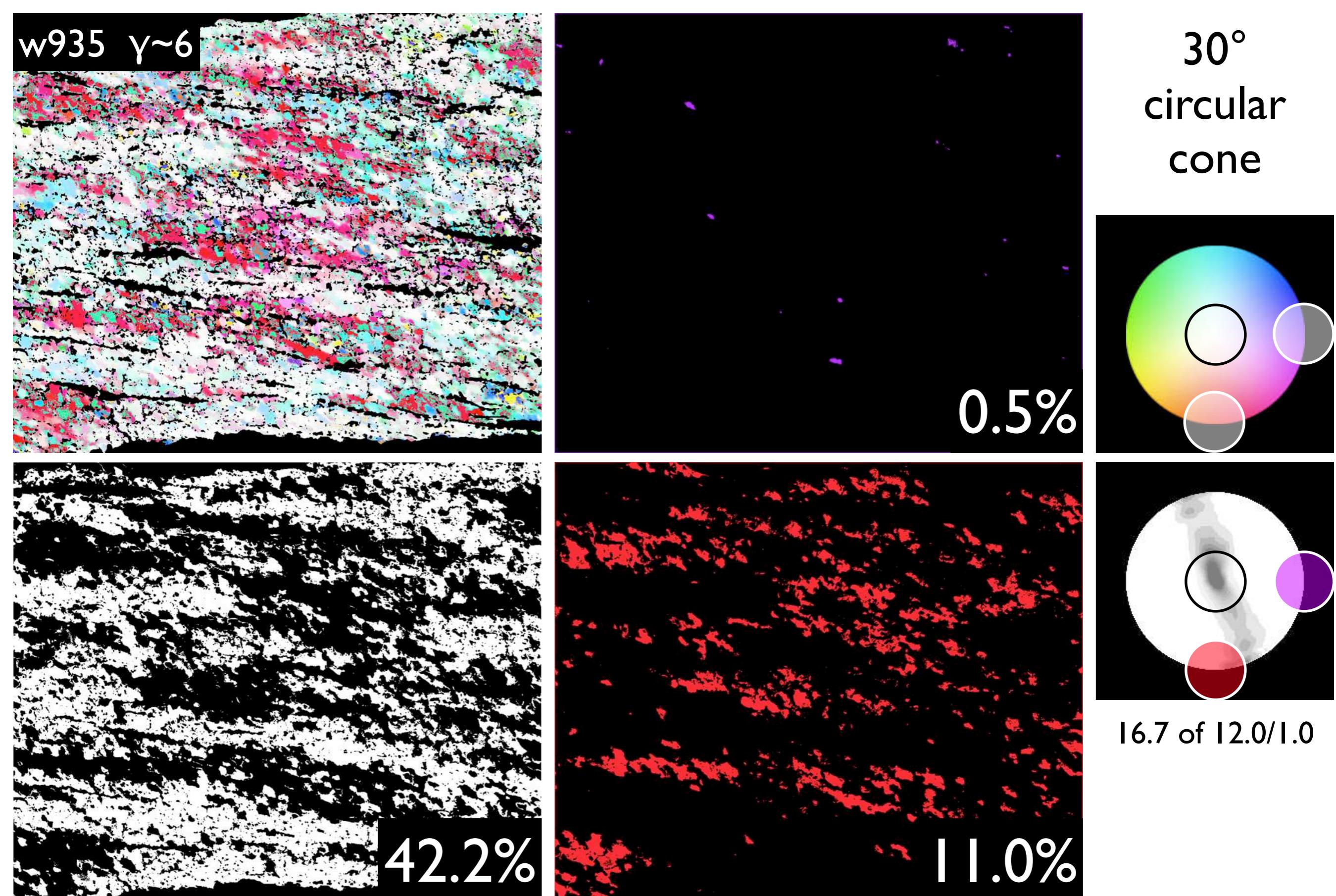
Figure 23.30
Orientation tracking VI.
High-strain sample w935: texture domains are color-coded thresholded misorientation images (misE, misH, misN); threshold level = 30, i.e., 30° cones are considered; CLUT and c-axis pole figure with schematic indication of texture domains on the right.
Measured area fraction of each domain is indicated, uniform density (UD) for 30° cone is 11.6%. Enrichment in domains is: 0.0 x, 3.6 x and 0.9 x.
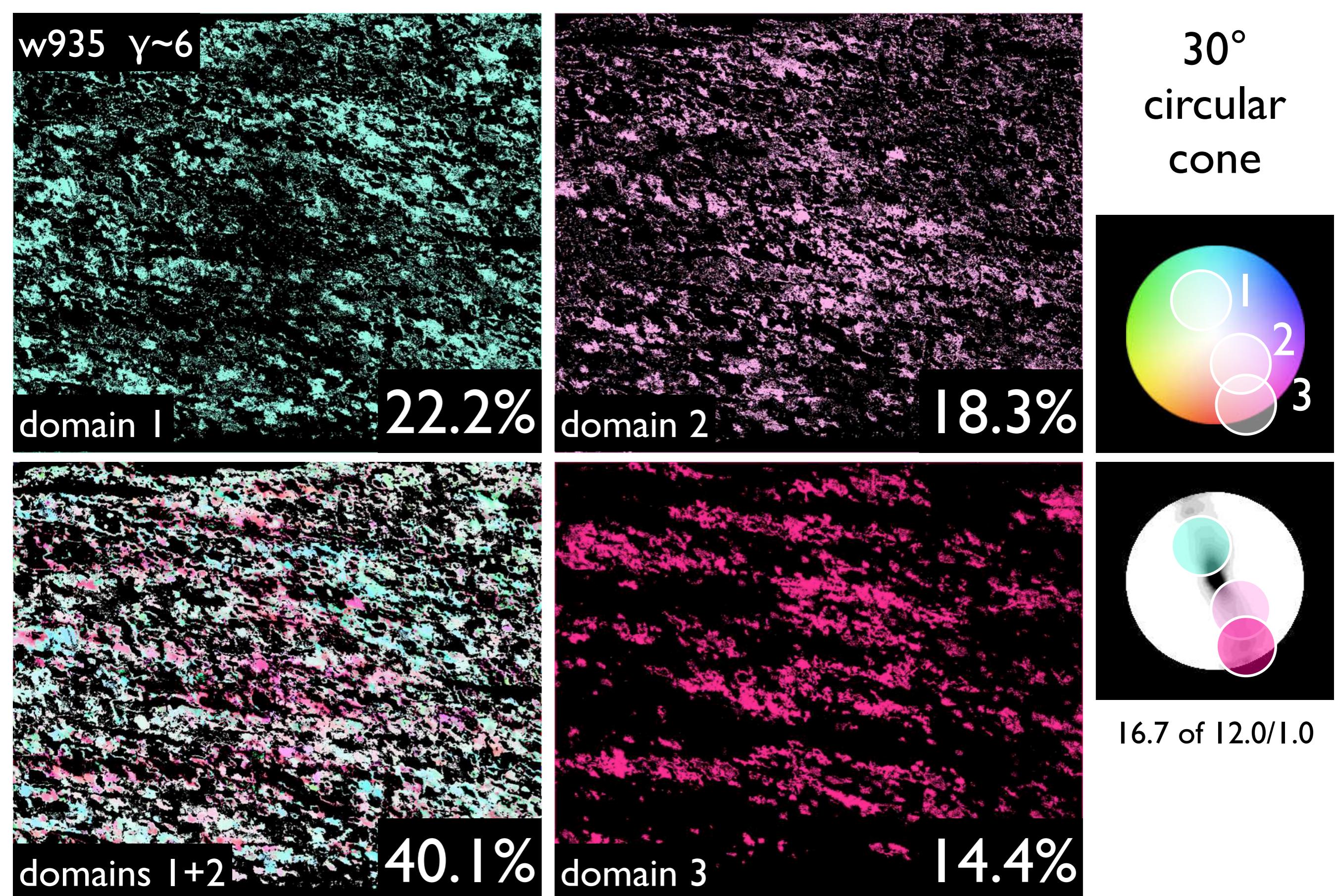
Figure 23.31

Orientation tracking VII.

High-strain sample w935: texture domains are shown as color-coded thresholded misorientation images (with respect to 3 pole figure maxima and a combination of 2); threshold level = 30, i.e., 30° cones are considered; CLUT and c-axis pole figure with schematic indication of texture domains on the right.

Measured area fraction of each domain is indicated, uniform density (UD) for 30° cone is 11.6%. Enrichment in domains is: 1.9 x, 1.6 x, (3.5x / 2 =) 1.7 x and 1.2 x.
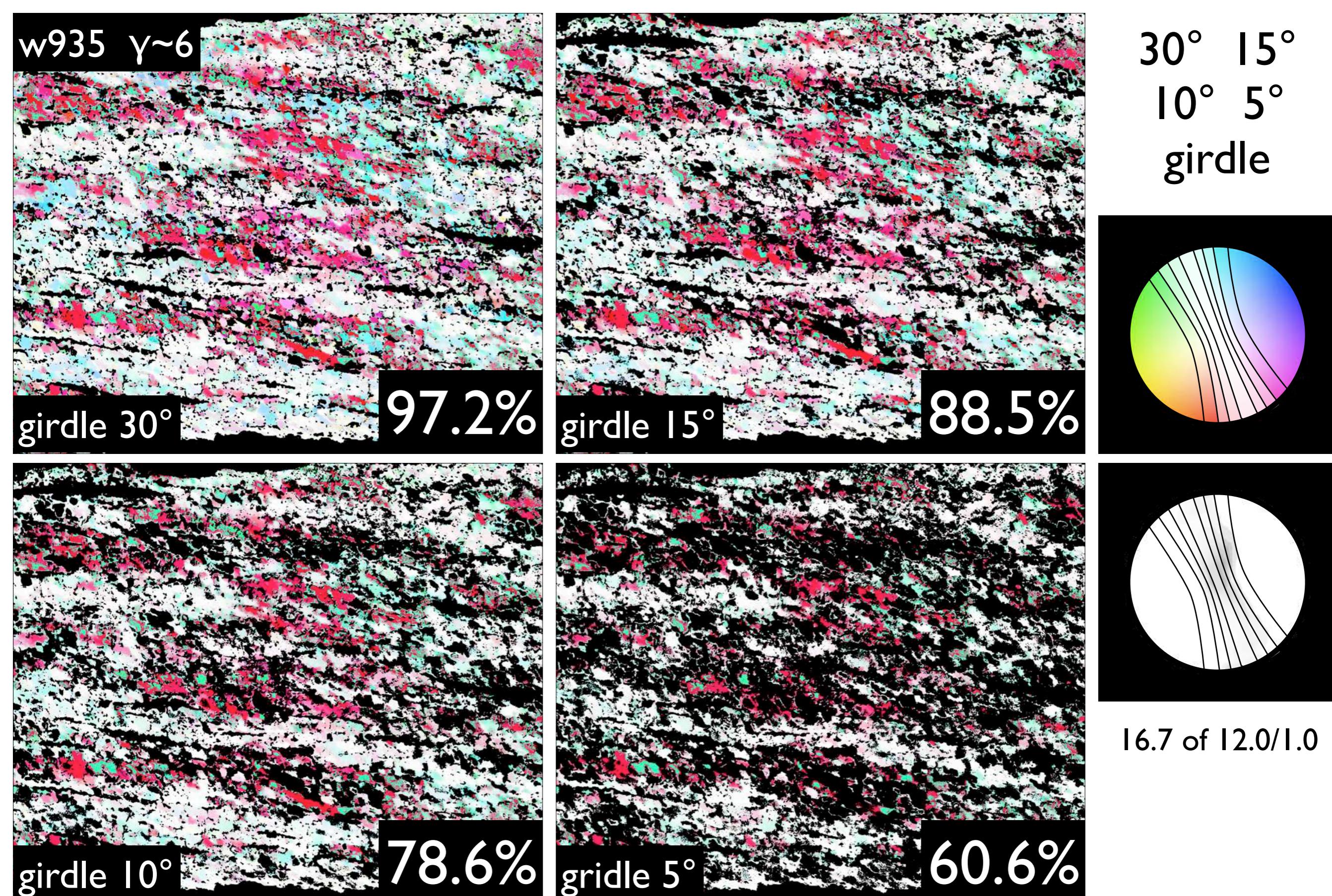
Figure 23.32
Orientation tracking VIII.
High-strain sample w935: concentration of c-axes in single girdles; misorientation images (MOIs) with respect to the girdle axis (69°/90°) are thresholded at 60°, 75°, 80° and 85° and inverted to yield girdle widths of 60°, 30°, 20° and 10°. Measured area fraction of each girdle is indicated. Uniform concentrations for 60°, 30°, 20° and 15° girdles are 54.3%, 29.4%, 20.1% and 10.3%, respectively. Enrichment factors are 1.8 x, 3.0 x, 3.9 x and 5.9 x.
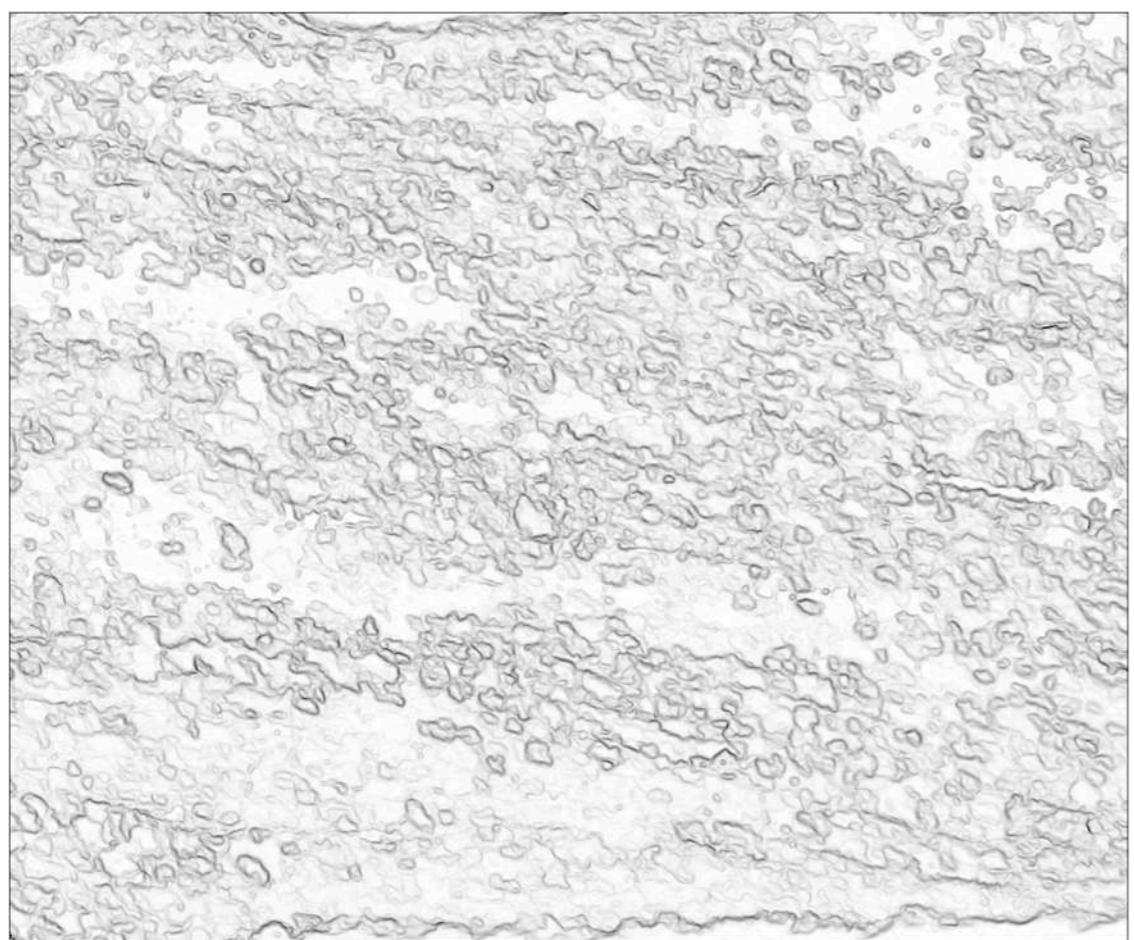
Figure 23.33
Texture domains and grain boundary density.
High-strain sample w935 (see Figure 23.32):
(a) misorientation image with respect to c-axis maximum Y_{max} (= misH);
(b) thresholded version of (a) representing misH texture domain;
(c) edge detection made from misorientation images (misE, misN, misH) using Lazy grain boundary macro (chapter 7): merged edge images;
(d) thresholded version of (b): separate threshold levels adapted to grain boundary density inside and outside texture domain.
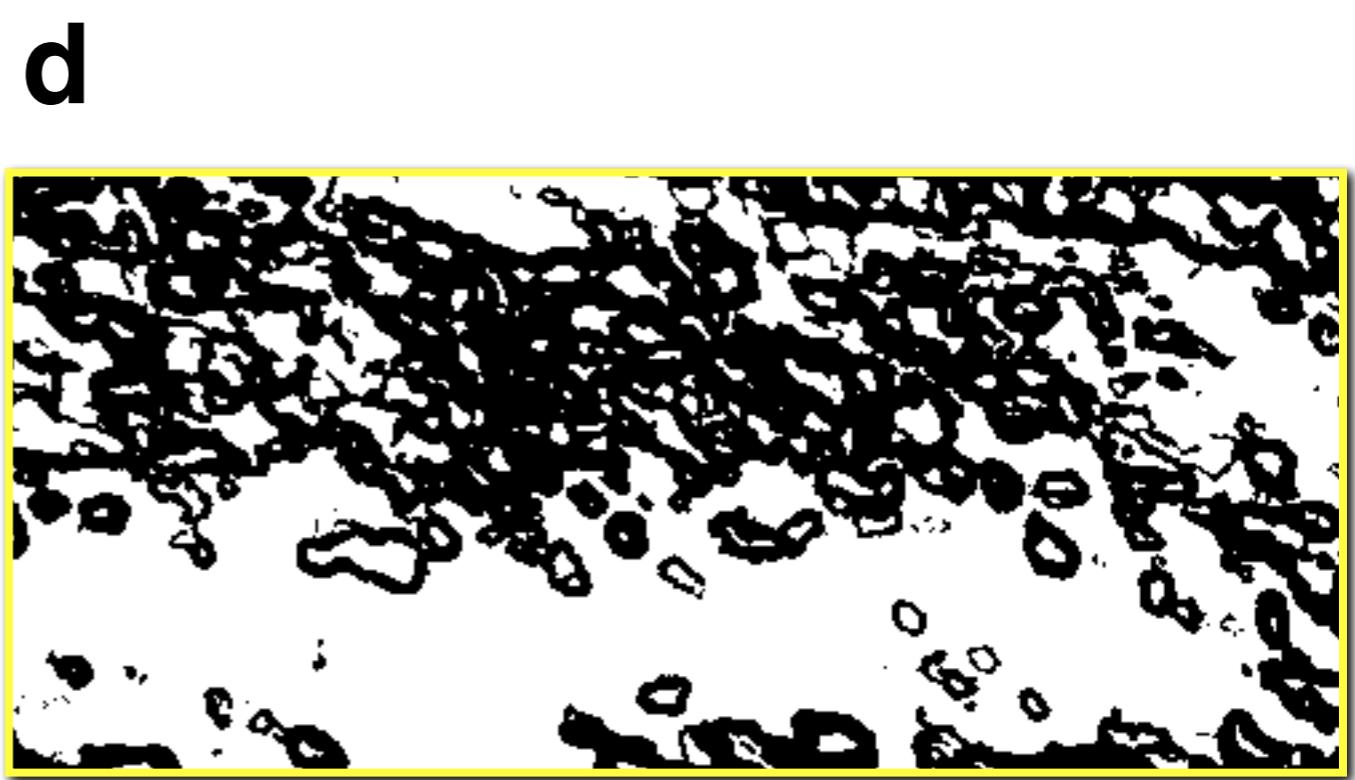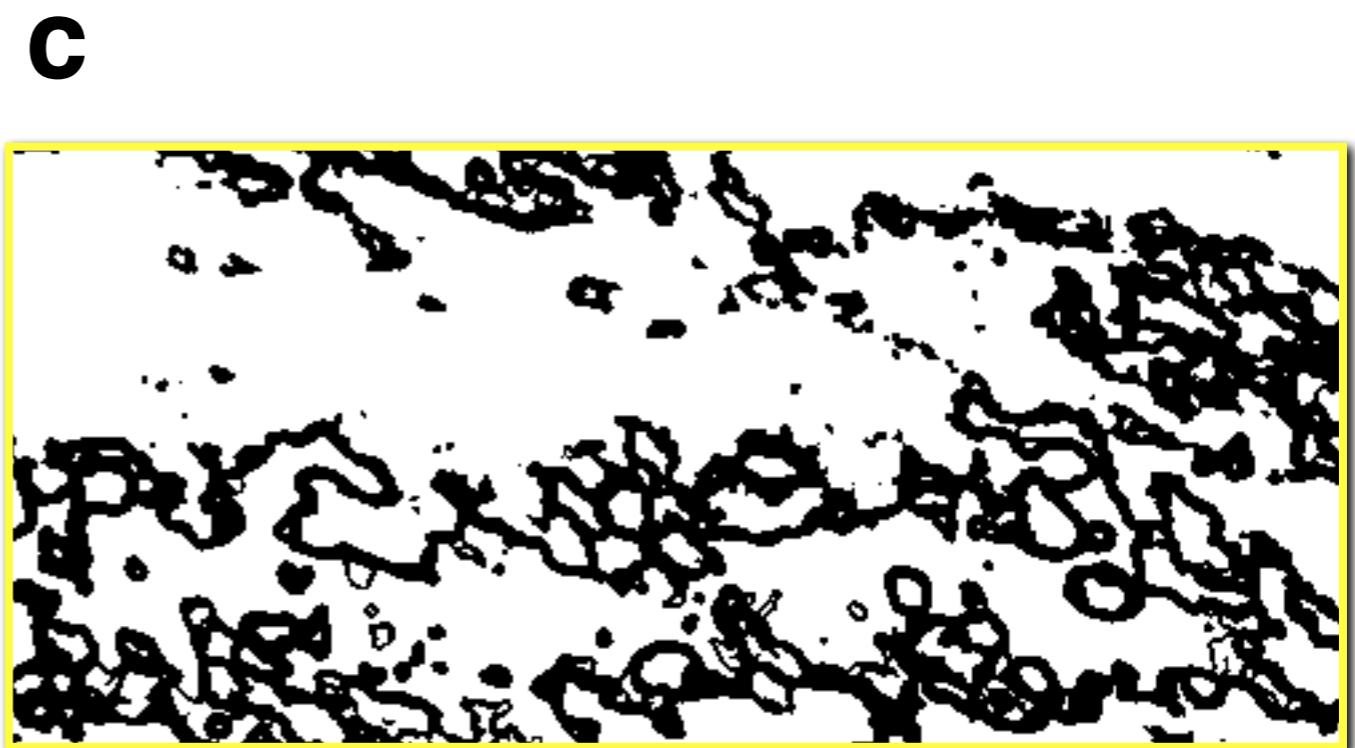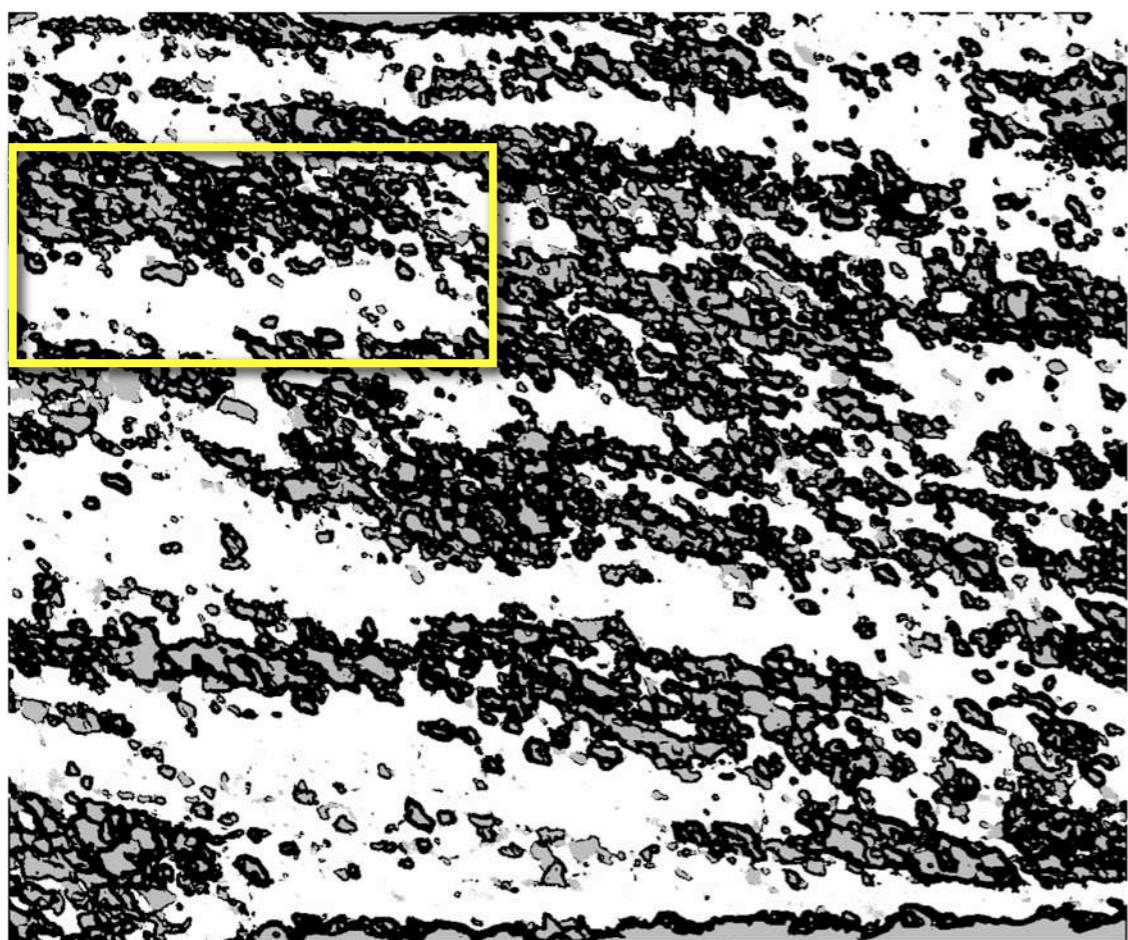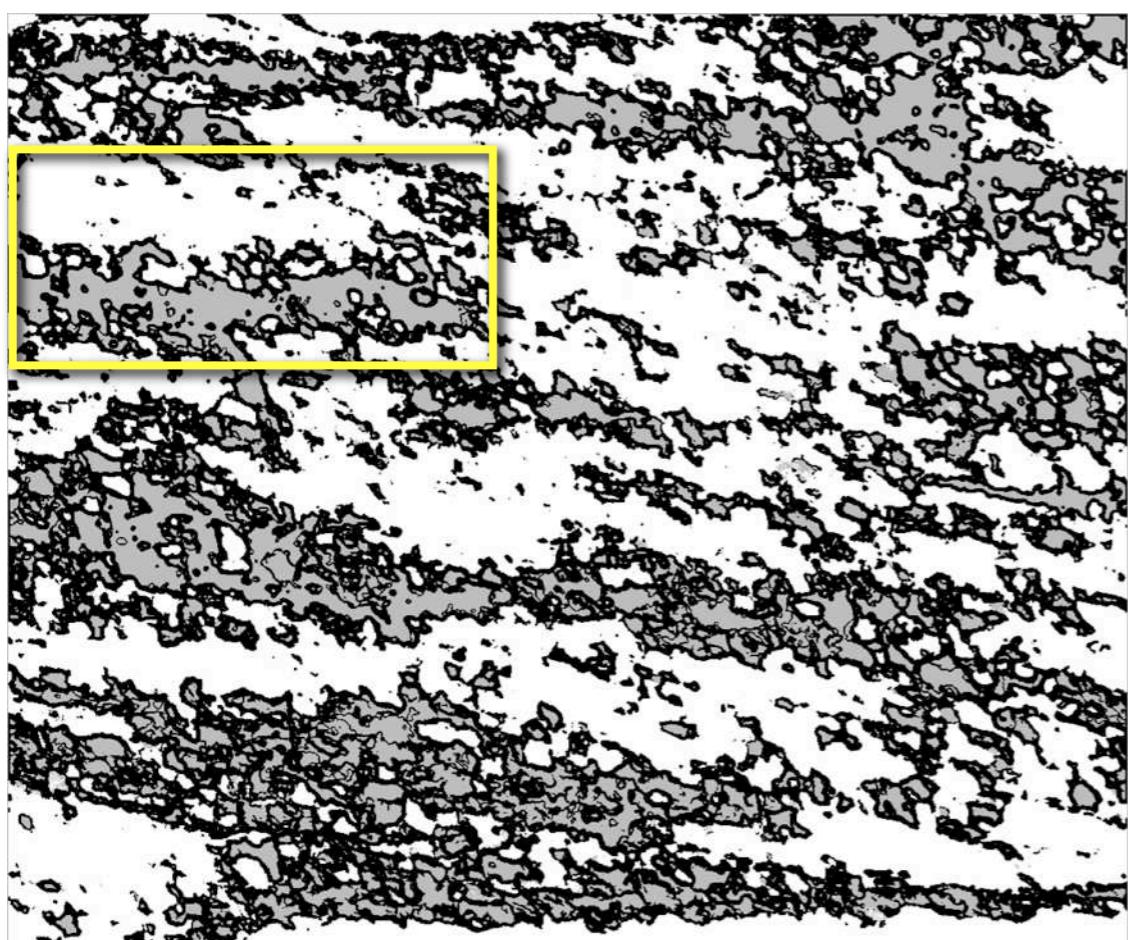
Figure 23.34
Texture domains and grain size.
High-strain sample w935 (see Figure 23.32):
(a) grain boundary density in misH texture domain;
(b) grain boundary density outside misH texture domain;
(c) enlarged detail of grain boundary density in misH texture domain;
(d) enlarged detail of grain boundary density outside misH texture domain.
Note different density and different grain size in (c) and (d).

a

orientation (φ, θ) of c-axis

b
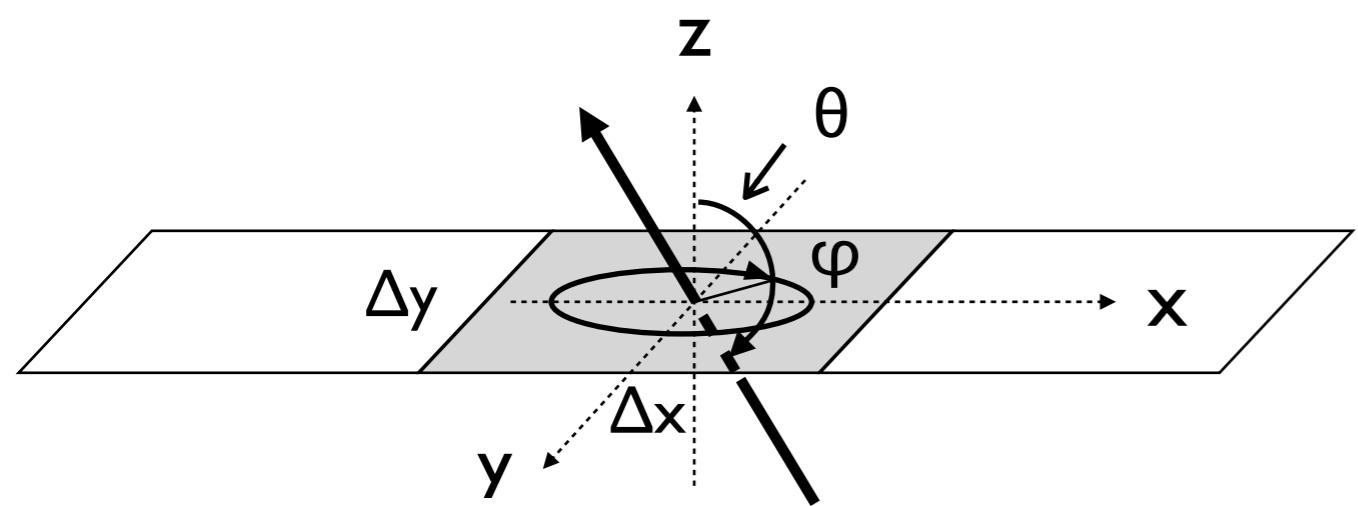
orientation gradient (Σ $β_i$) of c-axis
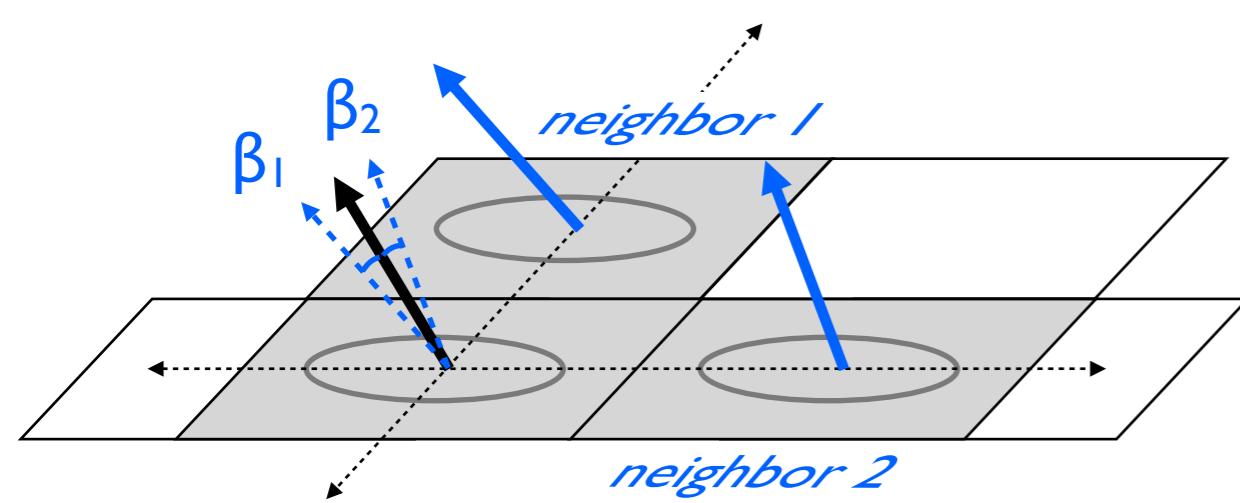
Figure 23.35
Orientation gradient imaging.
Schematic comparison of orientations and orientation gradients:
(a) orientation image: c-axis orientation is given by azimuth and inclination (φ, θ), at every pixel of the x-y image plane;
(b) orientation gradient image: orientation gradient = sum of misorientations ($β_i$) with respect to c-axis orientation of neighboring pixels.
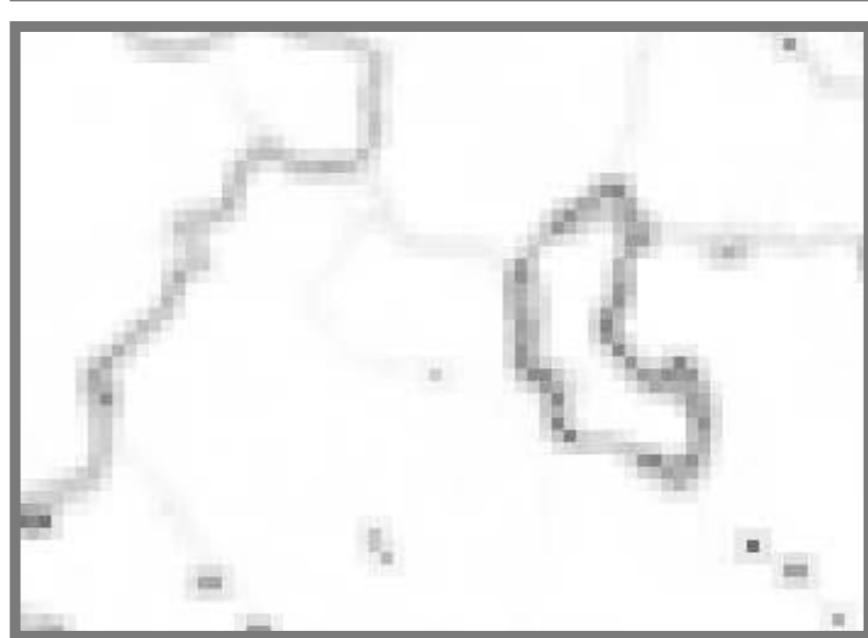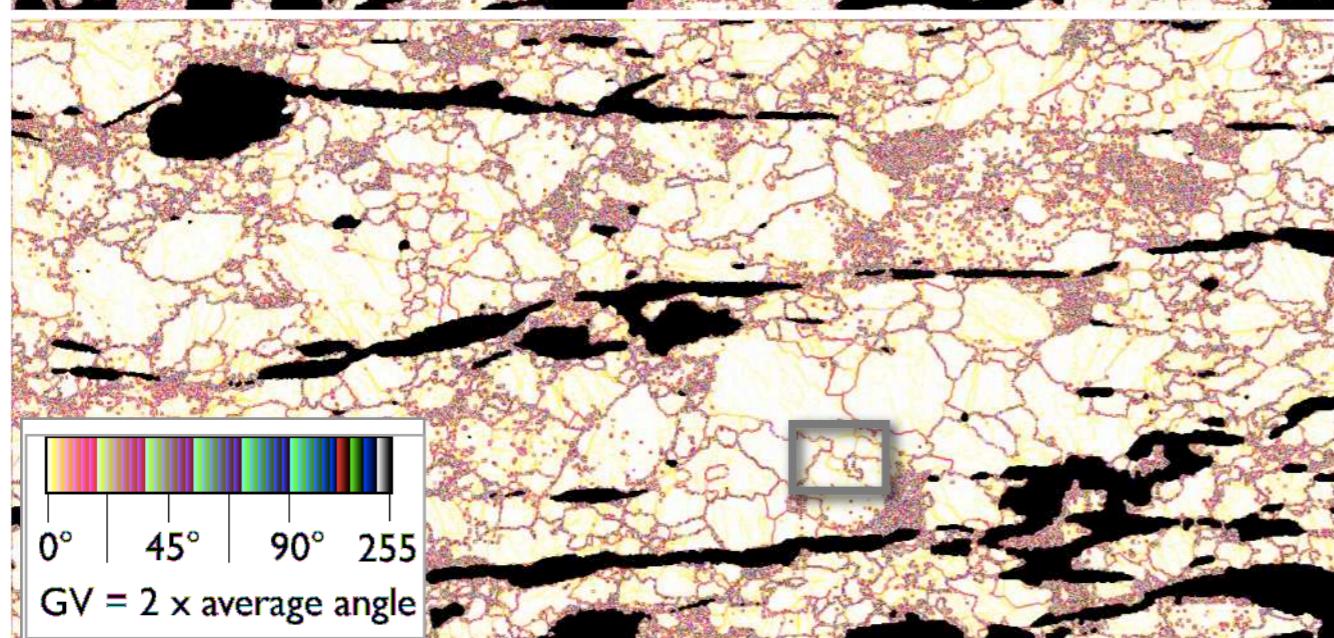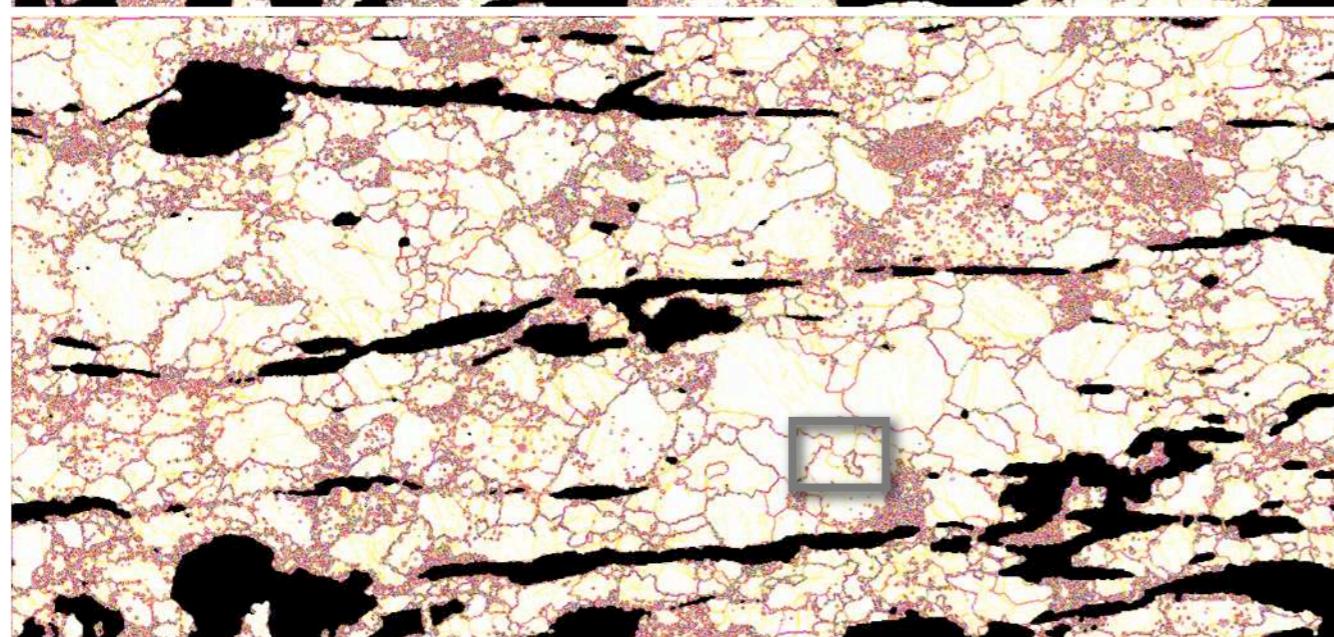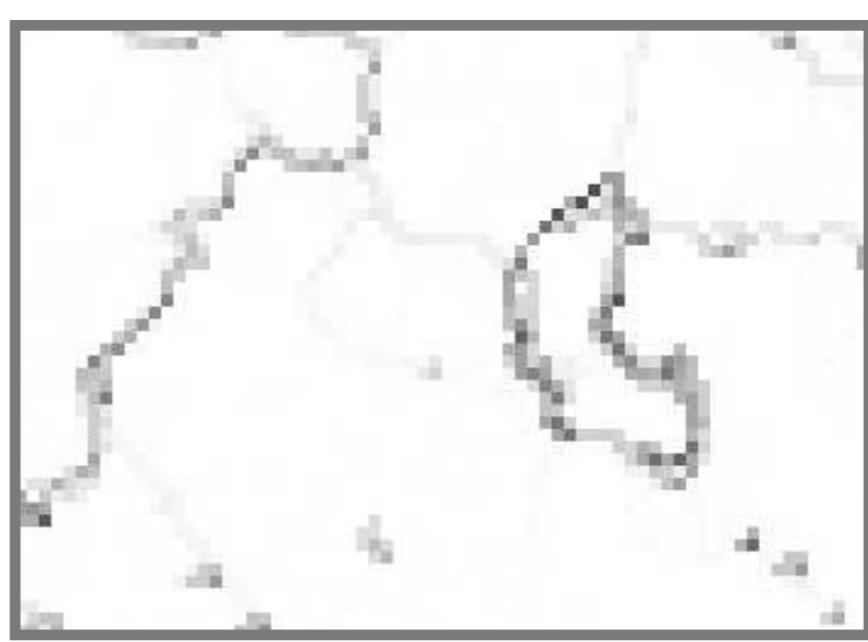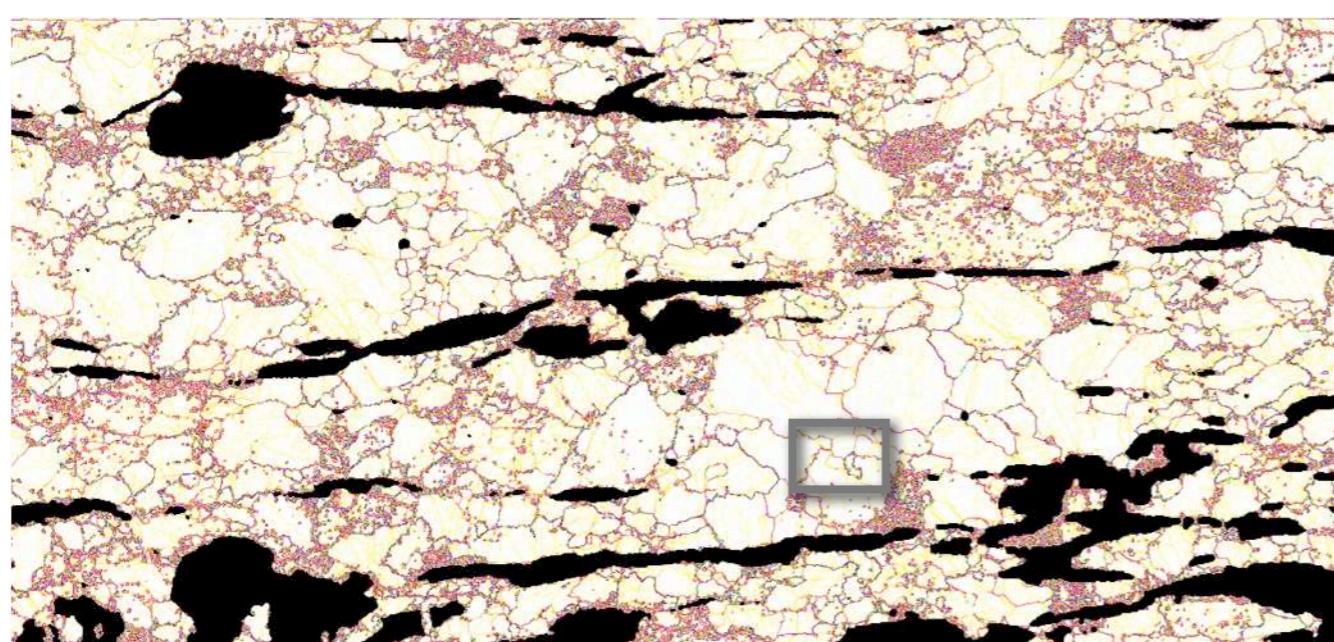
Figure 23.36

Orientation gradients.

Left: orientation gradient image (OGI) with 'System LUT' coloring (see inset); enlarged detail on right; sample is EBSD derived COI of quartzite (Figure 23.6).

(a) Gradient = sum of 2 neighbors (edge2s);

(b) gradient = 1/2 of sum of 4 neighbors (edge4a);

(c) gradient = 1/4 of sum of 8 neighbors (edge8a).
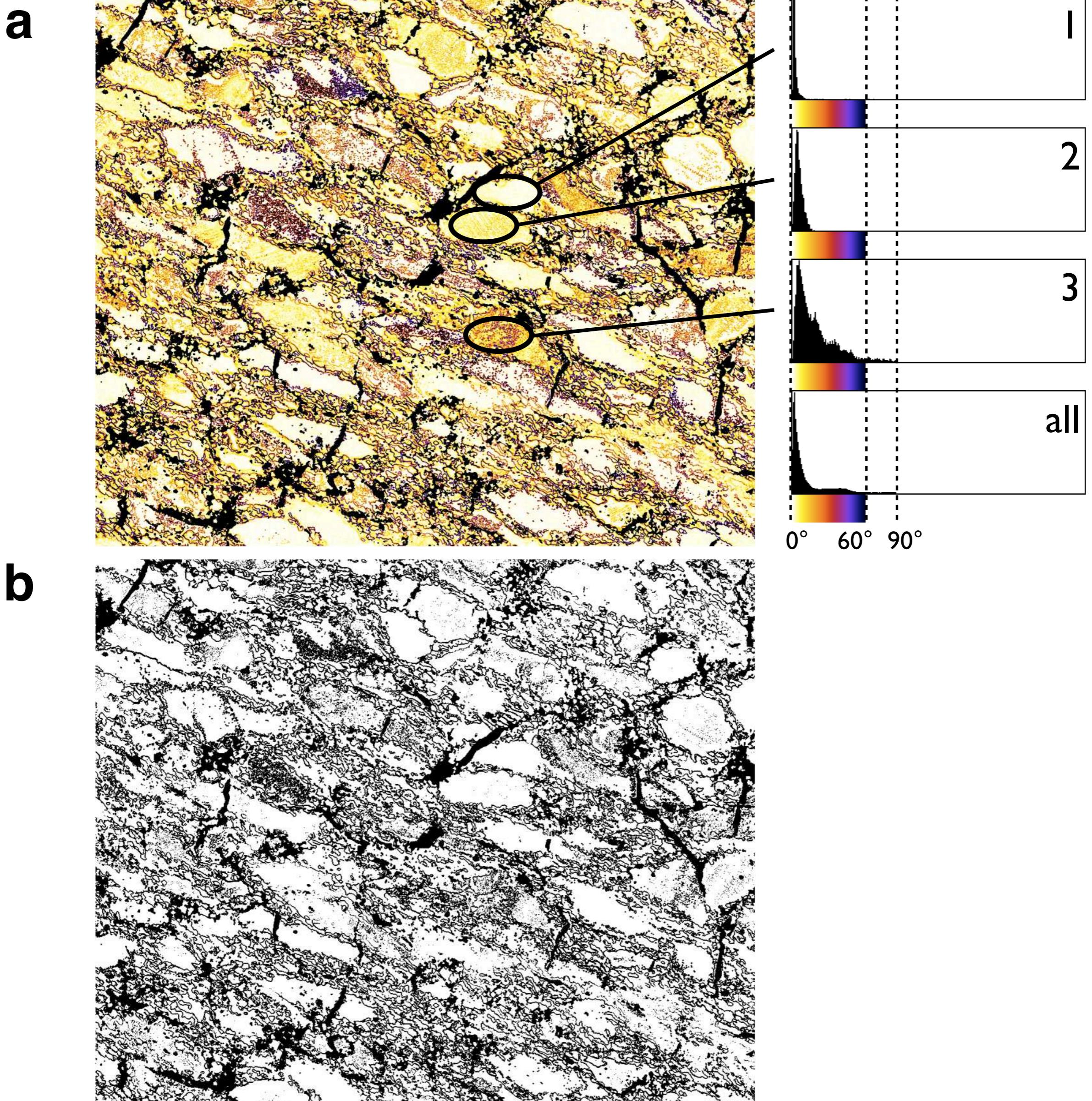
Figure 23.37
Orientation gradient and grain boundaries.
(a) Orientation gradient image (edge8a) with 'Fire-2' LUT; histograms of selected areas (1, 2, 3) and entire image (all) at right;
(b) thresholded version of (a): threshold level = 16, corresponding to an average orientation gradient of 8°.
(Mean / modal) orientation gradients of grains 1, 2, 3 and of the entire image are: (1.4° / 1°), (3° / 2.5°), (10.4° / 7°) and (10.4° / 1°), respectively.
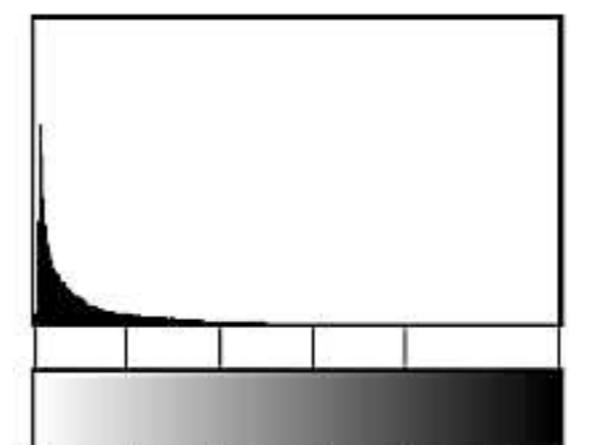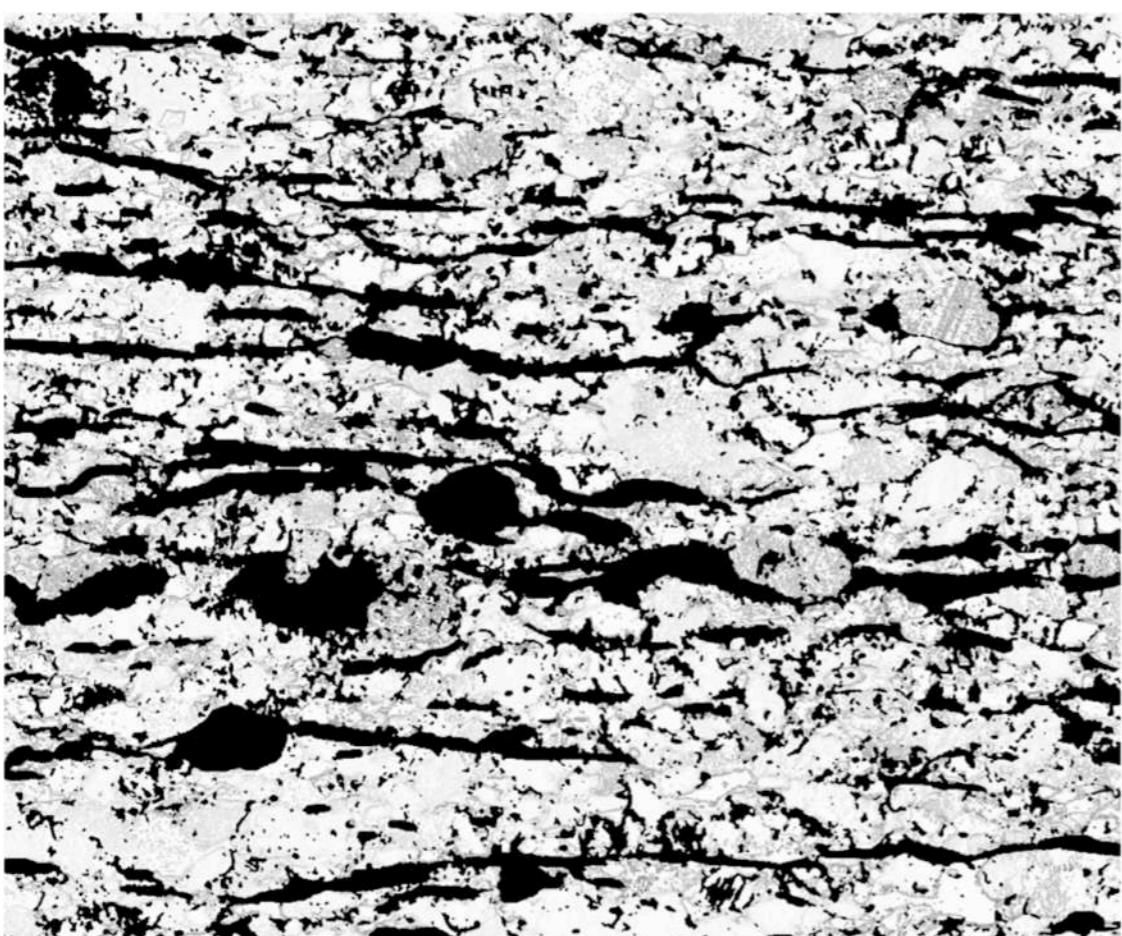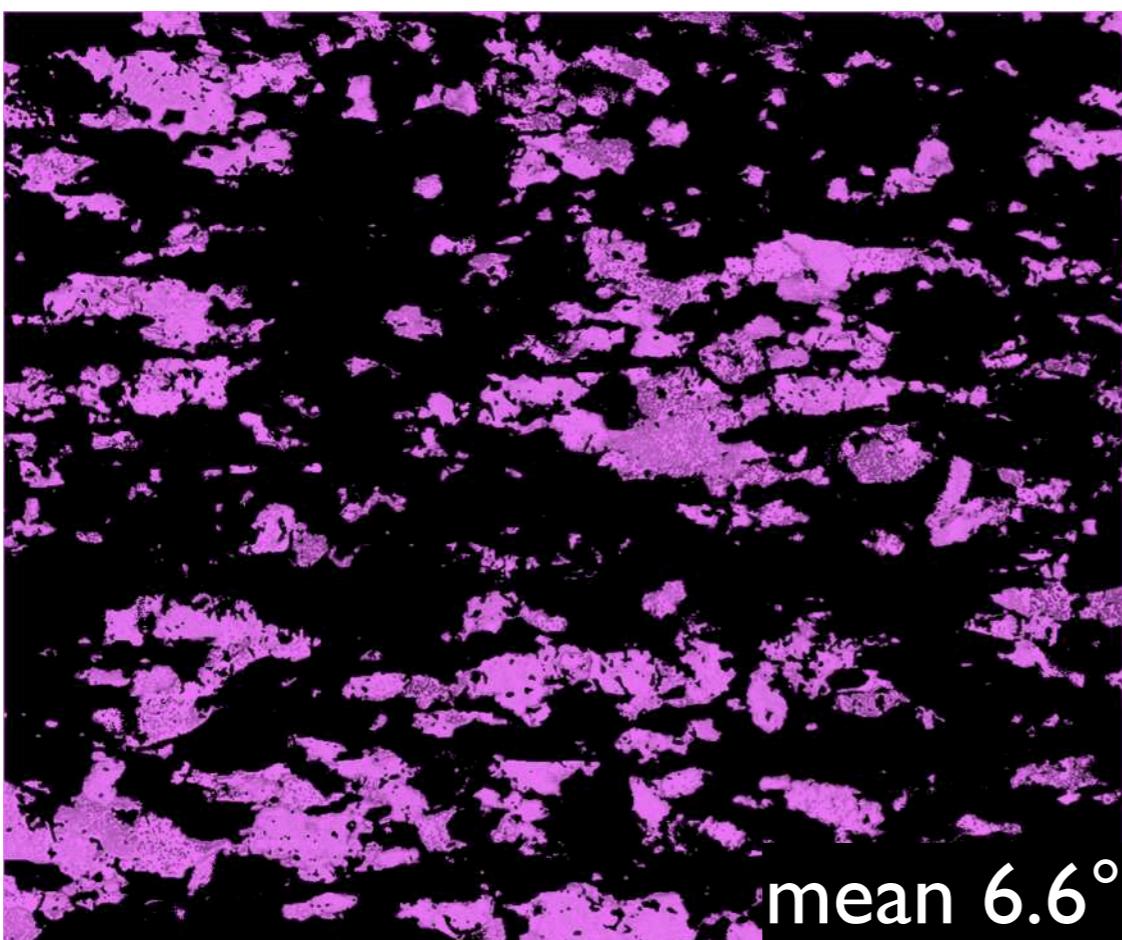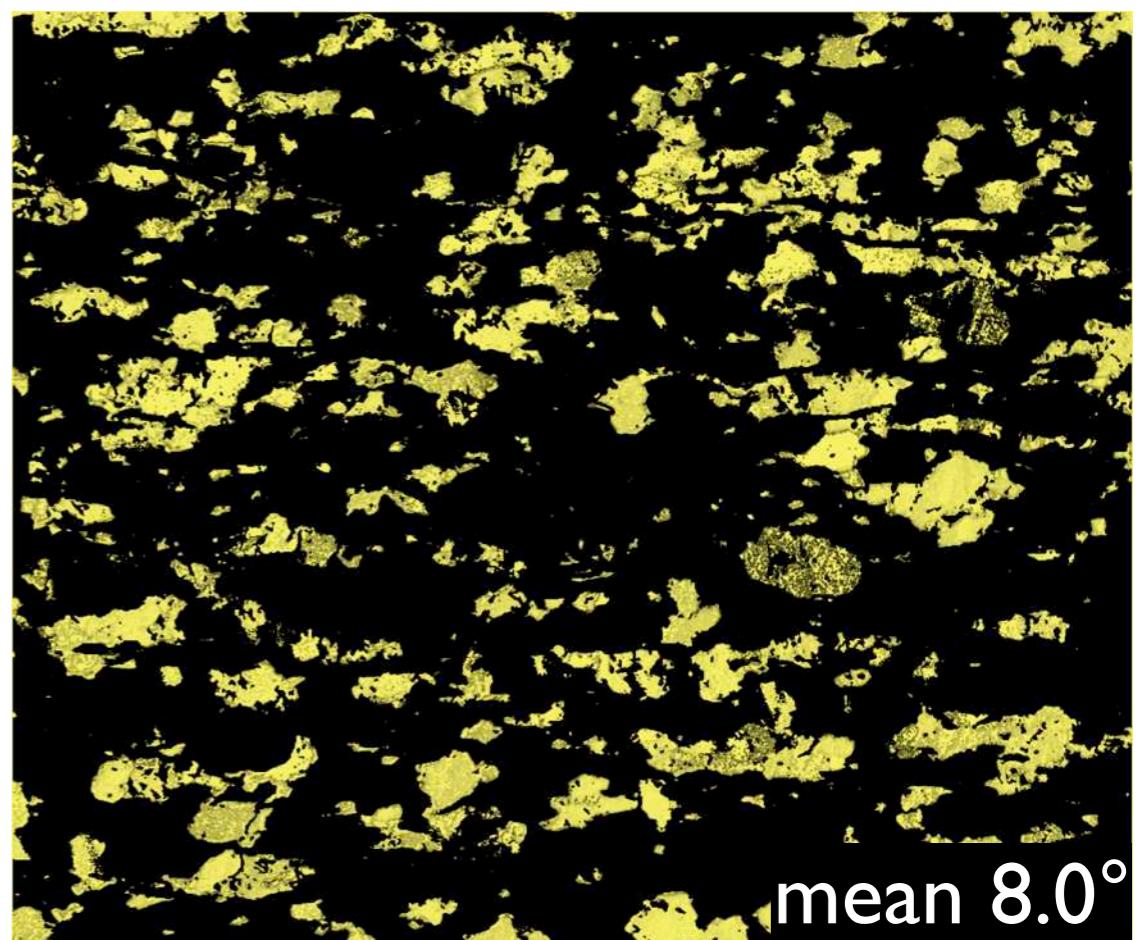
Figure 23.38
Orientation gradients in different texture domains.
(a) Orientation gradient image (OGI) using 8 neighbors (edge8a); average gradient indicated (mean); pole figure with 2 peripheral maxima high lighted in yellow and purple;
(b) same OGI as (a) masked by thresholded misorientation image (30° cone) with respect to purple direction (160°/90°); average orientation gradient in this domain is indicated;
(c) gradient image (edge8a) masked by thresholded misorientation image (30° cone) with respect to yellow direction (15°/90°); average orientation gradient in this domain is indicated (after Heilbronner 2010).
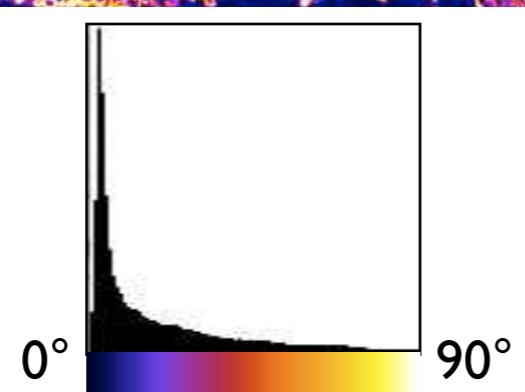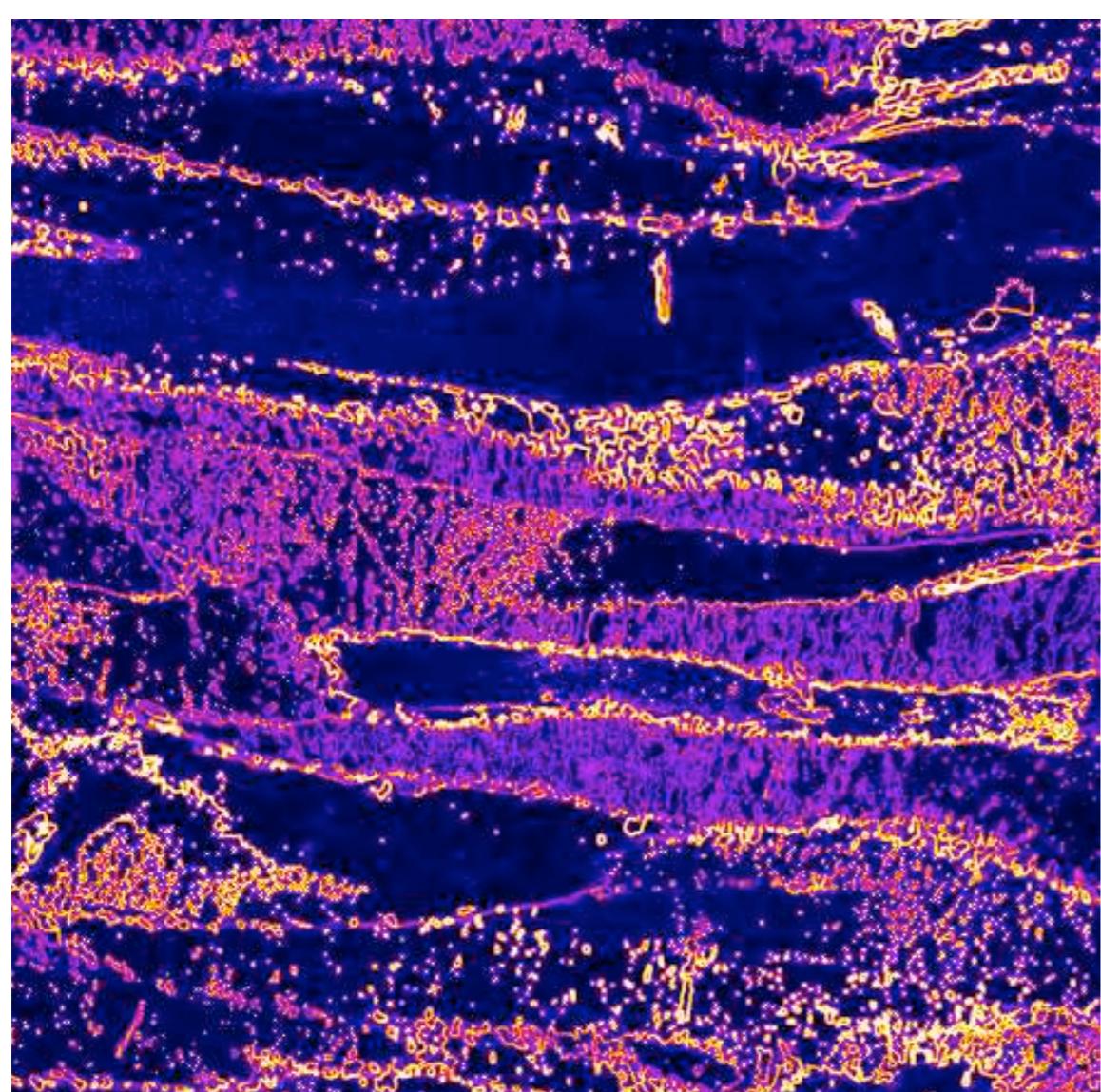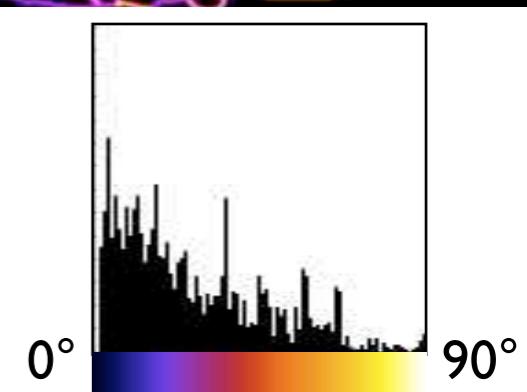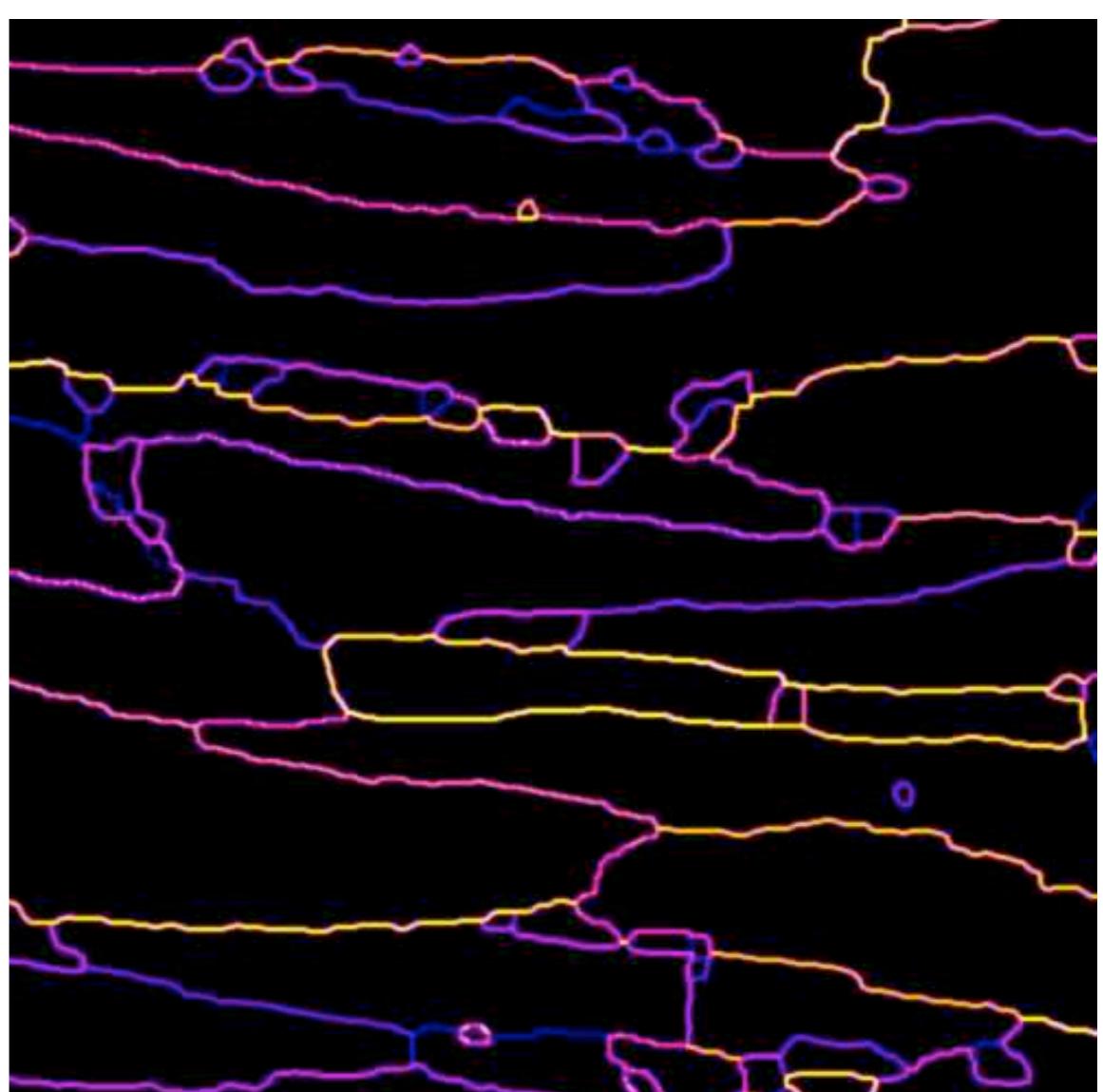
Figure 23.39
Orientation gradients for flat grains.
Deformed quartzite with ribbon grains:
(a) orientation gradient image (OGI); gradient = average of 4 neighbors (edge4);
(b) OGI of flat version of (a);
bottom: overview of c-axis orientation image (COI) and histogram of orientation gradients (0° - 90°). Note different distributions in histograms.
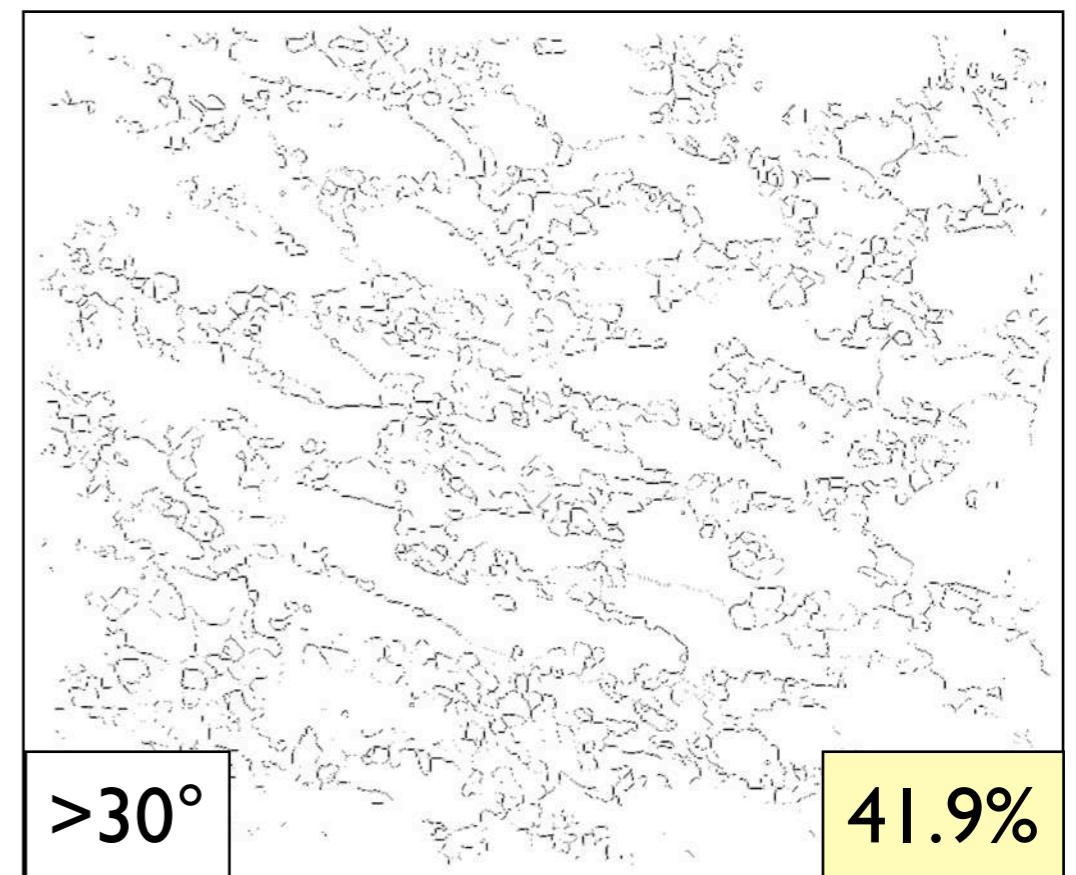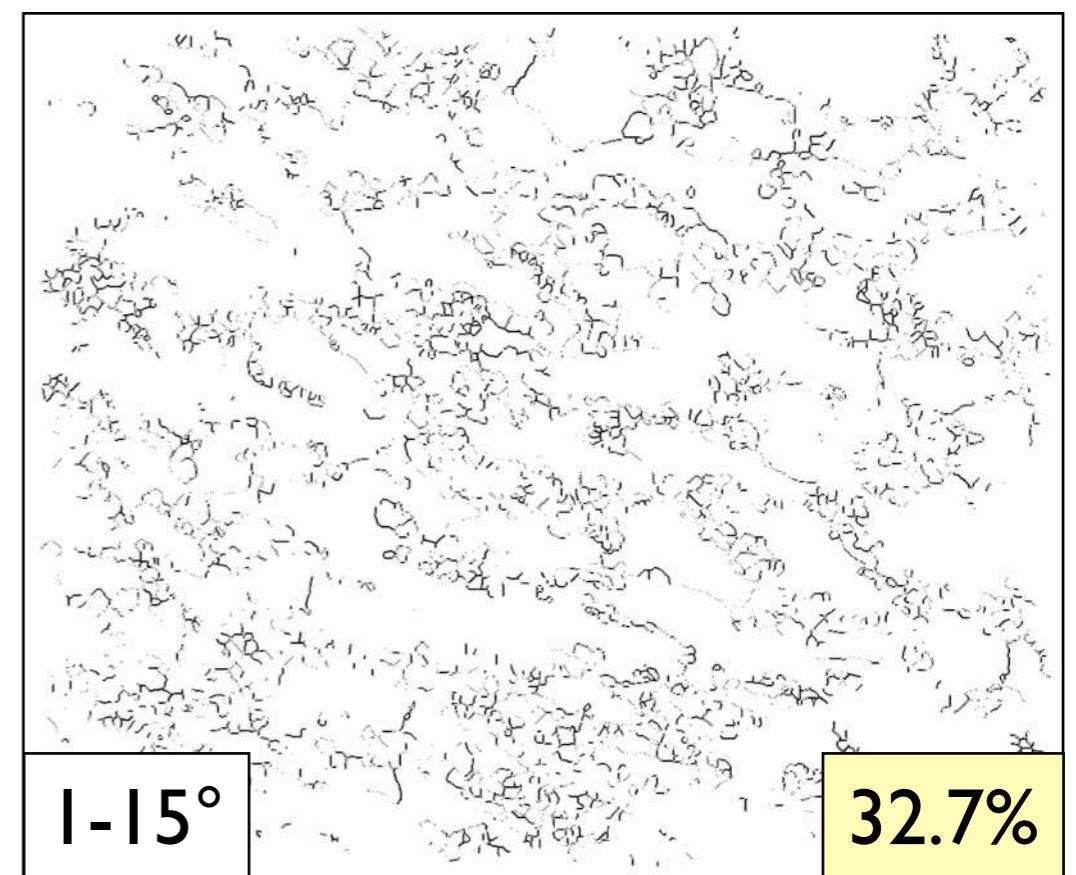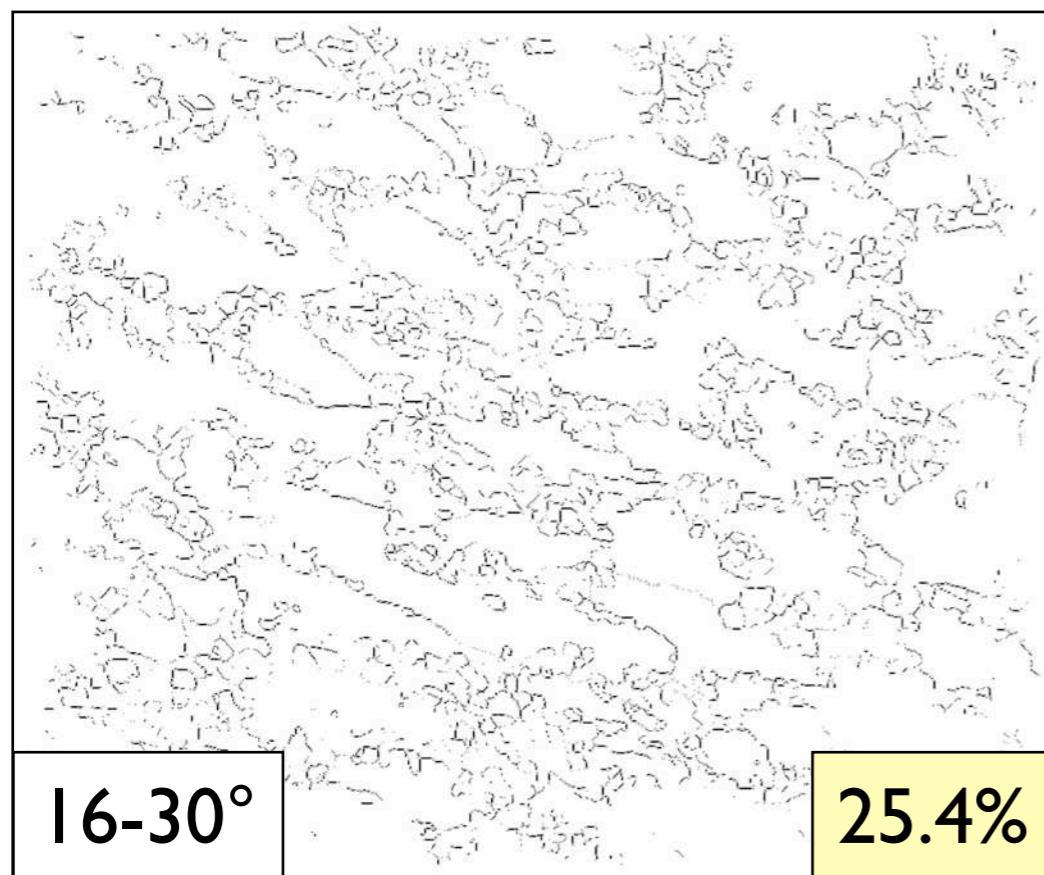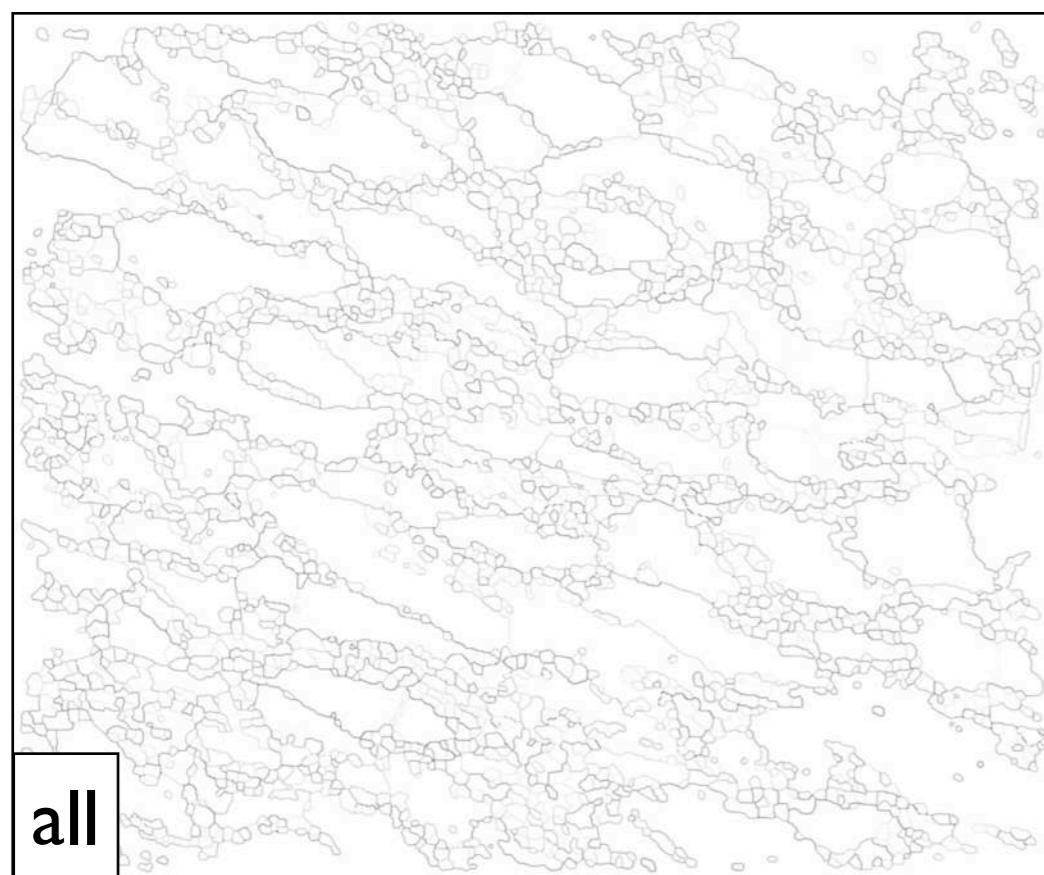
Figure 23.40
Orientation gradients of flat grains.
Orientation gradient images (OGI) of flat grains (COI in Figure 23.22):
(a) all gradients (average of 8 neighbors);
(b) bitmap of gradients between 1° and 15°, i.e, low angle boundaries;
(c) bitmap of gradients between 16° and 30°, i.e., medium angle boundaries;
(d) bitmap of gradients > 30°, i.e., high angle boundaries;
fractions of (b), (c) and (d) are indicated (yellow labels).
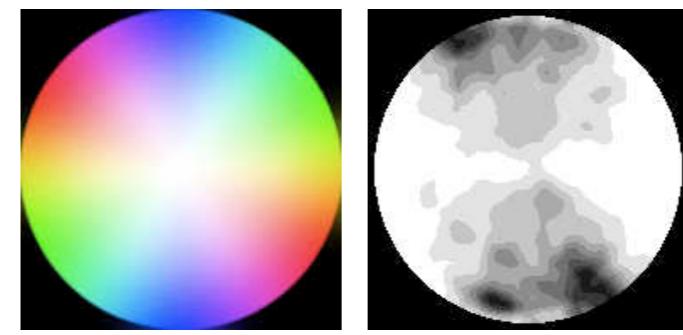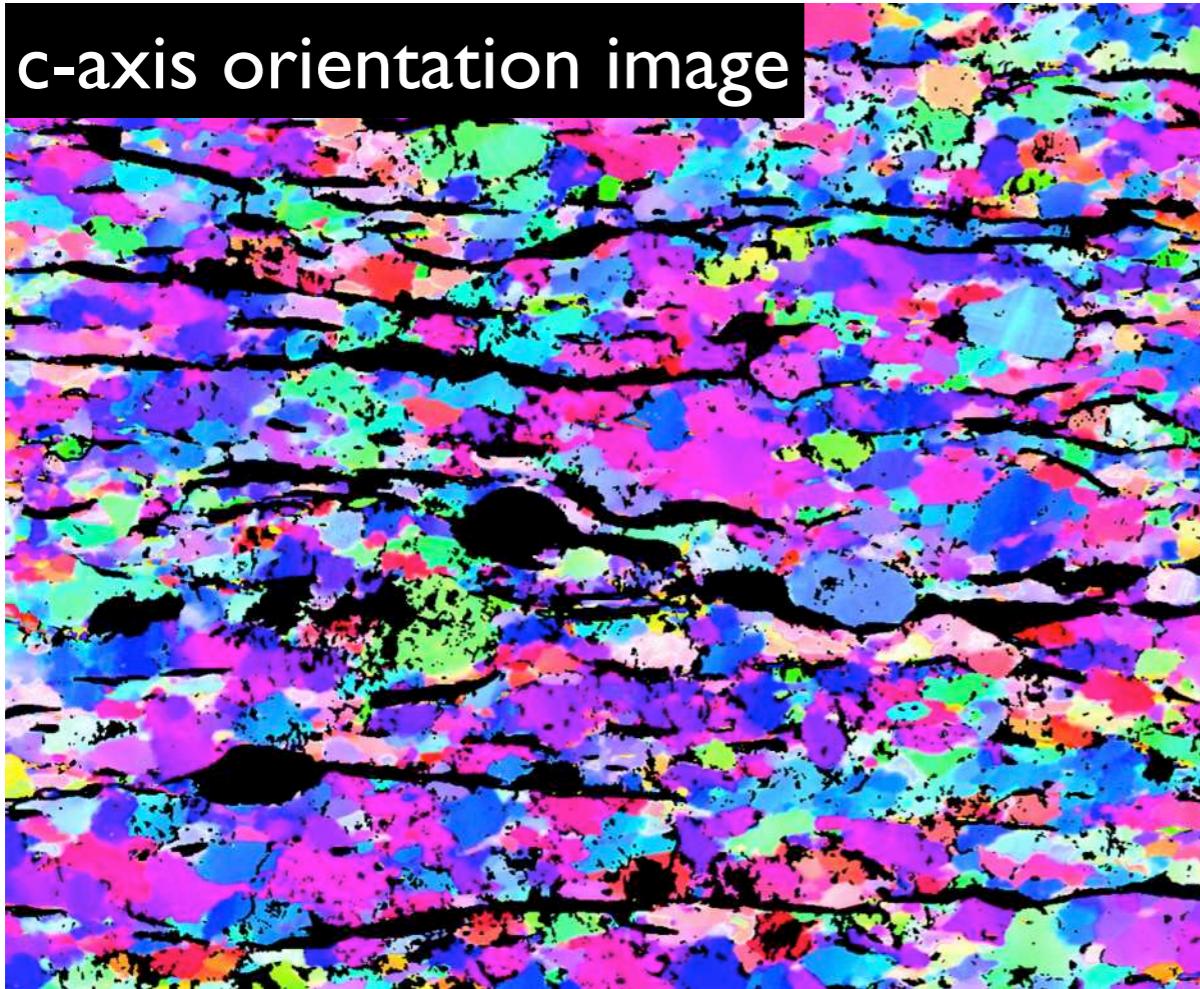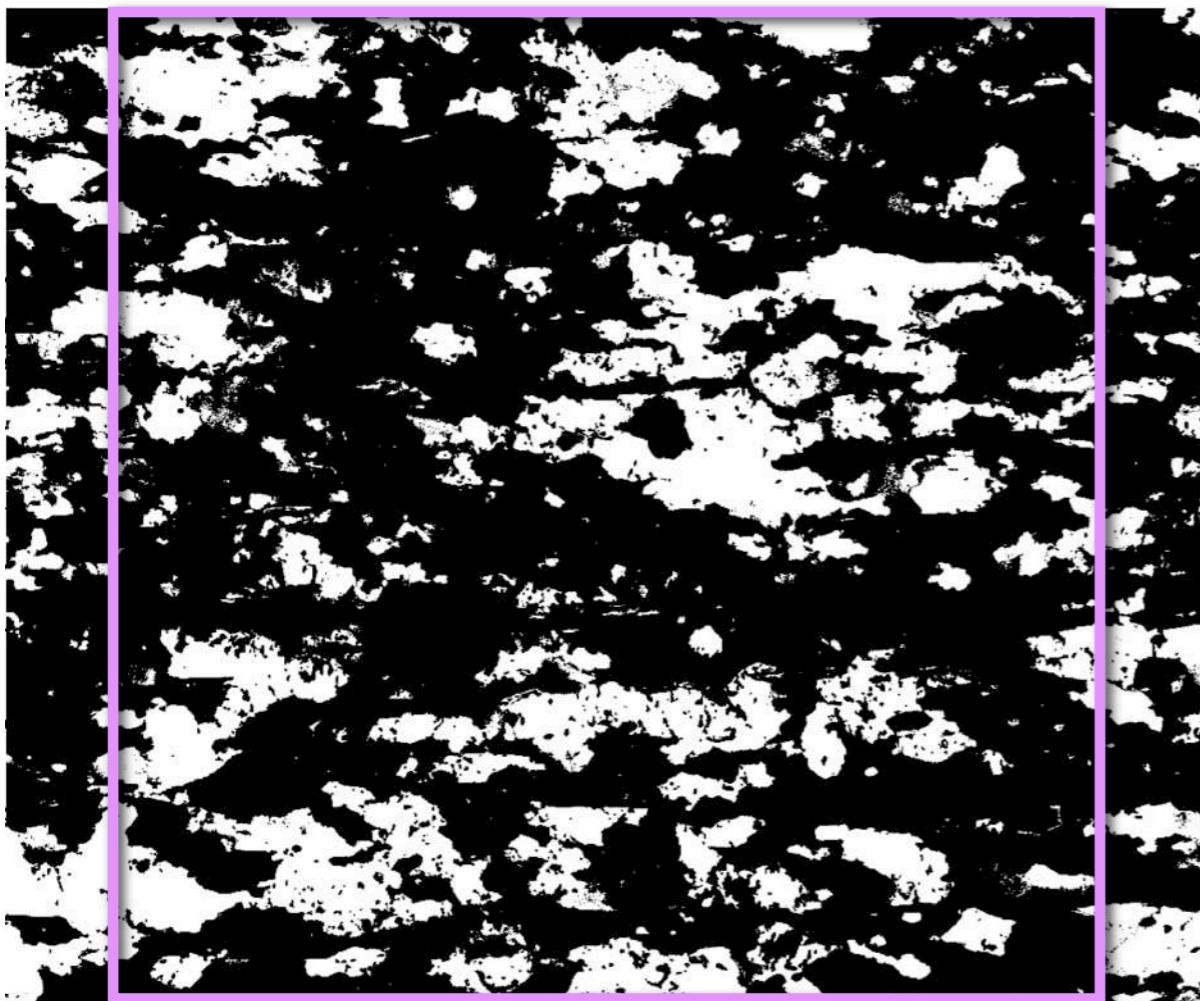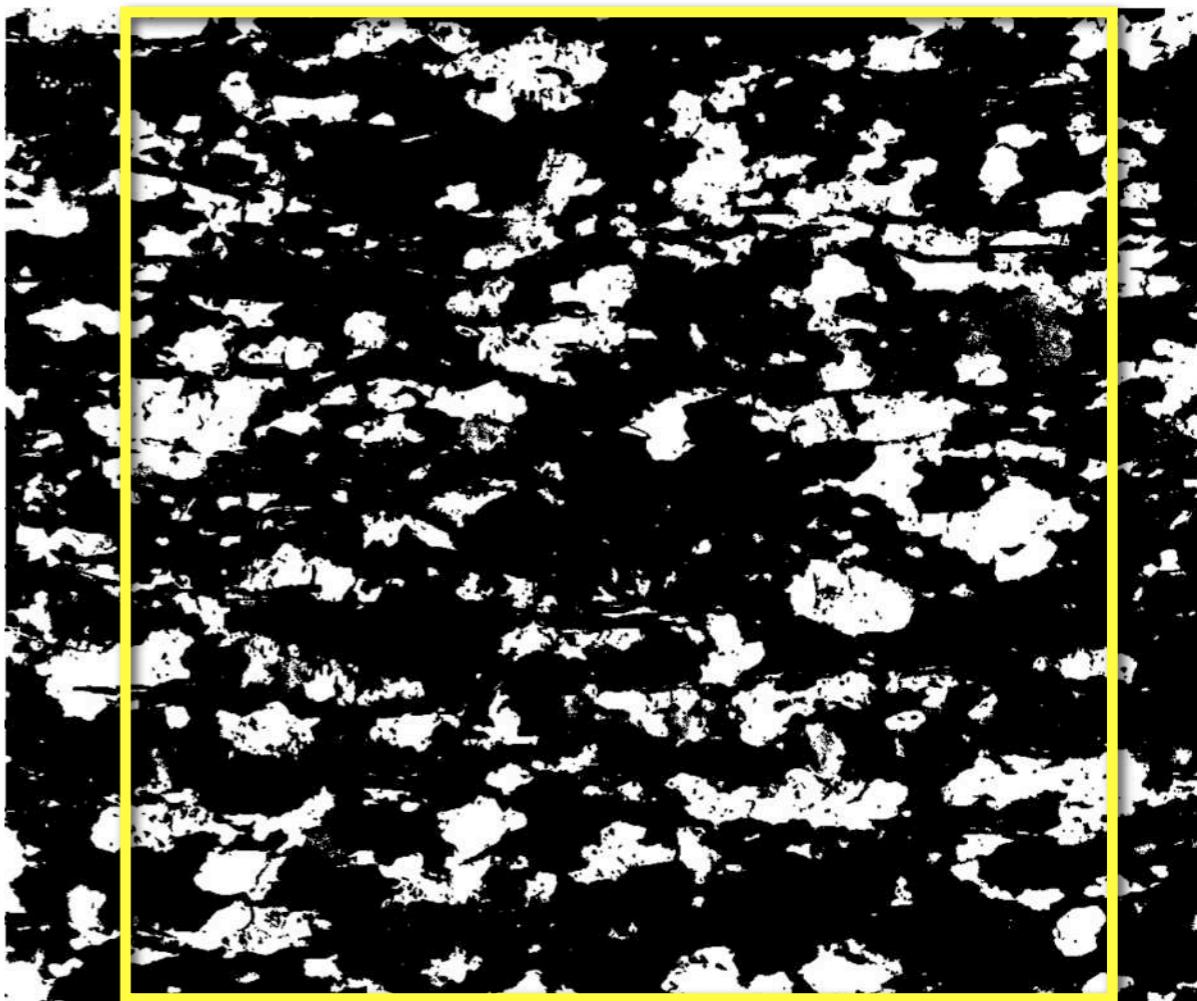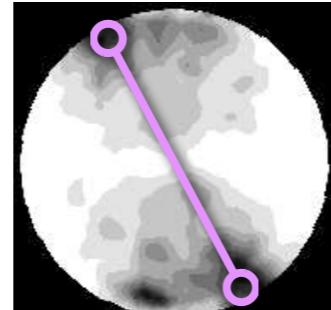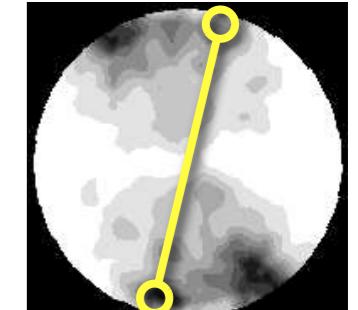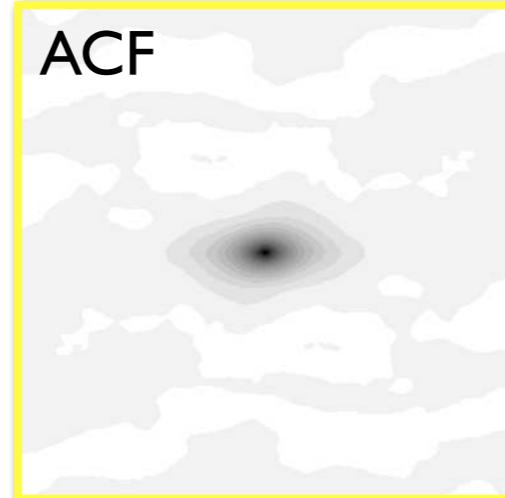
Figure 23.41

Shape of texture domains.

Autocorrelation functions (ACF) of texture domains of a naturally deformed quartz mylonite (for definition of domains see Fig.23.38):

(a) c-axis orientation image (COI) with pole figure;

(b) map and ACF of purple texture domain (reference direction 160° / 90°);

(c) map and ACF of yellow texture domain (reference direction 15° / 90°);

reference directions of texture domains indicated on pole figures; central 1/4 of ACFs are magnified 2x with respect to domain map (after Heilbronner 2010).